2007-11-21

Microchip Liquid Chromatography and Capillary Electrophoresis Separations in Multilayer Microdevices

Hernan Vicente Fuentes
Brigham Young University - Provo

MICROCHIP LIQUID CHROMATOGRAPHY AND CAPILLARY ELECTROPHORESIS SEPARATIONS IN MULTILAYER MICRODEVICES

by

HERNAN VICENTE FUENTES

A dissertation submitted to the faculty of

Brigham Young University

in partial fulfillment of the requirements for the degree of

Doctor of Philosophy

Department of Chemistry and Biochemistry

Brigham Young University

December 2007

a mi madre

BRIGHAM YOUNG UNIVERSITY

GRADUATE COMMITTEE APPROVAL

of a dissertation submitted by

HERNAN V. FUENTES

This dissertation has been read by each member of the following graduate committee and by majority vote has been found to be satisfactory.

_____	_____
Date	Adam T. Woolley, Chair
_____	_____
Date	Milton L. Lee
_____	_____
Date	Paul B. Farnsworth
_____	_____
Date	Matthew R. Linford
_____	_____
Date	Barry M. Willardson

BRIGHAM YOUNG UNIVERSITY

As chair of the candidate's graduate committee, I have read the dissertation of Hernan V. Fuentes in its final form and have found that (1) its format, citations, and bibliographical style are consistent and acceptable and fulfill university and department style requirements; (2) its illustrative materials including figures, and charts are in place; and (3) the final manuscript is satisfactory to the graduate committee and is ready for submission to the university library

_____ _____

Date

Adam T. Woolley
Chair, Graduate Committee

Accepted for the Department

_____

David V. Dearden
Graduate Coordinator

Accepted for the College

_____

Thomas W. Sederberg
Associate Dean, College of Physical and Mathematical Sciences

ABSTRACT

MICROCHIP LIQUID CHROMATOGRAPHY AND CAPILLARY ELECTROPHORESIS SEPARATIONS IN MULTILAYER MICRODEVICES

Hernan V. Fuentes
Department of Chemistry and Biochemistry

Doctor of Philosophy

In this dissertation, several microfabricated devices are introduced to develop new applications in the area of chemical analysis. Electrochemical micropumps, chip-based liquid chromatography systems and multilayer capillary electrophoresis microdevices with crossover channels were fabricated using various substrates such as poly(dimethylsiloxane) (PDMS), glass, and poly(methyl methacrylate) (PMMA).

I have demonstrated pressure-driven pumping of liquids in microfabricated channels using electrochemical actuation. PDMS-based micropumps were integrated easily with channel-containing PMMA substrates. Flow rates on the order of ~10 μL/min were achieved using low voltages (10 V).

The potential of electrolysis-based pumping in microchannels was further evaluated for pressure driven microchip liquid chromatography (LC). Two micropumps were connected with reservoirs for sample and mobile phase, situated at the ends of

microchannels for sample injection and separation, respectively. Columns micromachined in glass were coated covalently with an organic stationary phase to provide a separation medium. A pressure-balanced sample injection method was developed and allowed the injection of picoliter sample volumes into the separation channel. Fast (<40 s) separation of three fluorescently tagged amino acids was performed in a 2.5-cm-long microchip column with an efficiency of 3300 theoretical plates. Improved electrode designs that eliminate the stochastic formation of bubbles on the electrode surface will enhance pumping reproducibility.

Multilayer polymeric microdevices having fluidically and electrically independent crossover channels were made using phase-changing sacrificial layers (PCSLs). High-performance electrophoretic separations of fluorescently labeled amino acids were carried out in multilayer PMMA microchips. Neither pressure nor voltage applied in a crossover channel resulted in negative effects on the separation quality in the main fluidic path.

A fifty-fold reduction in crossover volumes was achieved in next-generation multilayered microchips. The ability to make minimal dead volume crossover channels facilitated the design and operation of multichannel array microdevices with a minimum number of electrical and fluidic inputs. Replicate electrophoretic separation of two peptides was performed in parallel for three independent microchannels connected to a single sample reservoir. My work demonstrates the value of PCSLs in making complex microfluidic structures that should expand the application of micro-total analysis systems.

ACKNOWLEDGEMENTS

Upon completion of my dissertation, my deepest gratitude goes to Dr. Adam T. Woolley, my advisor. During the last years, he has shaped my dream of being a researcher and directed it into becoming a reality. I will always appreciate his dedication and enthusiastic mentoring of my ideas and sometimes even my uncertainties. I thank my graduate committee members, Dr. Farnsworth, Dr. Linford, Dr. Lee, and Dr. Willardson for their valuable ideas and insightful suggestions during my progress reviews, which always kept my research in perspective. In particular, I feel great respect and admiration for Dr. Milton L. Lee for being not just an exemplary scientist, but also a personal example. I am grateful for his support and for the many resources he provided for my research.

I must acknowledge the Department of Chemistry and Biochemistry at Brigham Young University, their faculty, staff and all the facilities that were available to me to complete my work. Special thanks to the staff of the instrument shop for their contribution to and support of my work. In addition, I thank the Department of Electrical and Computer Engineering for facilitating my access to the instrumentation in the cleanroom, where I spent considerable research time.

During my time at BYU, I was fortunate to meet exceptional people to work with and who I consider my friends. With Dr. Ryan Kelly, Dr. Tao Pan and Bridget Peeni, together, we comprised the first generation of graduate students in microfluidics in Dr.

Woolley's laboratory, and I consider myself fortunate to have had such inspiring lab mates to work with.

Being away from home, sometimes friends occupy the space reserved for family. I found that comfort in two exceptional friends, Jenny Armenta and Jesse Contreras, to whom I express my gratitude for being an important part of this journey. I thank my family, especially my mother, who sacrificed all of these years away from her son with patience and always having faith in my goals. Finally, I thank my wife, Isabel Fuentes, for her understanding and patience throughout the final stage of this endeavor.

TABLE OF CONTENTS

LIST OF TABLES

LIST OF FIGURES

LIST OF ABBREVIATIONS

ALAL:	Ala-Leu-Ala-Leu
BOE:	buffered oxide etchant
BR:	buffer reservoir
CAD:	computer-aided design
CE:	capillary electrophoresis
CEC:	capillary electrochromatography
CGE:	capillary gel electrophoresis
CH:	channel substrate
COC:	cyclic olefin copolymer
CT:	connector tube
CZE:	capillary zone electrophoresis
DI:	deionized water
DNA:	deoxyribonucleic acid
EC:	electrolyte chamber
ED:	electrochemical detection
EFGF:	electric field gradient focusing
EL:	electrode
EOF:	electroosmotic flow
EP:	eluent pump
ER:	eluent reservoir
FITC:	fluorescein isothiocyanate
FLEEI:	Phe-Leu-Glu-Glu-Ile

GFP:	green fluorescent protein
HPLC:	high performance liquid chromatography
IEF:	isoelectric focusing
IP:	injection pump
IR:	infrared
LC:	liquid chromatography-
LC-MS:	liquid chromatography-mass spectrometry
LIF:	laser induced fluorescence
LOD:	limit of detection
MEKC:	micellar electrokinetic chromatography
MEMS:	micro-electro mechanical systems
MS:	mass spectrometry
OTLC:	open tubular liquid chromatography
PC:	polycarbonate
PCR:	polymerase chain reaction
PCSL:	phase-changing sacrificial layer
PDMS:	poly(dimethylsiloxane)
PI:	polyimide
PMMA:	poly(methyl methacrylate)
PP:	polypropylene
PT:	pressure transfer tube
RNA:	ribonucleic acid
R-PE:	R-phycoerythrin

RSD:	relative standard deviation
SC:	snugly fitting cap
SR:	sample reservoir
SW:	sample waste
TPE:	thermoset polyester
UV:	ultraviolet
WR:	waster reservoir
μCE:	microchip capillary electrophoresis
μTAS:	micro-total analysis system

1. INTRODUCTION

1.1 MINIATURIZATION IN CHEMICAL ANALYSIS

1.1.1 The journey to microchips

Analytical chemistry has always been an important field for basic and applied research, including areas such as biochemistry, medicine, biology, the environment and petrochemistry, among many others. For years, the goal of many analytical chemists has been to automate and integrate as many steps as possible in a single protocol, reducing the analysis time as well as sample and reagent consumption. Miniaturization is not a new concept in analytical separations; the potential advantages of using small-diameter columns have been recognized for decades. In 1958, Golay revolutionized analysis by gas chromatography through the introduction of capillary columns.[1] In the late 1960's, theoretical and experimental work by Horvath et al.[2,3] and Giddings[4] illustrated the possibility of performing liquid chromatography (LC) in capillary columns. Later studies by Novotny[5,6] and Yang[7,8] demonstrated improvements in separation efficiency, obtained using capillary LC. Similarly, in the early 1980s, the advantages of performing electrophoretic separations in narrow-bore (25- to 75-μm i.d.) capillaries (as opposed to conventional slab gels) were demonstrated by Mikkers[9] and Jorgensen et al.[10,11] Indeed, these pioneering studies were key to the development of modern analytical separation techniques as we know them today. Interestingly, even before capillary columns became popular and widely used, groundbreaking work in miniaturization was presented by Terry et al.[12,13] in which a gas chromatograph was micromachined in a silicon wafer. Despite the separation capabilities and miniaturized size of this device, this work did not attract

much attention due to the lack of experience of researchers in analytical chemistry in microsensing and microfabrication at that time. Over a decade later, Manz et al.[14] introduced the concept of a micro-total analysis system (μTAS), in which micromachining techniques such as those used in the microelectronics industry could be implemented in the fabrication of microdevices for sensing and automated sample measurement in the laboratory. The idea of integrating sampling, separation and detection capabilities in a single microdevice sparked separation scientists' interest in microfabrication. During the 1990s, several papers reported the chip-based implementation of techniques such as electrophoresis,[15-17] electrochromatography,[18-20] liquid chromatography,[21] isotachophoresis,[22] isoelectric focusing,[23] and capillary gel electrophoresis.[24-27] A survey of the current literature demonstrates that most column-based separation methods have been implemented in a microchip format.[28,29]

1.1.2 Materials and fabrication techniques for microfluidics

As stated in Fundamentals of Microfabrication, "Microfabrication is a process used to construct physical objects with dimensions in the micrometer to millimeter scale."[30] The manufacturing protocols to make miniaturized analytical devices can be delineated according to the chosen material, whether inorganic substrates (glass, quartz and silicon) or polymeric.

1.1.2.1 Inorganic materials

From the introduction of the μTAS concept, diverse fabrication procedures originally developed for micro-electro mechanical systems (MEMS) and for the microelectronics

industry (photolithography, thin-film deposition and wet chemical etching among others[30]) were applied to the fabrication of μTAS components. Micromachining of silicon has been used for years in microprocessors and integrated circuit technology; therefore, the first analytical microdevices were made of silicon.[12,13,31,32] However, the use of silicon in microfluidics is limited, in part because crystalline silicon is brittle and must be handled with care. The potentials applied in many microfluidic applications are incompatible with the breakdown voltage of silicon, which is <500 V.[33] Furthermore, silicon is opaque to visible and ultraviolet light, and hence, cannot be used with conventional optical methods of detection. Finally, the relatively high cost of silicon can be prohibitive for the fabrication of disposable microdevices. Glass substrates have been implemented widely for the fabrication of analytical microdevices, due in part to their favorable optical properties, well-known surface chemistry, high breakdown voltage, insulating properties and well-established fabrication procedures.[34-36] A brief review of the literature reveals that, while silicon is the most common material in the fabrication of MEMS, glass is the substrate of choice for many microfluidic applications.[36-38] Glass substrates can vary from low-cost soda lime glass[39] to high quality borosilicate[38] and Borofloat.[36] Some drawbacks of glass micromachining are the extreme health hazards involved with HF etching, the requirement of cleanroom conditions during fabrication and the use of high temperatures (>600˚C) for bonding. These factors make the process relatively slow and impractical for mass production, leading to high fabrication costs.[40] Moreover, in most cases the surface of glass microchannels must be modified for the analysis of large biomolecules such as proteins.[41] Quartz or fused silica has been used to make miniaturized electrophoretic devices.[42] Good mechanical strength and superior

optical properties compared to glass make quartz an appealing material for the fabrication of microfluidics; however, its high cost and complicated fabrication (e.g., bonding at >1000°C) have limited the application of quartz in μTAS devices.[43] The use of CaF_2 was reported by Pan et al. for the electrophoretic analysis of amino acids.[44] The optical transparency of CaF_2 (170-7800 nm) allowed Fourier transform infrared detection for the first time in microfabricated devices. Indeed, detection in CaF_2 microdevices could be extended to other methods including Raman, UV, fluorescence, etc. Unfortunately, as with quartz, the fabrication yield and bonding procedures are serious limitations for the use of CaF_2 in microfluidics.[44]

1.1.2.2 Polymer substrates

Perhaps one of the most important advancements in microfluidics in recent years has been the drift from the initially used and complex silicon and glass micromachining protocols to much simpler techniques involving materials such as polymers.[45-47] Indeed, polymeric materials hold great potential to advance (both in terms of design flexibility and the ease with which a simple prototype can be made) the development of future integrated devices. Implementation of these technologies should result in the realization of less expensive, more functional, disposable and faster microanalytical devices.

The use of polymeric materials to fabricate miniaturized analytical devices has expanded tremendously in the last few years.[37,45,47-52] In general, plastics are less expensive than glass or silicon substrates, and polymer-based microfluidics can be mass-produced by replica or molding techniques, reducing the manufacturing costs. Moreover, the variety

of polymers available, each with unique characteristics, allows the selection of a substrate depending on the particular application and detection mode in which the specific polymer is best exploited.[53] Plastics used in the fabrication of microfluidics can be classified as either thermoplastics or elastomers.[54] Thermoplastic materials are composed of weakly bonded chains, can be dissolved in organic solvents, soften upon heating and harden when cooled down. Typical examples of thermoplastic materials include poly(methyl methacrylate) (PMMA), polycarbonate (PC), poly(cyclic olefin copolymer) (COC) and polyimide (PI). Elastomers or thermoset materials on the other hand are cross-linked and insoluble in most organic solvents. Some examples of thermoset polymers include poly(dimethylsiloxane) (PDMS) and epoxy resists.

Polymers can be characterized by their glass transition temperature (T_g), melting temperature (T_m) and decomposition temperature. A more complete list of the properties of polymeric materials can be found in several texts.[55,56] **Table 1.1** lists the T_g values for several commonly used polymers in μTAS applications.

1.1.2.3 Silicon and glass microfabrication techniques

The processes developed for microelectronics can be applied to silicon and glass to make microstructures in planar substrates. Microfabrication using inorganic materials can be described as either bulk or surface micromachining.[30,57] In bulk micromachining, structures are created in the substrate itself, whereas surface micromachining uses deposition or growth of thin layers on a substrate followed by selective etching to form features.

Table 1.1 Common polymers for microfluidic devices and their μTAS applications.

Material	T_g (˚C)	μTAS Application
PMMA	105	DNA analysis[48,58-60] Electrophoretic analysis of amino acids, peptides and proteins[50,61,62] Isoelectric focusing of peptides[63] Interface to mass spectrometry (MS)[64-66] Electroosmotic flow properties[67] Electric field gradient focusing[68] On-chip solid phase extraction[69]
PDMS	128	Immunoassays[70,71] MS electrospray emitters[72,73] Electroosmotic flow properties[74,75] 2D-capillary electrophoresis[76] Electrophoretic analysis of amino acids and proteins[46,77,78] Multilayer microchips[79,80]
PC	150	PCR amplification followed by DNA analysis[81] Electrophoretic analysis of proteins, peptides and amino acids[82] MS electrospray emitters[83] Electroosmotic flow properties[84,85] DNA mutation detection[86]
COC	140	Electrophoretic separation and MS[87] MS electrospray emitters[88] On-chip LC-MS[89] Isoelectric focusing[90]
PI	350	Affinity assays, electrochemical and biochemical analysis[91] Nano-LC-MS[92]

Figure 1.1 illustrates the steps involved in the microfabrication of microfluidic structures using bulk and surface micromachining. Some fabrication steps such as photolithography, etching and thin-film deposition are common to bulk and surface micromachining. The processes used in bulk micromachining are described in detail in the following

paragraphs. The principles and applications of microfabrication using sacrificial materials or thin films for surface micromachining will be described in **Chapter 4**.[93]

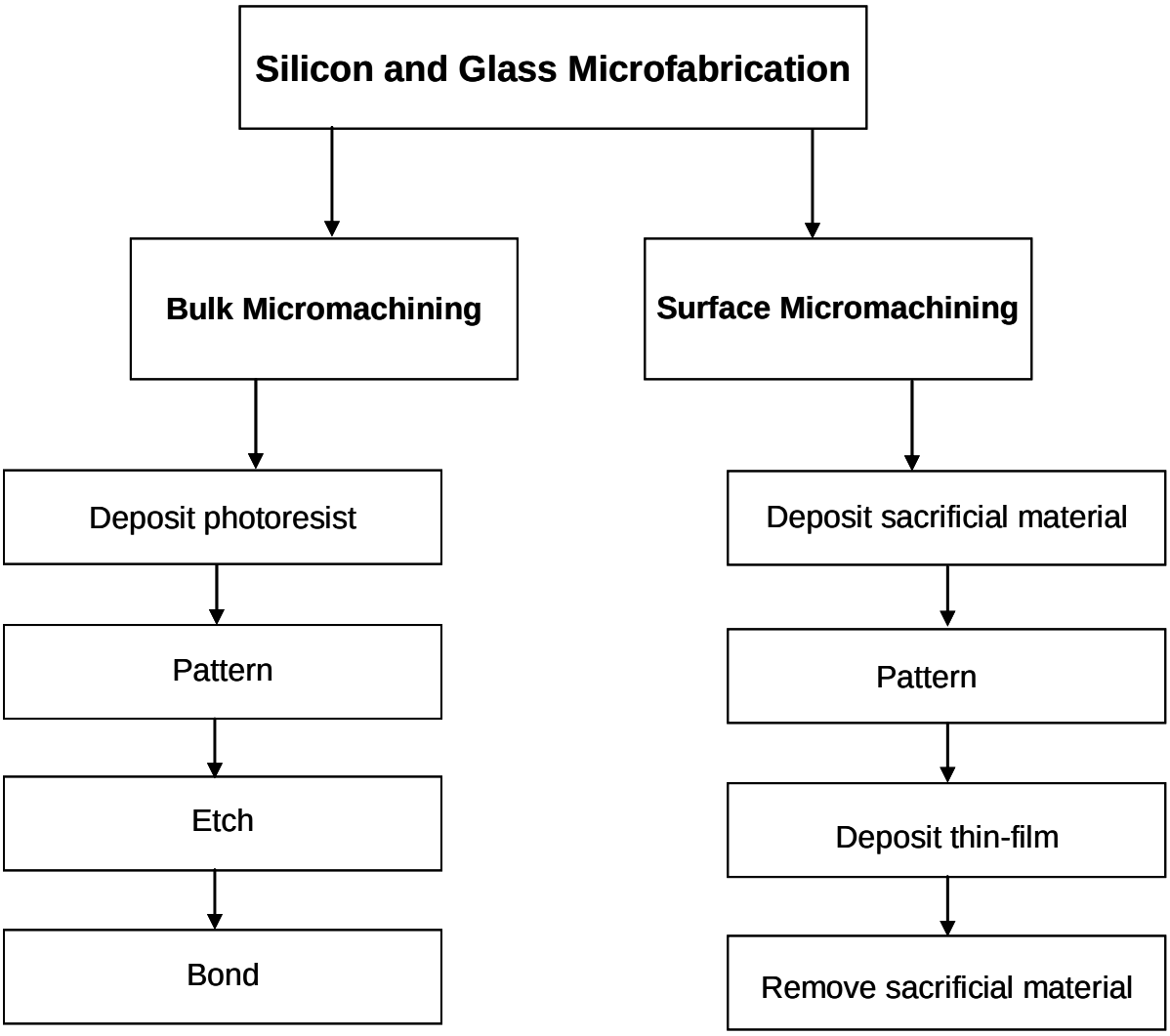

Figure 1.1 Schematic diagram of bulk and surface micromachining of microfluidics.

Photolithography. The process of transferring patterns into a substrate by optical methods is known as photolithography.[30] The general procedure of photolithography is outlined in **Figure 1.2.**

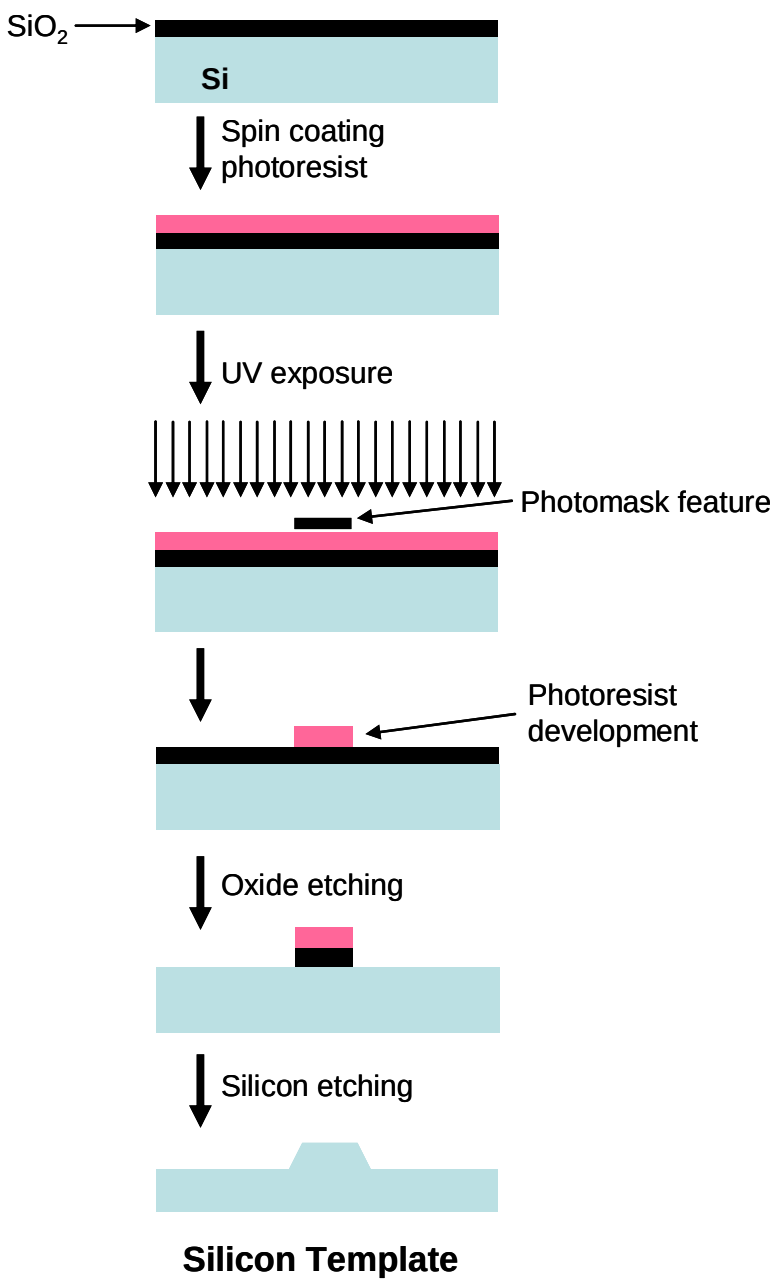

Figure 1.2. General procedure of photolithography (*reprinted with permission from reference 93, copyright 2007, CRC Press*).

The process starts by drawing the features to be transferred to the substrate using a computer-aided design (CAD) program. Patterns in the CAD program are then

transferred to a photomask using a pattern generator. A typical photomask consists of a chromium-covered glass plate.

Prior to the photolithographic process, the substrate must be cleaned to remove organic contaminants or dust particles. Photolithography must be performed in a cleanroom environment because dust particles in the air can settle on the substrates or the photomasks, leading to defects in the final devices.[36] In a cleanroom, the total number of dust particles per unit volume, temperature and humidity must be controlled tightly. The US FED 209B standard classifies cleanrooms according to the maximum allowable number of particles 0.5 μm and larger, per cubic foot (**Table 1.2**).[94] For example, a class 10 cleanroom has a count of 10 particles/ft^3 with diameters of 0.5 μm and larger. Current cleanroom classification is based on the ISO Standard 14644-1.[95] However, the US FED 209E standards are still widely used in many microfabrication facilities.

Table 1.2 US Federal Standard 209B for cleanroom classification.[94]

	Maximum particles/ft³				
Class	**≥ 0.1 μm**	**≥ 0.2 μm**	**≥ 0.3 μm**	**≥ 0.5 μm**	**≥ 5 μm**
1	35	7	3	1	
10	350	75	30	10	
100		750	300	100	
1,000				1,000	7
10,000				10,000	70
100,000				100,000	700

When silicon is used as the substrate, a layer of insulating silicon dioxide must be grown on the surface. This oxide layer is obtained by thermal oxidation in the presence of an oxidant such as oxygen. For photolithography, an adhesion promoter such as hexamethyl disilazane is applied on the substrate to increase the hydrophobicity of the surface and provide a chemically compatible interface for the photoresist.

Following this, a layer of an organic polymer resist is spin coated on the substrate. Spin speed is generally in the range of 1000-10,000 rpm; the thickness of the photoresist layer is correlated with the resist viscosity and spin speed. After the spinning step, the substrate is soft-baked for about 60-120 s at 90-100˚C to remove the solvent from the photoresist and increase resist adhesion to the substrate. Application procedures for photoresist have been studied extensively and optimized for specific applications.[30]

Once a uniform layer of photoresist is applied on the surface, the substrate is aligned with the photomask in an optical lithography system, and the photoresist is exposed to UV light. Depending on the type of photoresist used, the polymer chains are broken (positive resist) or linked together further (negative photoresist), which changes the solubility of the resist in a solvent developer. The exposed areas become more soluble for a positive photoresist or less soluble for a negative resist.[30] After development, the photoresist is left with the pattern from the optical mask. In general, positive resists generate a more clear edge definition than negative resists.[30,96] However, microfluidics with pattern linewidths ranging from 10-100 μm can be defined readily with both positive or negative photoresists.

A related pattern transfer process is the liftoff technique, which is commonly used for defining metal patterns in planar substrates.[97] For this process, a layer of resist is coated on the substrate and photolithographically patterned as described before (**Figure 1.3A-B**). Then, a metal is deposited on the resist, typically by thermal evaporation or sputtering (**Figure 1.3C**), resulting in a metal pattern effectively stenciled through the gaps in the resist. The photoresist in the substrate is normally over developed, resulting in overhangs that define a gap in the metal on the surface (**Figure 1.3C**). Finally, the photoresist is removed, lifting off the unwanted metal and leaving unaffected the metal in the patterned areas (**Figure 1.3D**).

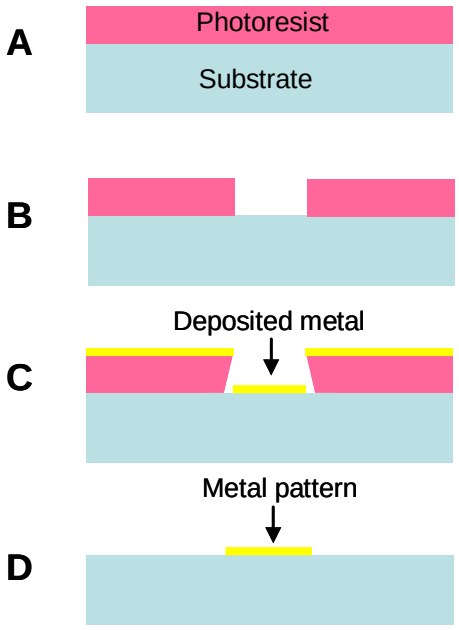

Figure 1.3. Lift-off process.

Etching techniques. The etching step is fundamental in bulk micromachining.[57] It involves the physical or chemical removal of materials in desired areas to permanently establish photolithographic patterns in the substrate. Microstructures such as microchannels, wells, membranes and diaphragms can be fabricated by etching protocols.[98] The two major types of etching are wet and dry etching. Wet etching techniques are generally more broadly accessible and widely used in making microfluidics. Dry etching involves the removal of substrate materials by gaseous reactants without liquid-phase solutions. Compared to chemical etchants, dry etching

provides higher resolution and better fidelity in transfer of resist patterns to a substrate. Dry-etch methods normally use plasma or reactive ion etching.[30,99] Because most of the microfabrication work presented in this dissertation used wet etching, I will focus on discussing this method. A comprehensive review of dry etching techniques can be found in several nano- and microfabrication textbooks.[30,57,100,101]

Wet or chemical etching involves using solutions with appropriate reactants to dissolve the substrate. The solutions used in etching, or etchants, attack the parts of the substrate that are not protected by a masking layer. Importantly, the etching solution must not dissolve this layer, or should at least etch the mask at a much slower rate than the material to be patterned. The basic wet etch process involves (a) diffusion of reactant to the surface, (b) surface reaction (absorption, reaction, desorption) and (c) diffusion of products away from the surface. Crystalline silicon can be etched with strong bases such as KOH, whereas HF solutions are used to etch glass or SiO_2 substrates.[102] Depending on the material, two types of etching are observed, isotropic and anisotropic (**Figure 1.4**).[97]

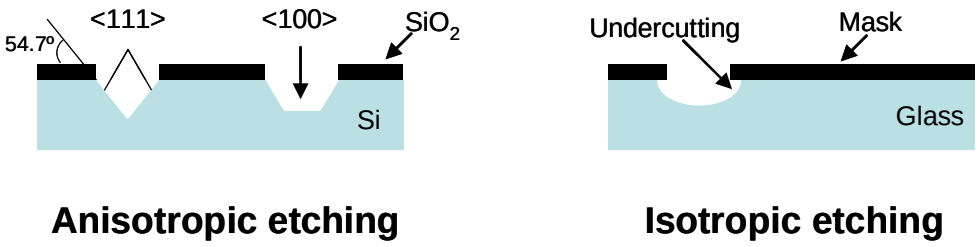

Figure 1.4 Anisotropic and isotropic etching profiles.

Isotropic etching is a process in which the etching of substrate takes place uniformly in all directions.[30,36,103] This etching process produces smooth, rounded microstructures and

is often observed when etching non-crystalline materials such as glass. Isotropic etching is not desirable in applications where the finished geometry of the microstructures must be controlled. In practice, the width of an isotropically etched microchannel will always be at least twice its depth due to undercutting of the mask. Hence, isotropic etching is not an appropriate choice to fabricate high-aspect-ratio microstructures.

In contrast to isotropic etching, anisotropic etching has different etch rates in different directions within the material. The classic example of this is the etching of crystalline silicon in KOH.[104] Silicon has a face-centered cubic unit cell in which single-crystal planes have different orientations. The growth of crystals proceeds at different rates in certain directions, and etching rates also vary. Planes in a crystalline material like silicon are designated by the Miller indices. Three planes in silicon are important in micromachining: <100>, <110> and <111>. Because of the importance of this orientation-dependent machinability, silicon suppliers normally cut wafers along these planes. For some applications, anisotropic etching is preferred over isotropic etching because it allows one to "shape" or micromachine the substrate in one direction much faster than another.[30,104] Some drawbacks of anisotropic etching include limited design freedom in the fabrication of channels with sharp bends and loss of space, since these planes are not generally vertical to the surface for etching holes or cavities.

Bonding techniques. To obtain enclosed, patterned structures in a planar substrate, the assembly of a cover plate is often required.[96] Sealing methods depend largely on the bulk

material used for microfabrication. **Figure 1.5** summarizes the main bonding techniques that have been developed for applications in glass and silicon substrates.[102,105-108]

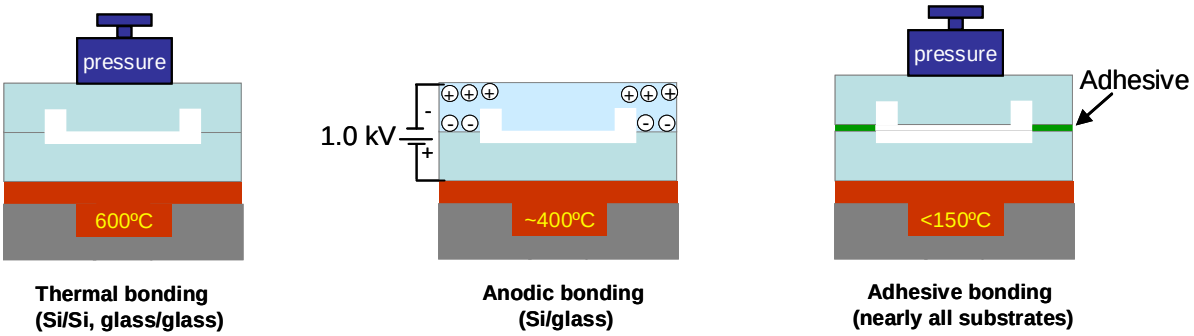

Figure 1.5 Bonding techniques for glass and silicon substrates.

Thermal or fusion bonding is a widely used technique to enclose structures in microchips;[36,105,109] this process can be used to obtain microdevices formed of the same material or different materials. The bonding of glass to glass for example produces well-bonded devices when the sealing is performed at temperatures near 600˚C and under pressure for several hours.[35] Because bonding is accomplished near the softening temperature of the material, the microstructures in the substrates can be distorted readily, compromising device integrity. Thermal stress is also a concern in the case of heterogeneous assembly, since different materials will have different thermal expansion coefficients. Moreover, thermal bonding requires flat, defect-free surfaces and imposes strict cleanliness conditions during bonding. To address these problems with high temperature, low-temperature glass-to-glass bonding techniques have been developed using 1% HF and 1 MPa applied pressure at room temperature.[110] In general, low-

temperature methods give lower device yields and have lower bonding strength compared to thermal sealing.

Anodic bonding uses a high electric field to affix substrates; this process is preferred for bonding glass and silicon.[108,111,112] When a voltage is applied across a glass-silicon sandwich at a temperature close to 450˚C, ions diffuse through the glass surface, creating a space-charge region which leads to a strong electrostatic attractive force between the two surfaces. This method does not require highly polished surfaces, and bonding can be effected in the presence of asperities up to 1 μm tall. Typical bonding times are 10 to 30 min, considerably shorter than thermal bonding. Anodic bonding also allows the formation of multilayer glass/silicon/glass structures in a single bonding step. However, bonding of two silicon or glass pieces together is only possible with prior deposition of silicon nitride or oxide films between the surfaces being affixed.[113]

Adhesive bonding uses a polymeric intermediate layer to attach two pieces together.[106,107,114] In this method, a thin film of adhesive polymer is coated on one of the substrates being bonded, and the second piece is held in contact with the adhesive-coated surface to effect bonding. Adhesive bonding offers some advantages compared to fusion and anodic bonding. The process is performed at temperatures generally below 150˚C and does not require extensive cleaning procedures, since the adhesives are normally "soft" materials that can conform to particles on the surface without compromising bonding quality. Drawbacks of this bonding technique include limited thermal range and stability, and the introduction of a new material (the adhesive layer) between the bonded

pieces, which may be undesirable in applications where control of surface properties is critical.

1.1.2.4 Polymer microtechnology

Fabrication of plastic microdevices uses a variety of techniques. Manufacturing methods can be divided into two areas: (1) direct fabrication and (2) replication.[48,115] Direct techniques include laser ablation and mechanical machining. The use of these protocols is restricted because the linewidths obtained are wide (~100-500 μm), and the surfaces are normally too rough to perform high-efficiency microfluidic separations. Due to these reasons, only replication techniques will be discussed herein.

Table 1.3 Overview of polymer replication techniques. *Adapted from Becker et al.*[115]

Process	Materials	Cost	Cycle time	Force/Temp	Geometry	Minimum dimensions
Hot Embossing	Thermoplastics	Low-medium	3-10 min	High (kN)/~T_g (100-200˚C)	planar	Sub-10 nm
Injection moulding	Thermoplastics	high	0.3-0.3 min	High (>kN) /above melting (150-400˚C)	Planar-spherical	10 μm
Casting	Elastomers	low	Min-h	No forces/25-80˚C	planar	~ 10 nm

Replication methods include injection molding, casting, and embossing (**Table 1.3**); these fabrication techniques had been used in the plastic industry for many years before microfluidics were developed. All replica methods use a replication mold or master with the inverse shape of the desired structure, from which copies in the polymeric material can be made. Approaches for master fabrication vary from conventional milling[50] to

highly sophisticated lithography processes such as those used for the fabrication of microchips in inorganic materials.[54,87,116,117] Unlike glass micromachining that requires cleanroom conditions during fabrication, polymer microchips can be made using replication techniques in a research laboratory environment, provided a mold is available. Indeed, one of the main advantages of replica molding microfabrication is the possibility of mass production of many microdevices from the same template.

Casting. Also known as "soft lithography", casting of microfluidic structures was introduced over ten years ago[118] and today is one of the most frequently used replication techniques.[46,47,54,79,119,120] Microdevice fabrication involves pouring a prepolymer solution formed by a two-component mixture of monomer and cross-linking agent directly on a photolithographically fabricated silicon or SU-8 master. The most common material used in soft lithography is a mixture of PDMS and curing agent, commercially available as Sylgard 184 from Dow Corning. PDMS is an attractive substrate in microfabrication due to its optical transparency down to ~230 nm and ease of integration with macro-scale components.[79] After curing at room temperature for about 48 h or at 100˚C for 45 min, the PDMS elastomer is peeled away from the mold and sealed to a flat surface to enclose the microstructures in the PDMS replica.[47] Patterned PDMS sheets can be sealed reversibly to a variety of materials including glass or another PDMS slab. Bonding strength of PDMS microdevices can be improved using an oxygen plasma to create covalent Si-O-Si bonds between PDMS and a glass, Si or PDMS surface. **Figure 1.6** depicts the casting process of PDMS using a photolithographically patterned and etched silicon template.

A primary advantage of PDMS casting is the ease of implementation, even for laboratories without sophisticated instrumentation or cleanroom capabilities. Moreover, a single mold can be used to make several casts. Finally, this technique facilitates the formation of three-dimensional devices by successive stacking of PDMS layers.[121]

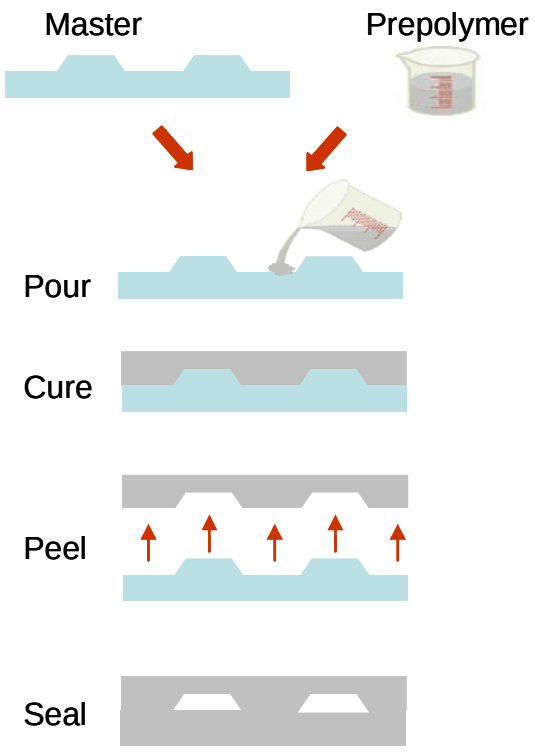

Figure 1.6. PDMS casting using soft lithography.

Chiu et al.[122] have explored the use of thermoset polyester (TPE) to fabricate microfluidic devices using a process similar to soft lithography. Compared to PDMS, TPE casting presents both advantages and disadvantages. For example, TPE is transparent in about 90% of the visible spectrum; it is a hard material and is compatible with nonpolar solvents such as cyclohexane, n-heptane and toluene.[122,123] On the other hand, connecting TPE with macro-scale components is difficult compared to PDMS.

Hot Embossing. The transfer of the patterns from a master surface, for example a silicon template, into a formable material such as a thermoplastic polymer is known as hot embossing.[54,116,124-126] This technique is easy to implement and does not require complicated instrumentation (except for the fabrication of the template). **Figure 1.7**

shows a schematic of the hot embossing microfabrication process using an etched silicon template for imprinting a microchannel into a PMMA piece.

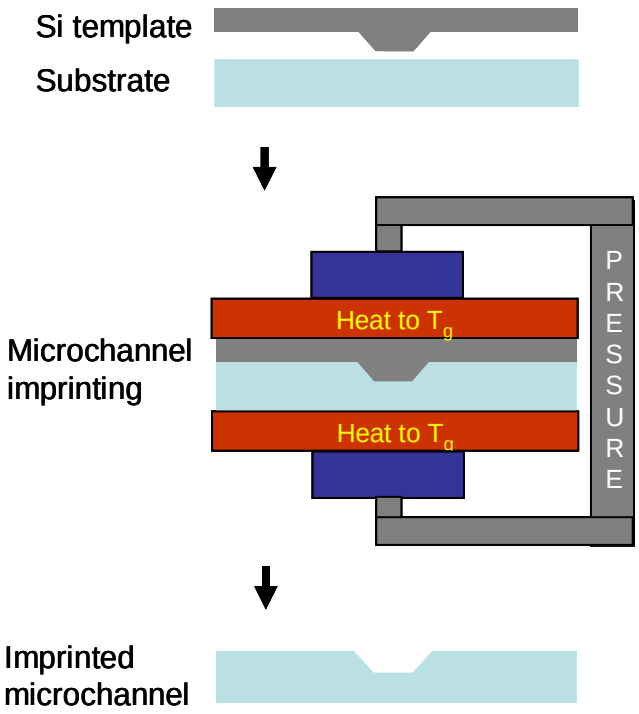

Figure 1.7 Hot embossing (imprinting) procedure.

The master and polymeric substrate are heated above the T_g of the polymer under applied embossing pressure. After an optimized embossing time, the template-substrate assembly is removed from heat and cooled. To obtain higher resolution and fidelity in the pattern transfer process, cooling is preferably done while the silicon template and polymer substrate are still in contact.

Hot embossing has been used in the fabrication of microfluidic chips for years.[59,116,126-128] The embossing conditions (temperature, pressure and time) can be optimized for specific substrates; some examples include microchips in PMMA, PC, and COC. The main advantages of hot embossing are the ability to mold small structures, and the good replication accuracy since a phase change is not involved. Moreover, depending on the master material, a single template can be used to fabricate multiple devices with good reproducibility.

Injection molding. One of the most common methods of shaping polymer substrates is a process called injection molding.[55,58] Injection molding is accomplished using relatively large machines (**Figure 1.8**).

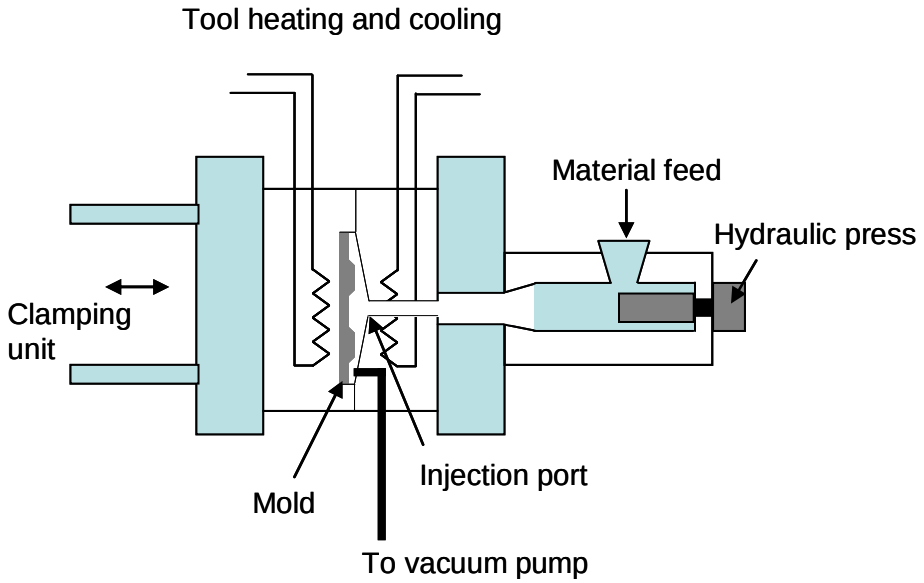

Figure 1.8 Schematic representation of an injection molding machine.

Using this technique, it is possible to generate structures having almost any geometry from a variety of thermoplastic polymers. Briefly, the process consists of injecting the melted substrate under high pressure into an evacuated cavity containing a master that shapes the material appropriately. Typical molds are made of either steel or aluminum, and are precision-machined to form the features of the desired part. After cooling, the polymer solidifies and the formed structures are removed from the mold. The injection molding technique has been utilized in the fabrication of microfluidic devices.[58,129,130] Microstructures can be fabricated with integrated components such as optical fibers or metal wires. The wide use of injection molding in microfluidics research is limited by the costs associated with complex instrumentation and fabrication of metal molds.

Bonding of polymer microfluidics. Microfabricated structures in polymeric microchips need to be sealed to complete the fluid conduits. Several methods have been explored for bonding of cover plates to substrates, including thermal and solvent bonding.

Similar to glass microdevices, polymeric microchips can be thermally bonded to create microcapillaries. The standard thermal bonding method involves heating a patterned substrate and cover plate to near the T_g of the material under applied pressure.[61,116] Alternate approaches have used heated weights[131] or boiling water.[125] Thermal bonding is attractive for enclosing polymer microchips because is easy to implement, does not require sophisticated instrumentation and can produce microstructures composed of one material.[48,49,114,132,133] However, the use of elevated temperature and pressure during bonding represents a challenge since the microstructures in the substrate can be distorted readily during this step, limiting the success rate. In addition, thermally bonded microdevices are sealed weakly and can be delaminated with <200 psi internal pressure.[62]

Unlike thermal enclosure, solvent bonding does not require temperature to effect bonding. Briefly, polymeric surfaces to be bonded are wetted with an organic solvent, which partially dissolves the polymer at the surface. When the two pieces are brought together under lightly applied pressure, interdiffusion and entangling of the polymer chains in both surfaces forms a high-strength bond.[134-136] In recent years, the use of solvent bonding to fabricate polymer microfluidic devices has increased tremendously.[51,126,132,137,138] In general, solvent bonding produces more robust and

strongly enclosed devices compared to thermal bonding. However, microchannels can be blocked during bonding by dissolved polymer, or swelling or softening of the substrate.

The method developed by Kelly et al.[62] used a sacrificial material to protect microchannel integrity during solvent bonding. Paraffin wax was introduced in the microchannels before solvent-assisted bonding of PMMA to prevent the solvent from dissolving and deforming the polymeric microstructures. At the end of the process the sacrificial paraffin wax was removed by melting it and rinsing with a solvent (e.g., hexanes). The resulting devices could withstand pressures of at least 2,200 psi and electric fields of >1,500 V/cm. These microdevices were used to perform high-efficiency electrophoretic separation of amino acids and peptides.

Other approaches have been explored for sealing plastic microfluidic devices, including adhesive bonding,[139-141] thermal lamination,[58] and resin-gas injection.[142] These methods produce robust microdevices and are relatively easy to implement. However, in most cases they lead to microchannels with walls composed of different materials, which result in an inhomogeneous zeta potential and potentially poor separation efficiencies.[143]

1.1.2.5 SU-8 micromachining

SU-8 is an epoxy-based negative photoresist.[144,145] SU-8 can be patterned by photolithography[146] and has been adopted thereby as a structural material for the fabrication of microfluidic chips for separations[147] and multilayer systems.[148] Many features make SU-8 an attractive material for microfabrication: SU-8 is optically

transparent to near UV and visible light, and SU-8 can be integrated easily with additional components in microfabricated structures. Recently SU-8 has gained interest for the fabrication of patterns for soft lithography,[119] hot embossing and solvent imprinting of microstructures in microchannels.[149] In contrast to other materials such as silicon, SU-8 templates can be fabricated with sharp turns. Fabrication of SU-8 templates does not involve etching and, thus the height of the features on the template depends only on the thickness of the SU-8 layer patterned.

1.2 CHIP-BASED CAPILLARY ELECTROPHORESIS

Initial interest in miniaturization was driven by the desire to reduce costs by using less sample and reagents, while increasing separation speed and throughput. For years, most developments in μTAS have focused on transferring widely accepted analytical techniques such as chromatography and electrophoresis to a microchip format.

Pumped flow and separations are perhaps the most widely exploited microfluidic applications. The most common flow pumping mechanism implemented to date has been electroosmosis, using an electric field to generate bulk flow in a conducting liquid.[15] Not surprisingly then, electrically driven separation methods have been utilized in most on-chip separations.[29,37,150,151]

1.2.1 From capillaries to microchannels

Capillary electrophoresis (CE) is one the most versatile separation techniques in bioanalytical chemistry.[152,153] CE describes a family of electrically driven methods used to separate a variety of large and small molecules in an electric field in a narrow tube.[10] The electric field causes charged molecules to migrate toward the opposite pole and separate from each other based on their charge to viscous drag ratio.[154] CE is recognized as a high-efficiency separation technique, because of the high electric field and flat electroosmotic flow profile. This contrasts with pressure-driven flow, such as in HPLC, in which frictional forces at the column walls lead to a parabolic or laminar flow profile. In addition, CE requires only small amounts of sample, and can be automated easily.

In principle, CE can separate only charged analytes; however, there are a number of operation modes that increase the versatility of CE. **Table 1.4** lists the most commonly used modes of CE and their applications.[154] Microchip electrophoresis (μCE), which can be considered a scaled-down version of conventional CE, was first demonstrated by Harrison et al.[35] Today, all the modes of CE described in **Table 1.4** have been transferred to microchips.[15,19,23,37] Typical μCE devices consist of microstructures embedded into a glass or polymer substrate, ranging in design from a single injection and separation channel to more complex platforms for capillary arrays,[155] two-dimensional separations,[50,156] sample treatment,[157] pre- and post-column reaction,[158,159] and multilayer systems,[160] among others.[37]

Chip-based CE has several advantages over bench-top counterpart systems. For example, it can speed up analysis while reducing reagent and waste stream volumes. Sophisticated sample-processing and analysis functions can also be carried out in an automated fashion. Moreover, because of the small dimensions of microfabricated channels, high electric fields can be applied to improve separation efficiency. Finally, Joule heat dissipation is more effective in micrometer-dimension channels. Indeed, these features make μCE an attractive technology for the next generation of CE systems.

Table 1.4 Different modes of capillary electrophoresis.

Mode	Basis of separation	Applications
Capillary zone electrophoresis (CZE)	Differences in the charge-to-mass ratio in free solution mobility	Separation of small and large charged analytes
Micellar electrokinetic chromatography (MEKC)	Hydrophobic/ionic interactions with micelle	Separation of neutral molecules and very hydrophobic compounds
Capillary gel electrophoresis (CGE)	Size (sieving) and charge	Denaturing gel molecular weight analysis of proteins; DNA sizing, sequencing and genotyping
Isoelectric focusing (IEF)	Isoelectric point in a pH gradient	Amphoteric molecules, determination of a protein's isoelectric point
Capillary electrochromatography (CEC)	Differential interaction of electrically driven solutes with a stationary phase	On-line concentration and high-efficiency separations

1.2.2 Theory of μCE

Microscale analytical systems have distinctive properties as a result of their small dimensions. Miniaturization is more than simply scaling down well-understood macrosystems. For example, because of the lack of turbulence, liquid flow is normally

laminar; moreover, properties such as surface tension and viscosity which have little effect in macro-systems become important in miniaturized devices.[161] Nevertheless, theoretical aspects of μCE systems are similar to those of conventional CE and will be discussed in the next paragraphs.[154,162]

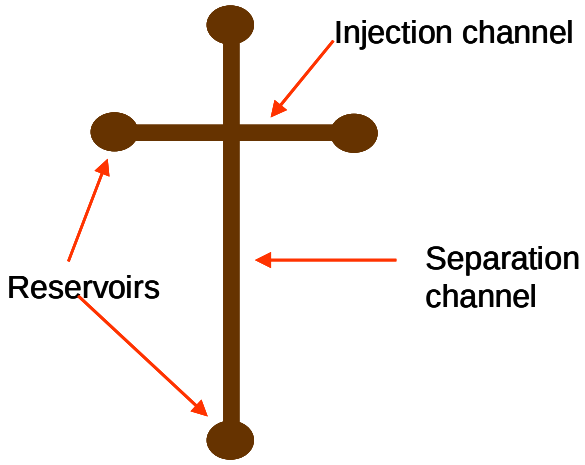

Electrophoretic separations in microchips are performed in microfabricated channels having wells at the ends, which serve as reservoirs. The simplest layout of a microchip consists of a cross structure as shown in **Figure 1.9.**

Figure 1.9. Layout of a CE microchip.

When a voltage is applied to a buffer-filled microchannel, charged analytes move toward the electrode of opposite polarity. The velocity of an ion in an electric field is given by:

$$\nu = \mu_e E \qquad (1.1)$$

where:

ν = ion velocity

μ_e = electrophoretic mobility

E = applied electric field

The mobility of a given ion in a medium is characteristic of that ion and depends on the

degree of dissociation, which is influenced by the pH of the solution. A particle with charge (q) is accelerated in an electric field by an electric force (F_e) given by:

$$F_e = qE \qquad (1.2)$$

The frictional force (F_f) on a spherical ion (radius = r) as it passes through a medium of viscosity, n , with velocity, ν , is given by:

$$F_f = -6\pi n r \nu \qquad (1.3)$$

During electrophoresis, these forces are equal in magnitude, but opposite in direction. Combining the two equations, the electrophoretic mobility of an ion is thus given by:

$$\mu_e = \frac{V}{E} = \frac{q}{6\pi n r} \qquad (1.4)$$

In equation (1.4), *V* is the applied voltage. It is clear that small, highly charged molecules will have greater mobilities compared to large and minimally charged species.

Unlike in pressure-driven chromatographic methods, fluid motion in electrophoresis relies on electroosmotic flow (EOF).[152] The surface of silica-based capillaries contains negatively charged weakly acidic silanol groups. Therefore, when a capillary is filled with a buffer solution, the negatively charged capillary wall attracts positively charged

ions from the buffer, forming a double layer of ions near the surface and a potential difference known as the zeta potential.[163] When a voltage is applied across this capillary, the cations within the double layer are attracted to the cathode. This overall movement of solvated ions carries the bulk solution along and is called electroosmotic flow.[164] An important benefit of EOF is that it causes movement in the same direction of nearly all species, regardless of charge. Normally, EOF goes from anode to cathode; however, anions can also move toward the cathode when the magnitude of the EOF is greater than the electrophoretic mobility of the anions. **Figure 1.10** depicts the migration of ions under an applied electric field in a buffer-filled capillary. Cations migrate fastest due to their attraction towards the cathode, while neutrals migrate faster than anions under EOF, but are not separated from each other.

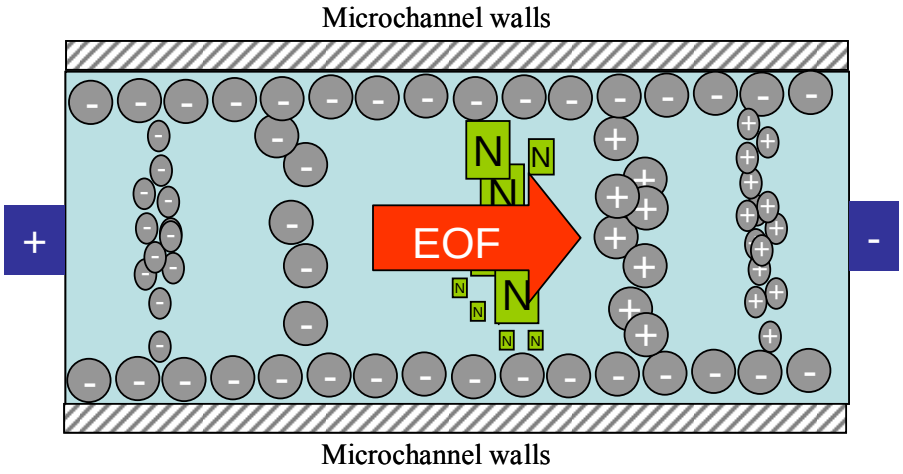

Figure 1.10. Solute migration under EOF.

1.2.3 Microchip CE analytical parameters

The analytical parameters for μCE can be described in terms of those used for column chromatography and electrophoresis.[152,154] The time required for a solute to migrate to the

point of detection is called the migration time. Solutes are separated electrophoretically due to differences in their mobilities. Under ideal conditions, analytes should travel along the microchannel with different speeds, forming narrow and well-defined zones; however, differences in solute velocities within a zone result in analyte dispersion, which translates into band broadening. For a Gaussian peak, the baseline width (W_b) can be expressed as:

$$W_b = 4\sigma \tag{1.5}$$

where σ is the peak standard deviation (in time, length or volume). The efficiency (N) in terms of theoretical plates in a separation microchannel can be expressed as:

$$N = (\frac{l}{\sigma})^2 \tag{1.6}$$

where (l) is the effective microchannel length measured from the injection intersection to the detection point. The efficiency can also be expressed in terms of molecular diffusion based on the diffusion coefficient of the solute (D).

$$\sigma^2 = \frac{2DlL}{\mu_e V} \tag{1.7}$$

In equation (1.7), L is the total length of the microchannel. Substituting equation (1.7) into equation (1.6), the number of theoretical plates in μCE can be expressed as:

$$N = \frac{\mu_e V}{2D} \qquad (1.8)$$

From equation (1.8), it is clear that high voltages benefit separation efficiency; this equation also shows that molecules with low diffusion coefficients (e.g., biomacromolecules) will have less dispersion compared to small molecules.

In addition to dispersion, other parameters affecting efficiency are: (i) Joule heating, (ii) injection plug length, (iii) solute interaction with microchannel walls, (iv) detector width, and (v) electrodispersion (for example, mismatched conductivities of sample and buffer).

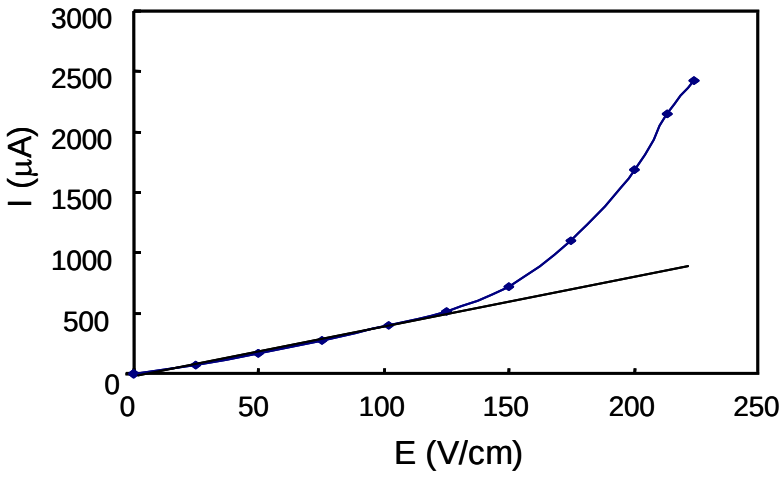

Figure 1.11. Current vs. voltage relationship in the presence of Joule heating (adapted from Schasfoort and Tüdos[162]).

The heat generated by the passage of current through a capillary filled with a conductive medium is called Joule heat.[165] Under optimal conditions (without Joule heating), the current vs. voltage relationship in a buffer-filled capillary should be linear. When Joule heating is present, the increase in temperature raises the solution conductivity, causing the current to increase more rapidly as a function of potential (**Figure 1.11**).

The Joule heat generated per time unit (Q/t) can be expressed in terms of the applied potential (V), the solution conductivity (λ) and the radius of the capillary (r):

$$Q/t = \frac{V^2 r^2 \pi \lambda}{L} \qquad (1.9)$$

Equation (1.9) shows that reducing the applied voltage or avoiding high-conductivity buffers can lower Joule heating. However, the best approach to reduce Joule heat is to use a small capillary diameter. Importantly, short lengths and small diameters of microfabricated channels can dissipate Joule heat more effectively than conventional capillaries; thus, higher electrical fields can be applied, potentially yielding greater separation efficiencies.

1.2.4 Operation of CE microchips

Microchip CE injection is achieved by applying a voltage across the injection channel, and then switching the voltage to the separation channel to inject and separate the sample plug at the microchannel intersection (**Figure 1.9**). This injection mode allows for the loading of narrow, well-defined sample zones, which can significantly reduce the distance required for adequate separation and resolution. The separated solute bands are then detected at the end of the separation channel.

In any separation technique, the injection of reproducible and well-defined sample plugs is critical to performance. In addition, sample introduction in microfabricated devices requires the injection of picoliter-volume plugs to avoid channel overloading and deteriorated separation performance.[166,167] Sample injection in microfluidics can be

performed using EOF (electrokinetic injection)[168] or pressure (hydrodynamic injection).[169] Each method has advantages and disadvantages; however, since electrokinetic injection is used more commonly in microfluidics, only EOF-based injection approaches will be discussed here. In general, electrokinetic methods require no moving parts, are easy to integrate, and are compatible with the voltages used during separation. Some drawbacks of these methods include possible sampling bias during injection and susceptibility to pH and EOF changes.

Cross injection is the most simple and common loading mode used in microfluidics.[35,105] A schematic representation of a cross injector is shown in **Figure 1.12**.[105]

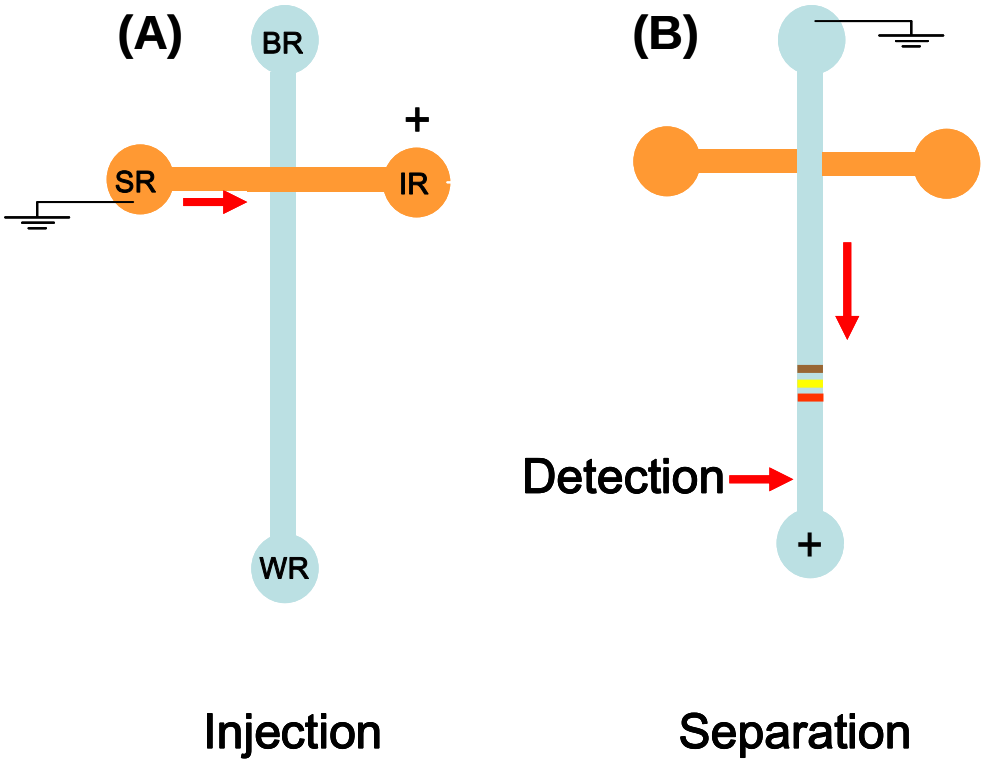

Figure 1.12. Schematic representation of a cross injector.

First, the microchannels are filled with separation buffer, and sample is loaded into the sample reservoir (SR). For injection, a voltage is applied across the injection channel, which drives the sample from the SR to the injection reservoir (IR, **Figure 1.12A**) while the buffer reservoir (BR) and waste reservoir (WR) are floating. Next, a potential is applied across the separation channel, causing the sample plug at the microchannel intersection to move towards the WR, during which separation and detection of analytes takes place (**Figure 1.12B**).

A similar approach, double-T injection, uses the same voltages and control inputs of a cross injector with a modified chip layout at the microchannel intersection (**Figure 1.13**).[16,43,170] This configuration allows better control of the sample plug length compared to cross injection but suffers from sample leakage from the injection channel into the separation channel, which is mostly due to convection and diffusion.[102]

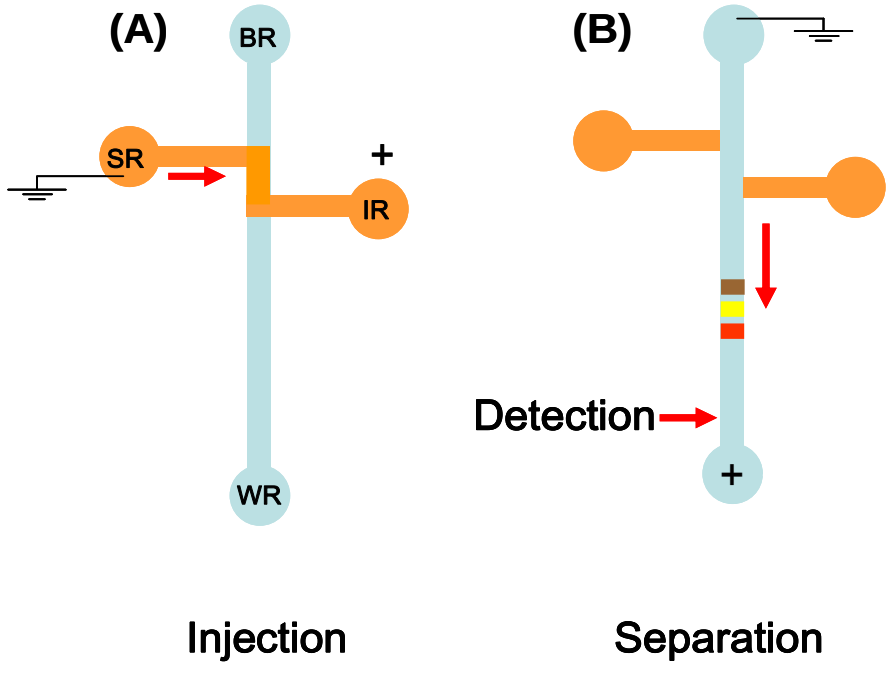

Figure 1.13. Schematic representation of a double-T injector.

Pinched injection was proposed by Jacobson et al.[105] in 1994 to improve sample plug definition and to address the problem of sample leakage into the separation channel. A schematic representation of the pinched injection mode is depicted in **Figure 1.14**.[171-173] Briefly, negatively charged analytes are driven electrokinetically from the SR to the IR by applying an elevated voltage in the IR while the other reservoirs are grounded (**Figure 1.14A**). For separation, a potential several-fold higher than the injection voltage is applied to the WR, the SR and IR are kept at the injection voltage, and the buffer reservoir is grounded (**Figure 1.14B**). The potential applied to the SR and IR prevents sample diffusion into the separation channel during injection, causing only the sample present in the channel intersection to be loaded into the separation channel.

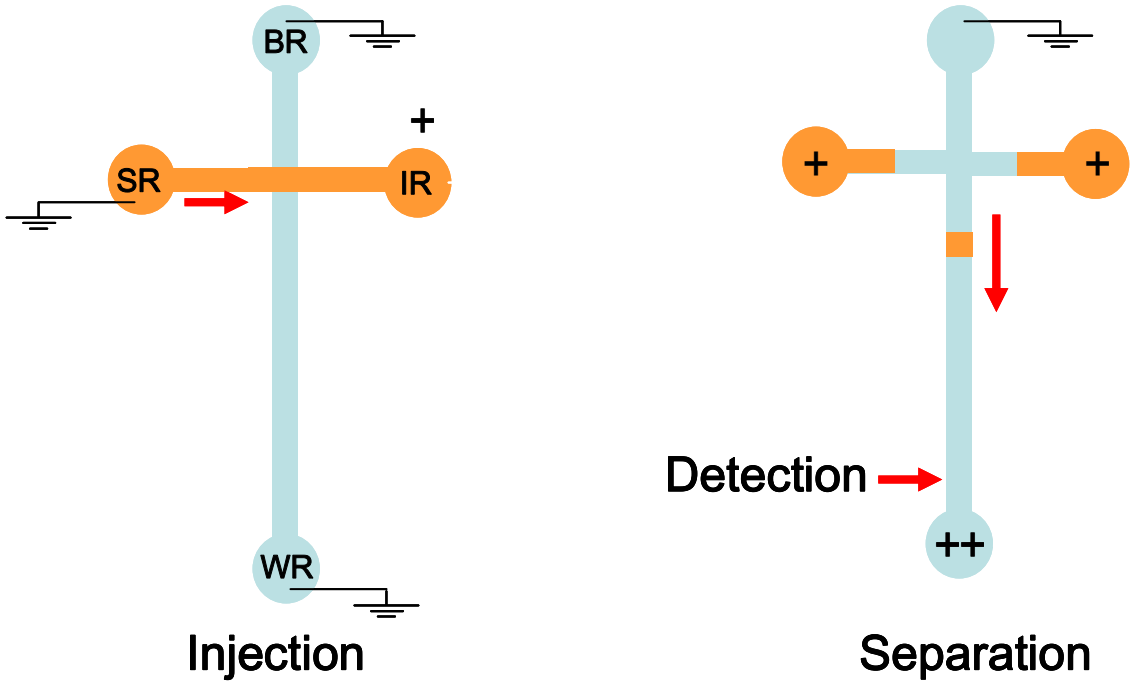

Figure 1.14. Schematic representation of the pinched injection approach. ***(Reprinted with permission from reference 93, copyright 2007, CRC Press*****).**

Detection methods. Detection in microfluidic devices presents a significant challenge due to the small dimensions of the microchannels and the amount of sample injected.[162] A number of detection methods, including optical, electrochemical and mass spectrometry techniques have been implemented to meet these challenges, and several reviews discuss the principles and applications of these approaches.[174-177]

Optical detection methods used in microfabricated devices include UV-visible absorption, chemiluminescence and laser induced fluorescence (LIF). These methods are attractive for microfluidic applications because no connections are required between the detector unit and the microfluidic device, which reduces zone broadening due to dead volume. A key problem with optical detection in microfluidics is the relatively poor limit of detection (LOD), due to the short optical pathlengths of microfabricated channels.

UV-visible absorbance is used widely in analysis techniques due to its nearly universal applicability. UV detection has been used in glass μCE devices,[178,179] but has seen little application in polymeric microchips because many polymer substrates readily absorb UV light. LIF is a technique with very low limits of detection (LOD), that can be incorporated in microchips. Indeed, LIF is the dominant detection method used in microfluidics.[102,174,176] Although few analytes have native fluorescence, non-fluorescent species can be derivatized with fluorescent dyes and detected using LIF. Some reagents used for this end include: *o*-phthaldahyde/?-mercaptoethanol[180] naphthalene dicarboxylaldehyde[181] and fluorescein isothyiocyanate (FITC).[62,114] Typical detection limits in LIF range from 10^{-10} to 10^{-12} M; moreover, with confocal epifluorescence,

subpicomolar detection levels have been achieved in a microchip.[182] Indeed, researchers have even reported detection limits down to a single molecule.[103,183] One disadvantage of LIF is the need for bulky instrumentation that reduces the advantages of miniaturization and limits portability. This issue has been addressed in part by Webster et al.[184] who integrated a light-emitting diode with a silicon photodiode in a microfabricated chip, eliminating the need for an external laser source or photodetector. **Figure 1.15** shows a schematic diagram of a confocal LIF system.

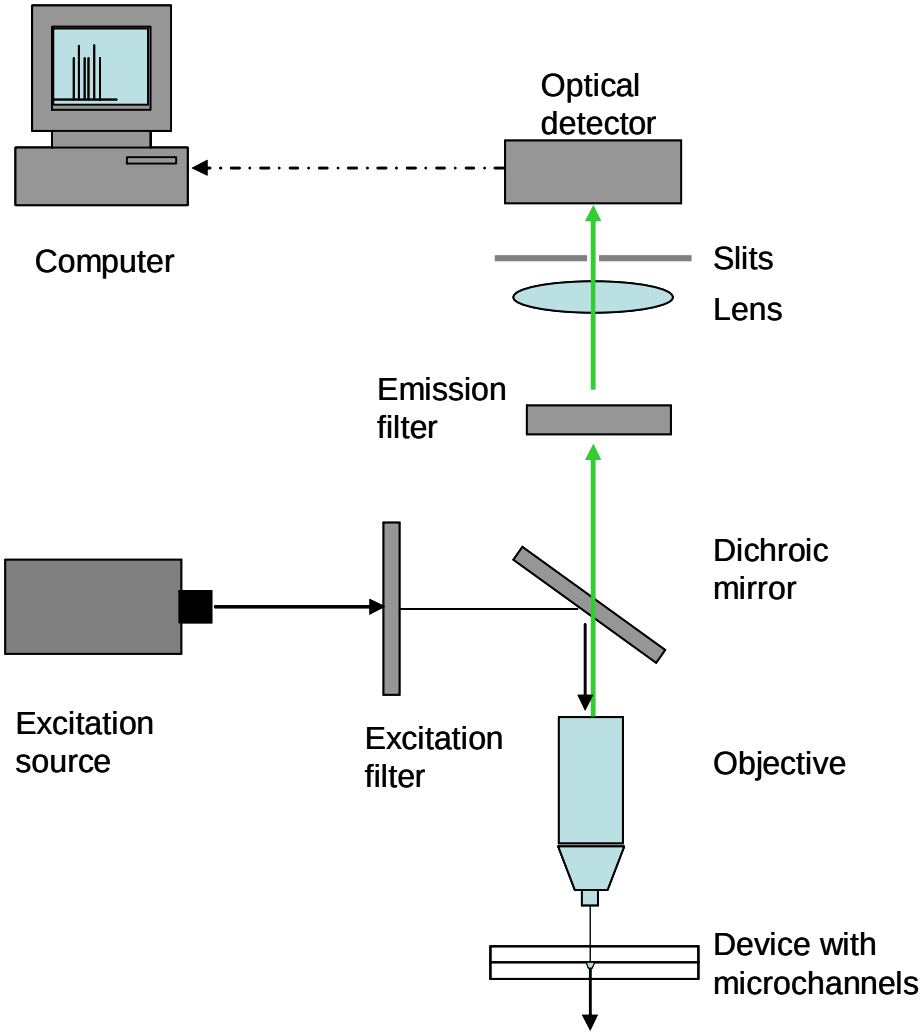

Figure 1.15 Schematic diagram of a confocal LIF system.

The three basic modes (amperometry, conductimetry and potentiometry) of electrochemical detection (ED) have been implemented in microchips.[174-176,185] The use of ED in microfluidic devices is attractive for several reasons. First, many compounds can be detected selectively and in low concentrations without derivatization.[186,187] Second, ED can be integrated easily in the microchip format because the electrodes can be microfabricated using photolithography techniques. Third, the background current generated is very small, leading to an increased signal-to-noise ratio and potentially lower LOD.[188,189] Finally, the reduced dimensions of microfabricated electrodes generally result in faster response times compared to conventional ED.[190,191] A major drawback of amperometric ED is the requirement that analytes be oxidized or reduced under the analytical conditions. Moreover, in microfabricated devices, the high voltages used for separation can potentially interfere with the detection electrodes. Some approaches to overcome this problem include end-channel detection, in which the working electrode is placed beyond the end of the separation channel,[192,193] or the use of a decoupler to ground the separation voltage before it reaches the detector.[194]

Mass spectrometry (MS) detection has been used with microfluidic devices for more than a decade.[195] Microchips are normally coupled to mass spectrometers via electrospray ionization interfaces.[64,196] Polymeric microdevices made of PMMA,[64,65] PDMS,[72] and PC[197] have been used for MS analysis of a variety of species, including small molecules[87] and proteins.[65] In recent years MS detection in microchips has been bolstered by the need to obtain structural information for proteomic studies.[198,199]

Other detection methods used in microfluidics include infrared absorbance,[44] Raman scattering spectroscopy,[200] and nuclear magnetic resonance.[201] Viskari and Landers[177] have published a review of unconventional detection methods for microfluidic devices.

The advances presented so far in miniaturized CE separations demonstrate that μCE is today an expanding and developing field, which is expected to continue to grow over the years.[37,202,203] However, as the demands for new analytical tools in the areas of proteomics, life sciences, pharmaceuticals and biomedicine increase, many challenges in design, integration and functionality arise for microfluidic systems. Some of these challenges are discussed next.

1.3 FUTURE TRENDS AND CHALLENGES IN MICROFLUIDICS

The number of papers on microfluidic applications has grown tremendously in the last decade (**Figure 1.16**),[37,109,204] and several companies have been established to commercialize products based on microfluidic applications (**Table 1.5**). Most of the developments in miniaturization so far have focused on discrete components such as microchannels, microvalves, micropumps, and electrochemical sensors. However, total integration is critical to realize true μTAS devices. A review of the current literature shows that a large amount of work in microfluidics has been directed to the development of chip-based platforms with integrated functional modules.

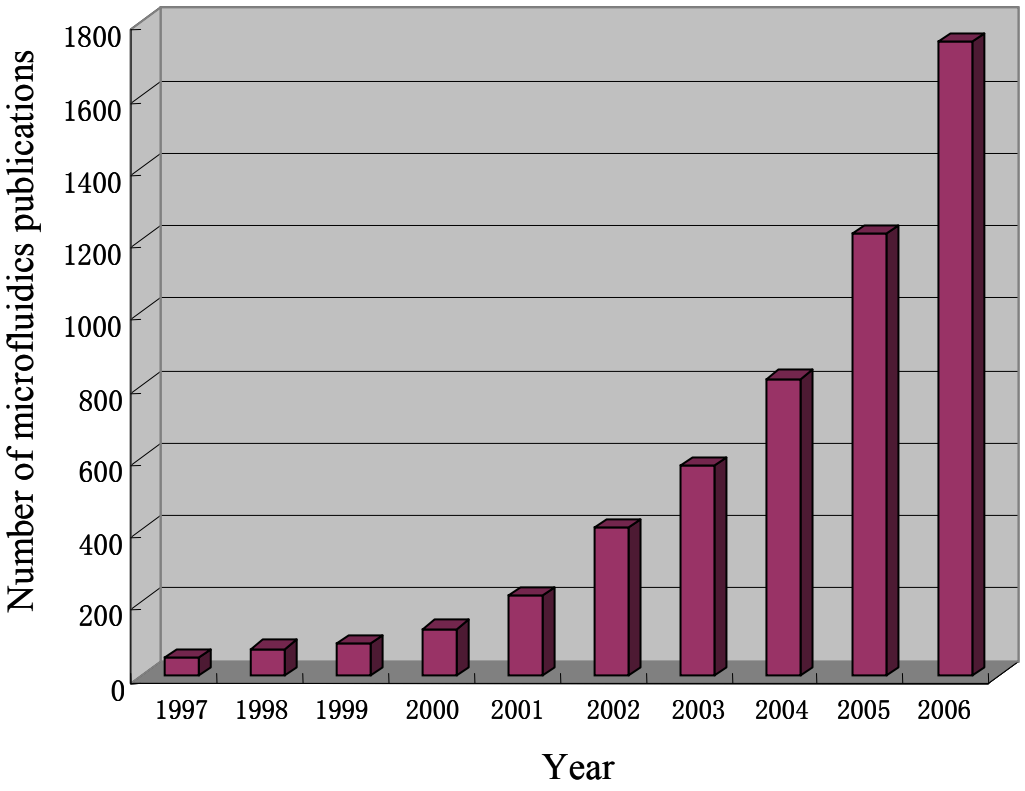

Figure 1.16 Growth of microfluidics literature in the last 10 years. (*Adapted from reference 204*).

Table 1.5 Selected companies commercializing microfluidic applications.

Company	Application	Website
Caliper	Tools for life science research	http://www.caliperls.com/
Agilent	2100 DNA bioanalyzer	http://www.chem.agilent.com/
Nanostream	Parallel micro-LC	http://www.nanostream.com/
Eksigent	Nano-HPLC	http://www.eksigent.com/
Micronit	Glass CE microchips	http://www.micronit.com
Nanogen	DNA and RNA analysis	http://www.nanogen.com/
Epigem	Microfabrication	http://www.epigem.co.uk
Dolomite	Microfluidic applications	http://www.dolomite-centre.com/

Figure 1.17 shows the concept of a fluidic analytical microdevice in which many functions including sampling, mixing and separation can be performed simultaneously in a planar platform.[205]

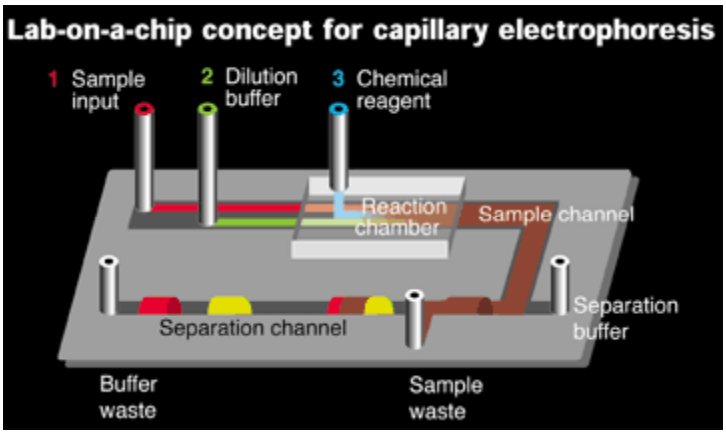

Figure 1.17. The lab-on-a-chip concept (*reprinted with permission from reference 205, copyright 1999, American Chemical Society*).

Chip-based analytical devices must be able to provide reliable data that meets current quality assurance requirements in analytical laboratories. Thus, more effort is required to implement aspects such as validation, calibration and method development in microfluidic devices. One of the main challenges to obtain an integrated and functional μTAS device is sample preparation. This becomes more critical if one considers the complexity of samples such as biological fluids. Even with preprocessed samples, the problem of how to get samples into the chip remains. This issue is often called the world-to-chip interface.[166,203] Microfluidic chips have micrometer-dimension channels and are usually a few millimeters thick, which makes most conventional coupling techniques unrealistic. In addition, samples usually are present in much larger volumes than the

nanoliter-range that microchips can handle. In the same way, manipulation of nanoliter volumes with conventional sample preparation protocols is impractical. Thus, new coupling methods that are compatible with the chip size need to be developed to address these problems.

In general, microfluidic devices must be able to manipulate μL to pL volume flows in micron-scale conduits. Flow control in microdevices is achieved through a combination of active and passive components including micropumps, valves, microchannels, reaction chambers, mixers, filters, microsensors and others. Any pumping actuation mechanism must be compatible with the separation and detection schemes in the chip. Currently, most microfluidic devices utilize electrokinetic pumps based on EOF. Unfortunately, this pumping strategy is incompatible with many applications in which samples cannot be exposed to high electric fields or when EOF does not occur. Therefore, new approaches are needed to effect pumping in microfabricated devices.

LC is presently the most important separation technique in analytical chemistry; however, on-chip LC methods are highly underdeveloped. Despite interest in the miniaturization of LC, creative ideas are needed to overcome various challenges such as applying pressure in microchannels, introducing small amounts of sample with minimal dead volume and depositing stationary phases inside microchannels. Indeed, the implementation of chip-based LC systems should enable the analysis of samples that cannot be exposed to high electric fields.

One weakness of miniaturization is the low yield of some methods for microdevice fabrication. The development of reliable and reproducible micromachining processes is a key concern, especially for mass production and commercialization of microchips. In addition, more flexible and reliable fabrication methods are needed to meet the demands for highly integrated microfabricated devices and expand the number of applications of microchips. Finally, it is necessary to develop manufacturing techniques for microfluidics that can be easily implemented by research groups with limited access to sophisticated instrumentation.

1.4 MICROPUMPS FOR MICROFLUIDIC APPLICATIONS

Micropumps transport samples and reagents from one point to another and are critical components of integrated and miniaturized microsystems. A variety of micropumps have been fabricated using micromachining techniques.[206,207] Although the classification of micropumps is somewhat arbitrary in the literature, micropumps can be divided into mechanical and non-mechanical pumps (**Figure 1.18**).[207]

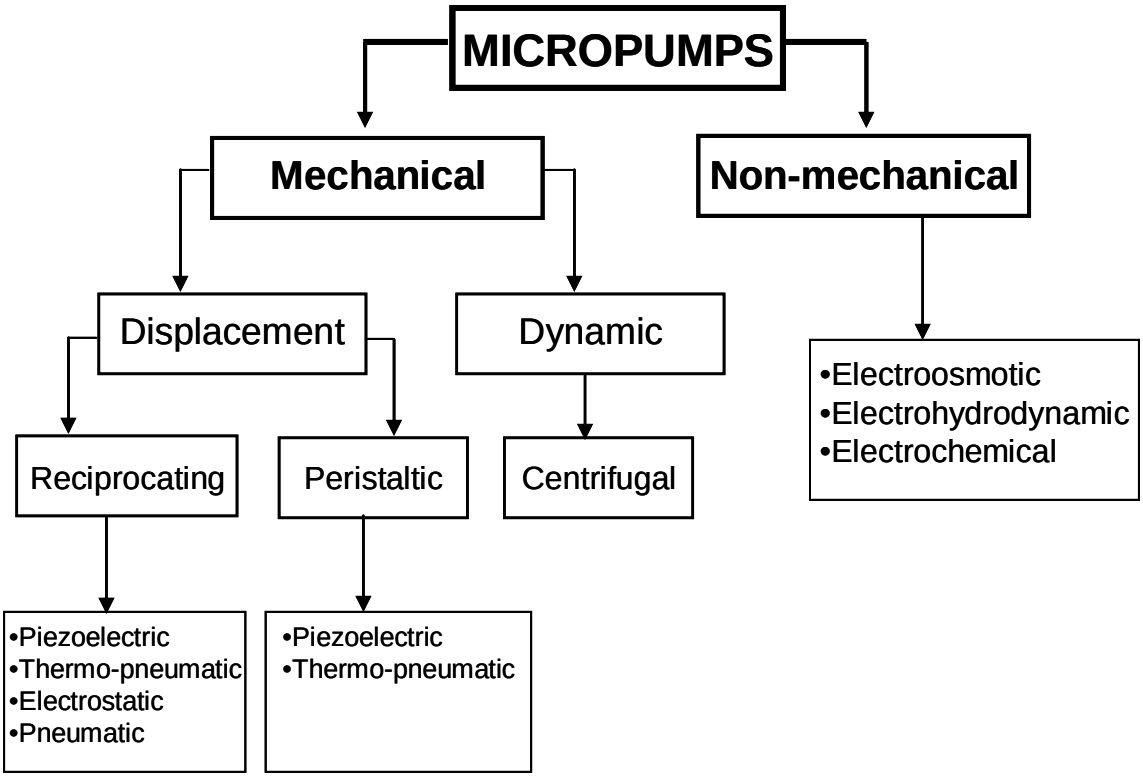

Figure 1.18. Micropump classification.

1.4.1 Mechanical micropumps

Mechanical micropumps require moving parts to produce pumping.[207] Based on the way in which mechanical energy is applied to the fluid, these micropumps can be further categorized as either displacement or dynamic.[206] There are two types of displacement micropumps (**Figure 1.18**). In both reciprocating and peristaltic pumps, the energy used for fluid pumping is applied by a force acting on a movable boundary. Usually, fluid flow is generated by means of pneumatic,[208] piezoelectric,[209] thermo-pneumatic[210] or electrostatic[211] actuators. In dynamic micropumps, energy is applied continuously to effect flow from the pump.

1.4.1.1 Reciprocating micropumps

Reciprocating micropumps are often referred to as membrane-actuated or check-valve pumps.[207] In these pumps, fluid flow is achieved by compression and expansion of a pressure chamber surrounded by a movable membrane (**Figure 1.19).**[212] The maximum pressure and flow that can be achieved by these micropumps depends on the actuation mechanism used. To produce unidirectional fluid flow, reciprocating micropumps need to be connected to a check valve. A major drawback of these pumps is the difficulty of integration with microfluidic devices.

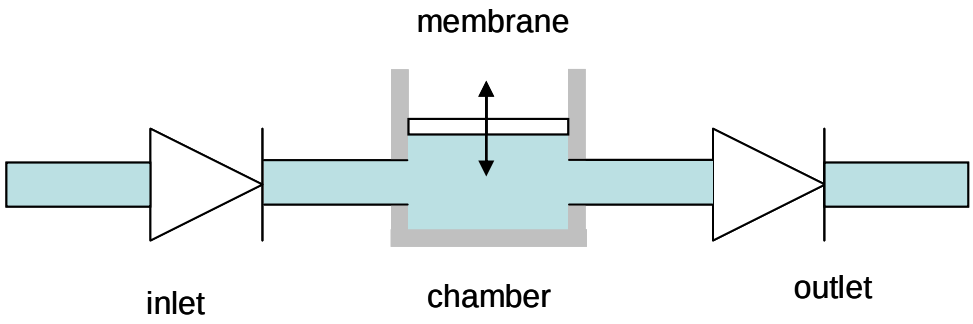

Figure 1.19. Principle of actuation of a reciprocating mechanical micropump.

1.4.1.2 Peristaltic micropumps

The operational principle of these pumps is based on the peristaltic motion of the chambers, which causes flow in the desired direction. **Figure 1.20** represents a general schematic representation of peristaltic pumping.[213] Unlike reciprocating pumps, peristaltic micropumps do not need check valves to direct fluid flow.[207] However, design and fabrication of peristaltic micropumps in conventional materials is somewhat complicated, which has limited their application in microfluidics.

PDMS is widely used as an actuator for peristaltic pumping. Normally, a layer of PDMS is bonded on top of the pump chambers. Fluid pumping occurs by sequential deflection of the PDMS layer on each of the micropump chambers, which causes directional fluid flow in the microdevice.

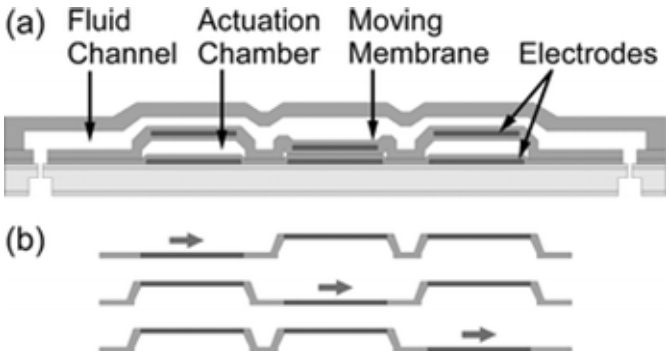

Figure 1.20. Schematic of an electrostatically actuated peristaltic micropump. (a) Design: the moving membrane is displaced up and down. (b) 3-phase peristaltic sequence. Arrows indicate pumping direction. *Reprinted with permission from ref. 213; copyright 2004 Royal Society of Chemistry*.

1.4.1.3 Piezoelectric actuation

The change in layer tension of a piezoelectric disc can be used for the deflection of a micropump chamber, increasing or decreasing the pressure depending on the direction of deflection. This pumping mechanism was first demonstrated by Smits[214] and has been used recently in polymeric microchips.[215,216] Piezoelectric actuation is attractive because the micropumps are relatively easy to fabricate, and can generate modest pressures (~300 kPa) and high flow rates (35 mL/min). One disadvantage of this actuation mechanism is the use of high voltages (>1.0 kV).[206,217]

Mechanical micropumps represent a sophisticated solution for pumping in microsystems. However, depending on the designs and materials used, costs of fabrication can be

prohibitive. Moreover, in some cases, the micropump materials are not compatible with reagents or samples used in microfluidic applications, which limits their utility.

1.4.2 Non-mechanical micropumps

In contrast to mechanical pumping actuators, non-mechanical micropumps do not use moving parts to effect flow. Normally these devices work by converting one energy form into the kinetic energy of the liquid being pumped.[206,207] Some non-mechanical pumps include: electroosmotic,[218] magnetohydrodynamic,[219] and electrochemical micropumps.[220] Non-mechanical pumps are attractive because they can be relatively easy to fabricate and offer accurate control of very low flow rates (nL-μL/min).[206,207]

1.4.2.1 Electrokinetic micropumps

The fundamentals of EOF were discussed in **Section 1.2.2**. Electroosmotic pumps (EOPs), which use EOF to generate pressure, are widely used in microfluidic applications.[29,207,218,221] The main advantages of EOPs are: absence of moving parts, fluid flow takes place over the entire length of a microchannel, and the flow can be controlled without valves by switching voltages.[206] In addition, EOPs have the advantage of being compatible with aqueous solutions, which is desirable for working with buffers and biological fluids. A major drawback of EOPs is the requirement of high voltages (~kV) for generating high-pressure flows. Working with high electric fields can cause Joule heating, which affects pumping efficiency. Moreover, to obtain considerable flow and pressure using EOPs, it is necessary in most cases to fill the capillary or channel with a porous medium (e.g., a packed silica particle bed),[218] or to construct small-diameter

microchannel network arrays,[221,222] which makes microchip fabrication difficult.[223] A paper by Lazar and Karger[221] used traditional photolithography, wet etching and bonding to fabricate a platform consisting of 100 microchannels connected to two buffers reservoirs. These devices were able to achieve pressures up to 80 psi and were used to deliver peptide samples for MS detection.

1.4.2.2 Electrohydrodynamic micropumps

Electrohydrodynamic pumping is performed by the Coulombic force created when an electric field positioned between two electrodes interacts with a dielectric fluid.[206] Two types of electrohydrodynamic pumps have been developed: induction and injection pumps.[207] These pumps are limited to liquids with low conductivity (10^{-12} to 10^{-6} S/m), like organic solvents or oils. Therefore, pumping of aqueous solutions such as biological fluids is restricted.

1.4.2.3 Electrochemical micropumps

The electrolysis of liquids such as water to produce gases is a well-known process. When an adequate voltage is applied to deionized (DI) water via platinum or gold electrodes, the electrolysis reactions are:

Anode: $2\,H_2O_{(l)} \rightarrow 4H^+ + O_{2\,(g)} + 4e^-$ (1.10)

Cathode: $4H^+ + 4e^- \rightarrow + 2H_{2\,(g)}$ (1.11)

Net equation: $2H_2O_{(l)} \rightarrow O_{2\,(g)} + 2H_{2\,(g)}$ (1.12)

The build-up of electrolysis gases in an enclosed chamber causes an increase in pressure that can be used for pumping by production of bubbles[224] or by deflection of a membrane that is in contact with the electrolyte solution.[220] Although solutions other than water have been used for electrochemical pumping,[225] aqueous electrolyte solutions are commonly used because of the low voltage needed to electrolyze water ($E^\circ = 1.23$ V).[226]

The maximum pressure generated by an electrochemical pump depends on the amount of gas generated during electrolysis. This relationship can be expressed using the ideal gas law:

$$pV = n_T RT \qquad (1.13)$$

where n_T is the total moles generated and is equal to the moles of hydrogen ($n\mathrm{H_2}$) plus moles of oxygen ($n\mathrm{O_2}$) ($n_T = 2n\mathrm{H_2} + n\mathrm{O_2}$). Based on Faraday's 1st Law of electrolysis, the amount of gas produced is determined by the current (I) that passes through the cell in a given time (t) according to:

$$n\mathrm{H_2} = \frac{It}{2F} \qquad (1.14)$$

$$n\mathrm{O_2} = \frac{It}{4F} \qquad (1.15)$$

Combining equations (1.13), (1.14) and (1.15), the pressure times volume of the electrolysis gases from water can be expressed as:

$$(pV)_{H_2} + (pV)_{O_2} = \left(\frac{3RT}{4F}\right)It \qquad (1.16)$$

According to equation (1.16), under ideal conditions, the pV relationship of electrolytically produced gases increases with time and current passing through the electrodes. However, in reality the increase in pressure is limited by the effects of H_2 and O_2 pressure on the cell potential (according to the Nernst equation), leaks in the system, solubility of gases in the electrolyte solution or other electrochemical reactions.[220,227]

Electrochemical pumps can work for bi-directional pumping by reversing the direction of the current, since the gases produced by electrolysis can recombine to form water. Electrochemically actuated micropumps have been used for dosing systems in applications in biology and medicine because they offer highly accurate and reproducible delivery.[228,229] Due to their simple design and implementation, the use of electrochemical micropumps for microfluidic applications has grown considerably in recent years.[230] Some applications include pumping in microchannels,[231] on-chip chromatography separations,[232,233] and valve actuation.[234]

1.5 MINIATURIZATION OF LIQUID CHROMATOGRAPHY

While μCE has seen great success and widespread implementation, the development of chip-based LC has been slower (**Figure 1.21**). Due to its versatility and efficiency, the miniaturization of LC is particularly attractive because the experimental conditions can

be adapted for the analysis of various samples with different analyte compositions and polarities.[235]

On the other hand, electrically-driven separation methods have some drawbacks, namely: (1) exposure of samples to high voltages, (2) Joule heating effects, and (3) sampling bias under applied electric fields. **Table 1.6** shows a comparison of CE and LC. Because of the non-universal nature of electrophoretic separations, the development of chip-based LC is critical for miniaturization to have the greatest impact in separation science.[236] A survey of the literature shows progress in developing pressure-driven separation microdevices[237] and, importantly, that interest remains high.

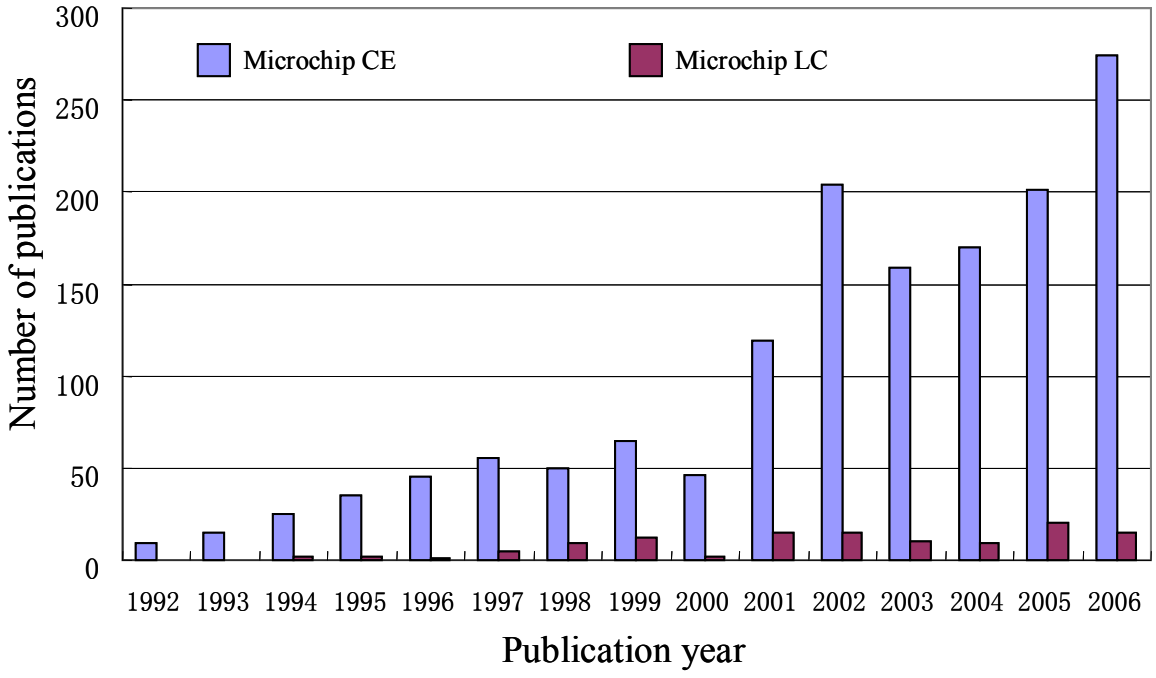

Figure 1.21. Comparison of reports on microchip LC and CE in the last 15 years. ***Citations containing the words on-chip capillary electrophoresis and on-chip liquid chromatography reported in the ISI Web of Science database were counted to generate the graph.***

Table 1.6 Comparisons between LC and CE.[238,239]

Liquid Chromatography	Capillary Electrophoresis
Pros: • Wide choice of detection modes • Good reproducibility • Many stationary phase options • Well-established methods Cons: • Uses high pressure pumps • Large organic solvent volumes	Pros: • Simpler instrumentation • High separation efficiency • Low solvent consumption Cons: • Incompatible with low or high pH • Requires high voltages

1.5.1 Advantages via miniaturization of LC

The efficiency of any chromatographic technique depends on the selection of mobile and stationary phases for the separation of a given analyte.[240] The advantages associated with shrinking LC and performing separations in micrometer-dimension channels are based on both improvements in efficiency and economical benefits. For example, reducing the column diameter potentially increases analyte interaction with stationary phase, and thus can improve the selectivity of the separation. In addition, the use of smaller diameter columns is associated with lower volumetric flow rates; therefore, less solvent is required and smaller sample amounts can be loaded into the column.

These advantages have motivated separation scientists to reduce the diameter of the columns. More than two decades ago, Ishii[241] classified LC separations based on the column internal diameter. Currently the different types of column chromatography are categorized based on the flow rate range rather than the column diameter (**Table 1.7**).

Table 1.7. Terminology used in LC techniques.[242]

Column i.d.	Flow rate	Name
3.2-4.6 mm	0.5-2.0 mL/min	Conventional HPLC
1.5-3.2 mm	100-500 µL/min	Microbore HPLC
0.5-1.5 mm	10-100 µL/min	Micro-LC
150-500 µm	1-10 µL/min	Capillary-LC
10-150 µm	10-1000 nL/min	Nano-LC

The reduction of column diameter is directly related to a reduction in LOD. During the chromatography process, compounds are subject to dilution as they travel along the column. The dilution at the end of the column for an analyte can be expressed as:[243]

$$D = \frac{c_o}{c_{\max}} = \frac{\pi d_c^2 \varepsilon \sqrt{2HL\pi}}{4V_{inj}} \qquad (1.17)$$

where c_o is the initial concentration of the solute in the sample, $c_{\max}$ is the concentration of the maximum of the peak, d_c is the column internal diameter, ε is the column porosity, L and H are the column length and plate height, respectively, and V_{inj} is the injection volume. Equation (1.17) shows that solute dilution during chromatography increases with the square of the column diameter; therefore, less dilution and hence, lower limits of detection can be obtained with smaller diameter columns.

1.5.2 On-chip LC approaches

The idea of making microfabricated chromatographic devices[13,31] was proposed before any work with microchip CE was published.[35] Since then, only a few reports of chip-based LC systems have appeared.[21,92,198,232,233,237,244-247] Based on the classification in **Table 1.7**, it is interesting to note that most microchannels fabricated in planar substrates fit in the capillary and nano-LC category. However, unlike conventional cylindrical microcolumns, micromachined channels have rectangular, trapezoidal or semi-circular cross-sections.

The first experimental results for a chip-based LC separation were presented in 1995.[21] A microfabricated column in silicon was used to separate a mixture of fluorescent dyes (fluorescein sodium and acridine orange), yielding a somewhat unimpressive maximum of 200 theoretical plates in 3 minutes. Difficulties applying pressure to microfluidic channels have led scientists to explore alternative approaches for miniaturizing LC.

Capillary electrochromatography (CEC) is a liquid-phase separation technique in which the mobile phase is transported through a stationary phase by EOF, rather than external pressure.[248] The separation mechanism in CEC, therefore, is the result of the combination of chromatographic partitioning and electrophoretic migration. As a hybrid technique of microcolumn (capillary) LC and CE, CEC combines some of the best features of the parent techniques such as the high efficiency of CE and the high selectivity of LC.[249] Chromatographic separations in microchips using CEC have been somewhat more successful compared to pressure-driven methods.[18,250-254] Fast (<45 s) microchip CEC

separation of peptides and amino acids has been reported,[250] and speed in microchip CEC was superior compared to capillary-based CEC separations.[250,251] However, CEC also has some drawbacks, mainly associated with the limitations of EOF discussed before. Moreover, some analytical separation problems are fundamentally incompatible with the principles of CEC, such as the separation of positively charged basic compounds.[249]

1.5.3 Major challenges in miniaturizing LC

1.5.3.1 Microchip LC integration

One of the main challenges in the development of miniaturized LC systems is the need to miniaturize other device components to minimize the dead volume contribution. By comparing the flow rates in **Table 1.7**, it can be calculated that to minimize dead volume effects in microscale systems, flow rates, injection and detection volumes as well as connecting tubes should be approximately 2000 times smaller for a 100 μm i.d. capillary compared to conventional LC.[242] Although microfabrication has the potential to allow monolithic integration of several components in a single substrate, most microfabricated LC devices reported to date have only miniaturized the separation column while still maintaining an external pumping mechanism such as syringe pumps,[21,38] or connection to external pressurized gas cylinders or vacuum systems.[255] Therefore, the development of pumping systems capable of applying pressure and generating the appropriate nL-μL flow rates in microfabricated channels is critical for the success of chip-based LC.

1.5.3.2 Column technology for microchip LC

A second major challenge for the development of chip-based LC is the introduction of stationary phases into microchannels.[236,237] Columns packed with porous materials are perhaps the most popular separation media for LC.[240] However, introducing small-diameter particles at desired locations within microchannels is not an easy task.[252] One of the main problems associated with the preparation of packed beds in microfluidic channels is the construction and positioning of a retaining frit at the end of the channel. Several approaches have been undertaken to deal with this limitation, including new frit designs[256] and entrapment of silica particles using sol-gel techniques. Verpoorte et al.[254] also reported the fritless fabrication of conventional particulate stationary phases for microfluidic applications. However, in this approach, the dimensions of the intersecting channels in the injection area, as well as those of a tapered column, needed to be controlled precisely to ensure uniform packing.

During the last decade, a new category of materials called monoliths has been developed and used for chromatographic separations.[257,258] A monolith is composed of a continuous piece of solid material with interconnected through-pores.[259] Monolithic silica columns can be fabricated for microscale separations, allowing for a higher efficiency and greater permeability compared to conventional packed columns. Polymer-based monoliths can be prepared by in-situ polymerization of monomers in a column, which avoids the tedious step of column packing.[259,260] Polymer monoliths prepared from materials such as acrylamide, styrene, divinyl benzene and methacrylate can be used for separations in CEC and HPLC.[261-264]

Monoliths have been used as separation media for chip-based CEC.[250,251] There are many reasons why a monolith is a good choice for microfluidic devices. First, there is no need for packing the small structure of a microchannel because the monolith can be polymerized in-situ.[259] Moreover, the walls of the channel can be modified by covalent bonding of the monolith to the channel surface.[265] By using light-initiated polymerization, the monolith can be confined to the illuminated areas in the microchannel. Thus, detection windows and injection arms can be defined by selective casting of the polymer.[251] Importantly, the high porosity and mass transfer achieved in monolithic structures should avoid the need for high-pressure pumping systems for potential applications in chip-based LC.[246]

In order to overcome the obstacles associated with placing a packing material in small channels, open tubular columns that use a stationary phase support attached to the wall surface have been proposed.[18,266] Indeed, microchannels have been coated using typical LC stationary phases.[233] Ramsey et al.[19] reported the fabrication of a wall-coated channel for performing open channel electrochromatography using octadecylsilane chemically bonded to the channel walls as a stationary phase.

Although the development of microchip LC has been slow compared to electrically driven methods, in recent years significant progress has been made in the areas of fluid pumping and microchip column technology. Theoretical studies and preliminary reports have demonstrated that chip-based LC separations can reduce the analysis time and

increase sample throughput. Further work should focus on developing "chip-to-world" interconnects with minimal dead volume.

1.6 DISSERTATION OVERVIEW

In my dissertation, I describe efforts to develop new approaches to increase the potential of microfluidic devices for applications in analytical chemistry. This chapter gave a brief overview of the history, methodologies, developments, applications, current challenges and future trends in miniaturization. At the end of this chapter are listed significant references covering relevant work in the area. **Chapters 2-6** focus on addressing some of the challenges in miniaturization mentioned in Section 1.3.

In **Chapter 2**, I present the design, fabrication and evaluation of electrochemically actuated pumps for microfluidic applications. Pressure-driven pumping was performed in microfabricated channels by an increase in pressure generated by electrolysis gases in an enclosed chamber. This chapter serves as a proof of concept for electrochemical pumping in microfluidic devices. **Chapter 3** is an extension of the work in **Chapter 2**, in which the electrochemical micropumps were integrated with microchannels, reservoirs and electrodes in glass substrates to develop microchip LC systems. A pressure-balanced injection mode was developed, and microdevices were evaluated for the chromatographic separation of fluorescently labeled amino acids.

Chapter 4, which also corresponds to Chapter 51 in the third edition of the Handbook of Capillary and Microchip Electrophoresis and Associated Microtechniques, edited by Prof. James P. Landers, introduces the following **Chapters 5-6**. In **Chapter 4,** I present the concepts, protocols and method development strategies to fabricate polymeric microchips using phase-changing sacrificial layers (PCSLs). The original fabrication of devices for μCE using PCSLs was accomplished by other reserchers in Prof. Woolley's laboratory. In **Chapter 5,** I implemented the PCSL fabrication approach to make multilayer polymeric microdevices in PMMA. The fluidic and electrical independence of these multilayer systems was evaluated. Moreover, high-efficiency electrophoretic separations were performed in microdevices with microchannels crossing one another. **Chapter 6** presents the PCSL-based fabrication of multilayer microdevices for multiplexed electrophoretic separations. The ability to make crossover microchannels facilitated the design and fabrication of multichannel microdevices with minimal fluidic inputs.

Finally, in **Chapter 7**, I give general conclusions regarding my work and consider future directions in the field.

1.7 REFERENCES

[1] Golay, M., *Gas Chromatography* Butterworths, London, 1958.
[2] Horvath, C. G. and Lipsky, S. R., Rapid Analysis of Ribonucleosides and Bases at the Picomole Level Using Pellicular Cation Exchange Resins in Narrow Bore Columns, *Anal. Chem.* 41, 1227, 1969.
[3] Horvath, C. G., Preiss, B. A., and Lipsky, S. R., Fast Liquid Chromatography: An Investigation of Operating Parameters and the Separation of Nucleotides on Pellicular Ion Exchangers, *Anal. Chem.* 39, 1422, 1967.
[4] Giddings, J. C., *Dynamics of Chromatography* Marcel Dekker, New York, 1965.
[5] Tsuda, T. and Novotny, M., Band-Broadening Phenomena in Microcapillary Tubes under Conditions of Liquid-Chromatography, *Anal. Chem.* 50, 632, 1978.
[6] Tsuda, T. and Novotny, M., Packed Microcapillary Columns in High-Performance Liquid-Chromatography, *Anal. Chem.* 50, 271, 1978.
[7] Yang, F. J., Open Tubular Column LC - Theory and Practice, *J. Chromatogr. Sci.* 20 (6), 241-251, 1982.
[8] Yang, F. J., Fused-Silica Narrow-Bore Microparticle-Packed-Column High-Performance Liquid-Chromatography, *J. Chromatogr.* 236, 265, 1982.
[9] Mikkers, F. E. P., Everaerts, F. M., and Verheggen, T. P. E. M., High-Performance Zone Electrophoresis, *J. Chromatogr.* 169, 11, 1979.
[10] Jorgenson, J. W. and Lukacs, K. D., Zone electrophoresis in open-tubular glass capillaries, *Anal. Chem.* 53, 1298, 1981.
[11] Jorgenson, J. W. and Lukacs, K. D., Capillary zone electrophoresis, *Science* 222, 266, 1983.
[12] Terry, S. C., Ph.D Dissertation, Stanford University, 1975.
[13] Terry, S. C., Jerman, J. H., and Angell, J. B., A Gas Chromatographic Analyzer Fabricated in a Silicon Wafer, *IEEE Trans. Electron Devices* ED26, 1880, 1979.
[14] Manz, A., Graber, N., and Widmer, H. M., Miniaturized Total Chemical-Analysis Systems - a Novel Concept for Chemical Sensing, *Sens. Actuators B* 1, 244, 1990.
[15] Harrison, D. J., Fluri, K., Seiler, K., Fan, Z. H., Effenhauser, C. S., and Manz, A., Micromachining a Miniaturized Capillary Electrophoresis-Based Chemical-Analysis System on a Chip, *Science* 261, 895, 1993.
[16] Effenhauser, C. S., Manz, A., and Widmer, H. M., Glass Chips for High-Speed Capillary Electrophoresis Separations with Submicrometer Plate Heights, *Anal. Chem.* 65, 2637, 1993.
[17] Jacobson, S. C., Hergenroder, R., Koutny, L. B., and Ramsey, J. M., High-Speed Separations on a Microchip, *Anal. Chem.* 66, 1114, 1994.
[18] Jacobson, S. C., Hergenroder, R., Koutny, L. B., and Ramsey, J. M., Open-Channel Electrochromatography on a Microchip, *Anal. Chem.* 66, 2369, 1994.
[19] Kutter, J. P., Jacobson, S. C., Matsubara, N., and Ramsey, J. M., Solvent-programmed microchip open-channel electrochromatography, *Anal. Chem.* 70, 3291, 1998.
[20] He, B., Tait, N., and Regnier, F., Fabrication of Nanocolumns for Liquid Chromatography, *Anal. Chem.* 70, 3790, 1998.

[21] Ocvirk, G., Verpoorte, E., Manz, A., Grasserbauer, M., and Widmer, H. M., High-Performance Liquid-Chromatography Partially Integrated onto a Silicon Chip, *Anal. Meth. Instr.* 2, 74, 1995.
[22] Walker, P. A., Morris, M. D., Burns, M. A., and Johnson, B. N., Isotachophoretic separations on a microchip. Normal Raman spectroscopy detection, *Anal. Chem.* 70, 3766, 1998.
[23] Hofmann, O., Che, D. P., Cruickshank, K. A., and Muller, U. R., Adaptation of capillary isoelectric focusing to microchannels on a glass chip, *Anal. Chem.* 71, 678, 1999.
[24] Woolley, A. T. and Mathies, R. A., Ultra-High-Speed DNA Fragment Separations Using Microfabricated Capillary Array Electrophoresis Chips, *Proc. Natl. Acad. Sci. USA* 91, 11348, 1994.
[25] Effenhauser, C. S., Paulus, A., Manz, A., and Widmer, H. M., High-Speed Separation of Antisense Oligonucleotides on a Micromachined Capillary Electrophoresis Device, *Anal. Chem.* 66, 2949, 1994.
[26] Schmalzing, D., Adourian, A., Koutny, L., Ziaugra, L., Matsudaira, P., and Ehrlich, D., DNA sequencing on microfabricated electrophoretic devices, *Anal. Chem.* 70, 2303, 1998.
[27] Waters, L. C., Jacobson, S. C., Kroutchinina, N., Khandurina, J., Foote, R. S., and Ramsey, J. M., Multiple sample PCR amplification and electrophoretic analysis on a microchip, *Anal. Chem.* 70, 5172, 1998.
[28] Jakeway, S. C., de Mello, A. J., and Russell, E. L., Miniaturized total analysis systems for biological analysis, *Fres. J. Anal. Chem.* 366, 525, 2000.
[29] Auroux, P. A., Iossifidis, D., Reyes, D., and Manz, A., Micro Total Analysis Systems. 2. Analytical Standard Operations and Applications, *Anal. Chem.* 74, 2637, 2002.
[30] Madou, M. J., *Fundamentals of microfabrication*, 2nd. ed. CRC, Boca Raton, Fl, 2002.
[31] Manz, A., Miyahara, Y., Miura, J., Watanabe, Y., Miyagi, H., and Sato, K., Design of an Open-Tubular Column Liquid Chromatograph Using Silicon Chip Technology, *Sens. Actuators B* 1, 249, 1990.
[32] Fintschenko, Y. and van den Berg, A., Silicon microtechnology and microstructures in separation science, *J. Chromatogr. A* 819, 3, 1998.
[33] Borrello, L., Bernardini, J., Dell'Orso, R., Dutta, S., Giassi, A., Messineo, A., Segneri, G., Starodumov, G., Tonelli, G., Verdini, P.G., Militaru, O., Fallica, P.G., and Valvo, G., Production and test of very high breakdown voltage detectors, *IEEE Trans. Nucl. Sci.* 49, 1035, 2002.
[34] Manz, A., Harrison, D. J., Verpoorte, E. M. J., Fettinger, J. C., Paulus, A., Ludi, H., and Widmer, H. M., Planar Chips Technology for Miniaturization and Integration of Separation Techniques into Monitoring Systems - Capillary Electrophoresis on a Chip, *J. Chromatogr.* 593, 253, 1992.
[35] Harrison, D. J., Manz, A., Fan, Z. H., Ludi, H., and Widmer, H. M., Capillary Electrophoresis and Sample Injection Systems Integrated on a Planar Glass Chip, *Anal. Chem.* 64, 1926, 1992.
[36] Simpson, P. C., Woolley, A. T., and Mathies, R. A., Microfabrication Technology for the Production of Array Electrophoresis Chips, *J. Biomed. Microdevices* 1, 7, 1998.
[37] Dittrich, P. S., Tachikawa, K., and Manz, A., Micro total analysis systems. Latest advancements and trends, *Anal. Chem.* 78, 3887, 2006.

[38] Sato, K., Hibara, A., Tokeshi, M., Hisamoto, H., and Kitamori, T., Integration of chemical and biochemical analysis systems into a glass microchip, *Anal. Sci.* 19, 15, 2003.
[39] Lin, C. H., Lee, G. B., Lin, Y. H., and Chang, G. L., A fast prototyping process for fabrication of microfluidic systems on soda-lime glass, *J. Micromech. Microeng.* 11 (6), 726-732, 2001.
[40] de Mello, A., Plastic fantastic?, *Lab Chip* 2, 31N, 2002.
[41] Youssouf, B. M., Wong, M., Chiem, N., Salimi-Moosavi, H., and Harrison, D. J., Protein separation and surfactant control of electroosmotic flow in poly(dimethylsiloxane)-coated capillaries and microchips, *J. Chromatogr. A* 947, 277, 2002.
[42] Jacobson, S. C., Moore, A. W., and Ramsey, J. M., Fused Quartz Substrates for Microchip Electrophoresis, *Anal. Chem.* 67, 2059, 1995.
[43] Fluri, K., Fitzpatrick, N., Chiem, N., and Harrison, D. J., Integrated Capillary Electrophoresis Devices with an Efficient Postcolumn Reactor in Planar Quartz and Glass Chips, *Anal. Chem.* 68, 4285, 1996.
[44] Pan, T., Kelly, R. T., Asplund, M. C., and Woolley, A. T., Fabrication of calcium fluoride capillary electrophoresis microdevices for on-chip infrared detection, *J. Chromatogr. A* 1027, 231, 2004.
[45] Becker, H. and Locascio, L. E., Polymer microfluidic devices, *Talanta* 56, 267, 2002.
[46] Duffy, D. C., McDonald, J. C., Schueller, O. J. A., and Whitesides, G. M., Rapid Prototyping of Microfluidic Systems in Poly(dimethylsiloxane), *Anal. Chem.* 70, 4974, 1998.
[47] McDonald, J. C., Duffy, D. C., Anderson, J. R., Chiu, D. T., Wu, H., Schueller, O. J. A., and Whitesides, G. M., Fabrication of microfluidic systems in poly(dimethylsiloxane), *Electrophoresis* 21, 27, 2000.
[48] Boone, T. D., Hugh Fan, Z., Hooper, H. H., Ricco, A. J., Tan, H., and Williams, S. J., Plastic advances microfluidic devices, *Anal. Chem.* 74, 78A, 2002.
[49] Soper, S. A., Ford, S. M., Qi, S., McCarley, R. L., Kelly, K., and Murphy, M. C., Polymeric microelectromechanical systems, *Anal. Chem.* 72, 642A, 2000.
[50] Shadpour, H. and Soper, S. A., Two-dimensional electrophoretic separation of proteins using poly(methyl methacrylate) microchips, *Anal. Chem.* 78, 3519, 2006.
[51] Shah, J. J., Geist, J., Locascio, L. E., Gaitan, M., Rao, M. V., and Vreeland, W. N., Capillarity induced solvent-actuated bonding of polymeric microfluidic devices, *Anal. Chem.* 78, 3348, 2006.
[52] Henry, A. C., Tutt, T. J., Galloway, M., Davidson, Y. Y., McWhorter, C. S., Soper, S. A., and McCarley, R. L., Surface Modification of Poly(methyl methacrylate) Used in the Fabrication of Microanalytical Devices, *Anal. Chem.* 72, 5331, 2000.
[53] Shadpour, H., Musyimi, H., Chen, J. F., and Soper, S. A., Physiochemical properties of various polymer substrates and their effects on microchip electrophoresis performance, *J. Chromatogr. A* 1111, 238, 2006.
[54] Becker, H. and Gartner, C., Microreplication technologies for polymer-based u-TAS applications, *In Lab on a Chip: Miniaturized Systems for (Bio)Chemical Analysis and Sythesis, Oosterbroek and van den Berg Ed.* 1st Ed., 21-64, Elsevier, Amsterdam, 2003.
[55] Carraher, C.E. Jr., *Introduction to polymer chemistry*, CRC, Boca Raton, FL, 2007.
[56] Young, R. J. and Lovell, P. A., *Introduction to Polymers*, CRC, Boca Raton, FL, 1991.

[57] Hsu, T.-R., *MEMS and Mycrosystems: Design and Manufacture,* Mc Graw Hill, 1st Ed. New York, 2002.
[58] McCormick, R. M., Nelson, R. J., Alonso-Amigo, M. G., Benvegnu, D. J., and Hooper, H. H., Microchannel Electrophoretic Separations of DNA in Injection-Molded Plastic Substrates, *Anal. Chem.* 69, 2626, 1997.
[59] Chen, Y. H. and Chen, S. H., Analysis of DNA fragments by microchip electrophoresis fabricated on poly(methyl methacrylate) substrates using a wire-imprinting method, *Electrophoresis* 21, 165, 2000.
[60] Llopis, S. L., Osiri, J., and Soper, S. A., Surface modification of poly(methyl methacrylate) microfluidic devices for high-resolution separations of single-stranded DNA, *Electrophoresis* 28, 984, 2007.
[61] Galloway, M., Stryjewski, W., Henry, A., Ford, S. M., Llopis, S., McCarley, R. L., and Soper, S. A., Contact conductivity detection in poly(methyl methacylate)-based microfluidic devices for analysis of mono- and polyanionic molecules, *Anal. Chem.* 74, 2407, 2002.
[62] Kelly, R. T., Pan, T., and Woolley, A. T., Phase-Changing Sacrificial Materials for Solvent Bonding of High-Performance Polymeric Capillary Electrophoresis Microchips, *Anal. Chem.* 77, 3536, 2005.
[63] Raisi, F., Belgrader, P., Borkholder, D. A., Herr, A. E., Kintz, G. J., Pourhamadi, F., Taylor, M. T., and Northrup, M. A., Microchip isoelectric focusing using a miniature scanning detection system, *Electrophoresis* 22, 2291, 2001.
[64] Yuan, C. H. and Shiea, J., Sequential electrospray analysis using sharp-tip channels fabricated on a plastic chip, *Anal. Chem.* 73, 1080, 2001.
[65] Meng, Z., Qi, S., Soper, S. A., and Limbach, P. A., Interfacing a Polymer-Based Micromachined Device to a Nanoelectrospray Ionization Fourier Transform Ion Cyclotron Resonance Mass Spectrometer, *Anal. Chem.* 73, 1286, 2001.
[66] Li, F. A., Wang, C. H., and Her, G. R., A sheathless poly(methyl methacrylate) chip-CE/MS interface fabricated using a wire-assisted epoxy-fixing method, *Electrophoresis* 28, 1265, 2007.
[67] Barker, S. L. R., Ross, D., Tarlov, M. J., Gaitan, M., and Locascio, L. E., Control of Flow Direction in Microfluidic Devices with Polyelectrolyte Multilayers, *Anal. Chem.* 72, 5925, 2000.
[68] Kelly, R. T., Li, Y., and Woolley, A. T., Phase-changing sacrificial materials for interfacing microfluidics with ion-permeable membranes to create on-chip preconcentrators and electric field gradient focusing microchips, *Anal. Chem.* 78, 2565, 2006.
[69] Wang, X. C., Yang, X. H., and Zhang, X. M., Preparation of the capillary-based microchips for solid phase extraction by using the monolithic frits prepared by UV-initiated polymerization, *Anal. Sci.* 22, 1099, 2006.
[70] Eteshola, E. and Leckband, D., Development and characterization of an ELISA assay in PDMS microfluidic channels, *Sens. Actuators B* 72, 129, 2001.
[71] Jang, Y. H., Oh, S. Y., and Park, J. K., In situ electrochemical enzyme immunoassay on a microchip with surface-functionalized poly(dimethylsiloxane) channel, *Enz. Microb. Tech.* 39, 1122, 2006.

[72] Chan, J. H., Timperman, A. T., Qin, D., and Aebersold, R., Microfabricated polymer devices for automated sample delivery of peptides for analysis by electrospray ionization tandem mass spectrometry, *Anal. Chem.* 71, 4437, 1999.
[73] Kim, J. S. and Knapp, D. R., Miniaturized multichannel electrospray ionization emitters on poly(dimethylsiloxane) microfluidic devices, *Electrophoresis* 22, 3993, 2001.
[74] Buch, J. S., Wang, P. C., DeVoe, D. L., and Lee, C. S., Field-effect flow control in a polydimethylsiloxane-based microfluidic system, *Electrophoresis* 22, 3902, 2001.
[75] Martin, I. T., Dressen, B., Boggs, M., Liu, Y., Henry, C. S., and Fisher, E. R., Plasma modification of PDMS microfluidic devices for control of electroosmotic flow, *Plasma Proc. Polymers* 4, 414, 2007.
[76] Chen, X. X., Wu, H. K., Mao, C. D., and Whitesides, G. M., A prototype two-dimensional capillary electrophoresis system fabricated in poly(dimethylsiloxane), *Anal. Chem.* 74, 1772, 2002.
[77] Xiao, D., Le, T. V., and Wirth, M. J., Surface modification of the channels of poly(dimethylsiloxane) microfluidic chips with polyacrylamide for fast electrophoretic separations of proteins, *Anal. Chem.* 76, 2055, 2004.
[78] Xiao, Y., Yu, X. D., Wang, K., Xu, J. J., Huang, J., and Chen, H. Y., Study on the separation of amino acids in modified poly(dimethylsiloxane) microchips, *Talanta* 71, 2048, 2007.
[79] Thorsen, T., Maerkl, S. J., and Quake, S. R., Microfluidic Large-Scale Integration, *Science* 298, 580, 2002.
[80] Kim, J. Y., Baek, J. Y., Lee, K. A., and Lee, S. H., Automatic aligning and bonding system of PDMS layer for the fabrication of 3D microfluidic channels, *Sens. Actuators A* 119, 593, 2005.
[81] Liu, Y., Ganser, D., Schneider, A., Liu, R., Grodzinski, P., and Kroutchinina, N., Microfabricated Polycarbonate CE Devices for DNA Analysis, *Anal. Chem.* 73, 4196, 2001.
[82] Shadpour, H., Hupert, M. L., Patterson, D., Liu, C. G., Galloway, M., Stryjewski, W., Goettert, J., and Soper, S. A., Multichannel microchip electrophoresis device fabricated in polycarbonate with an integrated contact conductivity sensor array, *Anal. Chem.* 79, 870, 2007.
[83] Wen, J., Lin, Y. H., Xiang, F., Matson, D. W., Udseth, H. R., and Smith, R. D., Microfabricated isoelectric focusing device for direct electrospray ionization-mass spectrometry, *Electrophoresis* 21, 191, 2000.
[84] Bianchi, F., Chevolot, Y., Mathieu, H. J., and Girault, H. H., Photomodification of polymer microchannels induced by static and dynamic excimer ablation: effect on the electroosmotic flow, *Anal. Chem.* 73, 3845, 2001.
[85] Pugmire, D. L., Waddell, E. A., Haasch, R., Tarlov, M. J., and Locascio, E., Surface characterization of laser-ablated polymers used for microfluidics, *Anal. Chem.* 74, 871, 2002.
[86] Hashimoto, M., Barany, F., Xu, F., and Soper, S. A., Serial processing of biological reactions using flow-through microfluidic devices: coupled pcr/ldr for the detection of low-abundant dna point mutations, *Analyst* 132, 913-921, 2007.
[87] Kameoka, J., Craighead, H. G., Zhang, H. W., and Henion, J., A polymeric microfluidic chip for CE/MS determination of small molecules, *Anal. Chem.* 73, 1935, 2001.

[88] Bedair, M. F. and Oleschuk, R. D., Fabrication of porous polymer monoliths in polymeric microfluidic chips as an electrospray emitter for direct coupling to mass spectrometry, *Anal. Chem.* 78, 1130, 2006.
[89] Ro, K. W., Liu, H., and Knapp, D. R., Plastic microchip liquid chromatography-matrix-assisted laser desorption/ionization mass spectrometry using monolithic columns, *J. Chromatogr. A* 1111, 40, 2006.
[90] Li, C., Yang, Y., Craighead, H. G., and Lee, K. H., Isoelectric focusing in cyclic olefin copolymer microfluidic channels coated by polyacrylamide using a UV photografting method, *Electrophoresis* 26, 1800, 2005.
[91] Rossier, J., Reymond, F., and Michel, P. E., Polymer microfluidic chips for electrochemical and biochemical analyses, *Electrophoresis* 23, 858, 2002.
[92] Yin, H., Killeen, K., Brennen, R., Sobek, D., Werlich, M., and vandeGoor, T., Microfluidic chip for peptide analysis with an integrated HPLC column, sample enrichment column, and nanoelectrospray tip, *Anal. Chem.* 77, 527, 2005.
[93] Fuentes, H. V. and Woolley, A. T., Using Sacrificial Materials to Fabricate Polymeric Microfluidic Devices, in *Handbook of Capillary and Microchip Electrophoresis and Associated Microtechniques*, Landers, J. P., Ed. CRC Press, Boca Raton, FL, 2007.
[94] Whyte, W., *Cleanroom Technology: Fundamentals of Design , Testing, and Operation*, Wiley, New York, 2001.
[95] *http://www.iso.org/iso/iso_catalogue/catalogue_tc/catalogue_detail.htm?csnumber=25052* (accessed Nov. 5th, 2007).
[96] Verpoorte, E. and De Rooij, N. F., Microfluidics meets MEMS, in *Proc. IEEE* 91 (6), 930-953, 2003.
[97] Sze, S. M., *Semiconductor Devices: Physics and Technology,* 2nd Edition, John Wiley and Sons, Ney York, 2002.
[98] Gardeniers, J. G. E., Oosterbroek, R. E., and van den Berg, A., Silicon and Glass Micromachinning for μTAS, in *Lab on a Chip*, 1st. ed., Oosterbroek, R. E. and van den Berg, A. Ed. Elsevier, Amsterdam, 2003
[99] Shaw, K. A., Zhang, Z. L., and Mac Donald, N. C., A Single Mask, Single-Crystal Silicon, Reactive Ion Etching Process for Microelectromechanical Structures, *Sens. Actuators A* 40, 63, 1994.
[100] Contescu, C. I. and Putyera, K., Dekker *Encyclopedia of Nanoscience and Nanotechnology* Schwarz J. A. Ed., New York, Marcel Dekker, 2004.
[101] Franssila, S., *Introduction to Microfabrication*, John Wiley and Sons, England, 2004.
[102] Fan, Z. H. and Harrison, J. D., Micromachining of capillary electrophoresis injectors and separators on glass chips and evaluation of flow at capillary intersections, *Anal. Chem.* 66, 177, 1994.
[103] Fister, J. C., Jacobson, S. C., Davis, L. M., and Ramsey, J. M., Counting single chromophore molecules for ultrasensitive analysis and separations on microchip devices, *Anal. Chem.* 70, 431, 1998.
[104] Seidel, H., Csepregi, L., and Heuberger, A., Anisotropic etching of crytalline silicon in alkaline solutions, *J. Electrochem. Soc.* 137, 3612, 1990.
[105] Jacobson, S. C., Hergenroder, R., Koutny, L. B., Warmack, R. J., and Ramsey, J. M., Effects of injection schemes and column geometry on the performance of microchip electrophoresis devices, *Anal. Chem.* 66, 1107, 1994.

[106] Wang, H. Y., Foote, R. S., Jacobson, S. C., Schneibel, J. H., and Ramsey, J. M., Low temperature bonding for microfabrication of chemical analysis devices, *Sens. Actuators B* 45 199, 1997.
[107] Huang, Z., Sanders, J. C., Dunsmor, C., Ahmadzadeh, H., and Landers, J. P., A method for UV-bonding in the fabrication of glass electrophoretic microchips, *Electrophoresis* 22, 3924, 2001.
[108] Fonslow, B. R. and Bowser, M. T., Free-Flow Electrophoresis on an Anodic Bonded Glass Microchip, *Anal. Chem.* 77, 5706, 2005.
[109] Abgrall, P. and Gue, A.-M., Lab-on-chip technologies: making a microfluidic network and coupling it into a complete microsystem-A review, *J. Micromech. Microeng.* 17, R15, 2007.
[110] Nakanishi, H., Nishimoto, T., Nakamura, R., Yotsumoto, A., Yoshida, T., and Shoji, S., Studies on SiO_2-SiO_2 bonding with hydrofluoric acid. Room temperature and low stress bonding technique for MEMS, *Sens. Actuators A* 79, 237, 2000.
[111] Kamholz, A. E., Weigl, B. H., Finlayson, B. A., and Yager, P., Quantitative analysis of molecular interaction in a microfluidic channel: The T-sensor, *Anal. Chem.* 71, 5340, 1999.
[112] Petersson, F., Nilsson, A., Jonsson, H., and Laurell, T., Carrier medium exchange through ultrasonic particle switching in microfluidic channels, *Anal. Chem.* 77, 1216, 2005.
[113] Berthold, A., Nicola, L., Sarro, P. M., and Vellekoop, M. J., Glass-to-glass anodic bonding with standard IC technology thin films as intermediate layers, *Sens. Actuators A* 82, 224, 2000.
[114] Liu, J., Pan, T., Woolley, A. T., and Lee, M. L., Surface-Modified Poly(methyl methacrylate) Capillary Electrophoresis Microchips for Protein and Peptide Analysis *Anal. Chem.* 76, 6948, 2004.
[115] Becker, H. and Gartner, C., Polymer microfabrication methods for microfluidic analytical applications, *Electrophoresis* 21, 12, 2000.
[116] Martynova, L., Locascio, L. E., Gaitan, M., Kramer, G. W., Christensen, R. G., and MacCrehan, W. A., Fabrication of plastic microfluid channels by imprinting methods, *Anal. Chem.* 69, 4783, 1997.
[117] Becker, H. and Heim, U., Hot embossing as a method for the fabrication of polymer high aspect ratio structures, *Sens. Actuators A* 83, 130, 2000.
[118] Effenhauser, C. S., Bruin, G. J. M., Paulus, A., and Ehrat, M., Integrated capillary electrophoresis on flexible silicone microdevices: analysis of dna restriction fragments and detection of single dna molecules on microchips, *Anal. Chem.* 69, 3451, 1997.
[119] Unger, M. A., Chou, H.-P., Thorsen, T., Scherer, A., and Quake, S. R., Monolithic microfabricated valves and pumps by multilayer soft lithography, *Science* 288, 113, 2000.
[120] Anderson, J. R., Chiu, D. T., Jackman, R. J., Cherniavskaya, O., McDonald, J. C., Wu, H., Whitesides, S. H., and Whitesides, G. M., Fabrication of topologically complex three-dimensional microfluidic systems in pdms by rapid prototyping, *Anal. Chem.* 72 , 3158, 2000.
[121] Jo, B. H., Van Lerberghe, L. M., Motsegood, K. M., and Beebe, D. J., Three-dimensional micro-channel fabrication in polydimethylsiloxane (PDMS) elastomer, *J. Microelectromech. Syst.* 9, 76, 2000.

[122] Fiorini, G. S., Lorenz, R. M., Kuo, J. S., and Chiu, D. T., Rapid prototyping of thermoset polyester microfluidic devices, *Anal. Chem.* 76, 4697, 2004.
[123] Fiorini, G. S., Jeffries, G. D. M., Lim, D. S. W., Kuyper, C. L., and Chiu, D. T., Fabrication of thermoset polyester microfluidic devices and embossing masters using rapid prototyped polydimethylsiloxane molds, *Lab Chip* 3, 158, 2003.
[124] Castaño-Álvarez, M., Fernández-Abedul, M. T., and Costa-García, A., Poly(methylmethacrylate) and Topas capillary electrophoresis microchip performance with electrochemical detection, *Electrophoresis* 26, 3160, 2005.
[125] Kelly, R. T. and Woolley, A. T., Thermal bonding of polymeric capillary electrophoresis microdevices in water, *Anal. Chem.* 75, 1941-1945, 2003.
[126] Kricka, L. J., Fortina, P., Panaro, N. J., Wilding, P., Alonso-Amigo, G., and Becker, H., Fabrication of plastic microchips by hot embossing, *Lab Chip* 2, 1, 2002.
[127] Grasß, B., Neyer, A., Jöhnck, M., Siepe, D., Eisenbeisß, F., Weber, G., and Hergenroder, R., A new PMMA-microchip device for isotachophoresis with integrated conductivity detector, *Sens. Actuators B* 72, 249, 2001.
[128] Heckele, M. and Schomburg, W. K., Review on micromolding of thermoplastic polymers, *J. Micromech. Microeng.* 14, 1, 2004.
[129] Sassi, A. P., Paulus, A., Cruzado, I. D., Bjornson, T., and Hooper, H. H., Rapid, parallel separations of D1S80 alleles in a plastic microchannel chip, *J. Chromatogr. A* 894, 203, 2000.
[130] Mair, D. A., Geiger, E., Pisano, A. P., Frechet, J. M. J., and Svec, F., Injection molded microfluidic chips featuring integrated interconnects, *Lab Chip* 6, 1346, 2006.
[131] Ford, S. M., Davies, J., Kar, B., Qi, S. D., McWhorter, S., Soper, S. A., and Malek, C. K., Micromachining in plastics using X-ray lithography for the fabrication of microelectrophoresis devices, *J. Biomech. Eng.* 121, 13, 1999.
[132] Wang, J., Pumera, M., Chatrathi, M. P., Escarpa, A., Konrad, R., Griebel, A., Dorner, W., and Lowe, H., Towards disposable lab-on-a-chip: poly(methylmethacrylate) microchip electrophoresis device with electrochemical detection, *Electrophoresis* 23, 596, 2002.
[133] Doherty, E. A. S., Meagher, R. J., Albarghouthi, M. N., and Barron, A. E., Microchannel wall coatings for protein separations by capillary and chip electrophoresis, *Electrophoresis* 24, 34, 2003.
[134] Glasgow, I. K., Beebe, D. J., and White, V. E., Design rules for polyimide solvent bonding, *Sens. Mater.* 11, 269, 1999.
[135] Harper, C. A. and Petrie, E. M., *Plastic materials and processes: A concise enclyclopedia*, Wiley Interscience, New York, 2003.
[136] Lin, C. B., Lee, S. B., and Liu, K. S., The microstructure of solvent-welding of PMMA, *J. Adhes.* 34 (1-4), 221-240, 1991.
[137] Griebel, A., Rund, S., Schonfeld, F., Dorner, W., Konrad, R., and Hardt, S., Integrated polymer chip for two-dimensional capillary gel electrophoresis, *Lab Chip* 4, 18, 2004.
[138] Brown, L., Koerner, T., Horton, J. H., and Oleschuk, R. D., Fabrication and characterization of poly(methylmethacrylate) microfluidic devices bonded using surface modifications and solvents, *Lab Chip* 6, 66, 2006.
[139] Wu, H., Huang, B., and Zare, R. N., Construction of microfluidic chips using polydimethylsiloxane for adhesive bonding, *Lab Chip* 5, 1393, 2005.

[140] Satyanarayana, S., Karnik, R. N., and Majumdar, A., Stamp-and-stick room-temperature bonding technique for microdevices, *J. Microelectromech. Syst.* 14, 392, 2005.
[141] Song, L., Fang, D., Kobos, R. K., Pace, S. J., and Chu, B., Separation of double-stranded DNA fragments in plastic capillary electrophoresis chips by using $E_{99}P_{69}E_{99}$ as separation medium, *Electrophoresis* 20, 2847, 1999.
[142] Lai, S. Y., Cao, X., and Lee, L. J., A packaging technique for polymer microfluidic platforms, *Anal. Chem.* 76, 1175, 2004.
[143] Bianchi, F., Wagner, F., Hoffmann, P., and Girault, H. H., Electroosmotic flow in composite microchannels and implications in microcapillary electrophoresis systems, *Anal. Chem.* 73, 829, 2001.
[144] Sikanen, T., Tuomikoski, S., Ketola, R. A., Kostiainen, R., Franssila, S., and Kotiaho, T., Characterization of SU-8 for electrokinetic microfluidic applications, *Lab Chip* 5, 888, 2005.
[145] Tuomikoski, S. and Franssila, S., Free-standing SU-8 microfluidic chips by adhesive bonding and release etching, *Sens. Actuators A* 120, 408, 2005.
[146] Lee, K. Y., LaBianca, N., Riston, S. A., Zolgharnain, S., Gelorme, J. D., Shaw, J., and Chang, T. H. P., Micromachining applications of a high resolution ultrathick photoresist, *J. Vac. Sci. Tech. B.* 13, 3012, 1995.
[147] Sikanen, T., Heikkila, L., Tuomikoski, S., Ketola, R. A., Kostiainen, R., Franssila, S., and Kotiaho, T., Performance of SU-8 Microchips as Separation Devices and Comparison with Glass Microchips, *Anal. Chem.*, 2007.
[148] Agirregabiria, M., Blanco, F. J., Berganzo, J., Arroyo, M. T., Fullaondo, A., Mayora, K., and Ruano-Lopez, J. M., Fabrication of SU-8 multilayer microstructures based on successive CMOS compatible adhesive bonding and releasing steps, *Lab Chip* 5, 545, 2005.
[149] Sun, X., Peeni, B. A., Yang, W., Becerril, H. A., and Woolley, A. T., Rapid prototyping of poly(methyl methacrylate) microfluidic systems using solvent imprinting and bonding, *J. Chromatogr. A* 1162, 162, 2007.
[150] Verpoorte, E., Microfluidic chips for clinical and forensic analysis, *Electrophoresis* 23, 677, 2002.
[151] Vilkner, T., Janasek, D., and Manz, A., Micro Total Analysis Systems. Recent Developments, *Anal. Chem.* 76, 3373, 2004.
[152] Landers, J. P., Handbook of Capillary Electrophoresis, 2nd Edition, *CRC, Boca Raton, FL*, 1997.
[153] Monnig, C. A. and Kennedy, R. T., Capillary Electrophoresis, *Anal. Chem.* 66 (12), R280-R314, 1994.
[154] Camilleri, P., *Capillary electrophoresis: Theory and practice* CRC Press, Boca Raton, FL, 1993.
[155] Emrich, C. A., Tian, H. J., Medintz, I. L., and Mathies, R. A., Microfabricated 384-lane capillary array electrophoresis bioanalyzer for ultrahigh-throughput genetic analysis, *Anal. Chem.* 74 , 5076, 2002.
[156] Ramsey, J. D., Jacobson, S. C., Culbertson, C. T., and Ramsey, J. M., High-efficiency, two-dimensional separations of protein digests on microfluidic devices, *Anal. Chem.* 75, 3758, 2003.

[157] Broyles, B. S., Jacobson, S. C., and Ramsey, J. M., Sample filtration, concentration, and separation integrated on microfluidic devices, *Anal. Chem.* 75 , 2761, 2003.
[158] Jacobson, S. C., Hergenroder, R., Moore, A. W., and Ramsey, J. M., Precolumn Reactions with Electrophoretic Analysis Integrated on a Microchip, *Anal. Chem.* 66, 4127, 1994.
[159] Jacobson, S. C., Koutny, L. B., Hergenroder, R., Moore, A. W., and Ramsey, J. M., Microchip Capillary Electrophoresis with an Integrated Postcolumn Reactor, *Anal. Chem.* 66, 3472, 1994.
[160] Fuentes, H. V. and Woolley, A. T., Phase-changing sacrificial layer fabrication of multilayer polymer microfluidic devices, *Anal. Chem.* (in press), 2007.
[161] Hsieh, S. S., Lin, C. Y., Huang, C. F., and Tsai, H. H., Liquid flow in a micro-channel, *J. Micromech. Microeng.* 14, 436, 2004.
[162] Schasfoort, R. B. M. and Tudos, A. J., *Separation and detection on a chip,* In*:* BioMEMS, Urban, G.A. Ed., Springer, The Netherlands, 2006.
[163] Van Theemsche, A., Deconinck, J., Van den Bossche, B., and Bortels, L., Numerical solution of a multi-ion one-potential model for electroosmotic flow in two-dimensional rectangular microchannels, *Anal. Chem.* 74, 4919, 2002.
[164] Hayes, M. A. and Ewing, A. G., Electroosmotic Flow-Control and Monitoring with an Applied Radial Voltage for Capillary Zone Electrophoresis, *Anal. Chem.* 64, 512, 1992.
[165] Hjerten, S., Zone broadening in electrophoresis with special reference to high-performance electrophoresis in capillaries - an interplay between theory and practice, *Electrophoresis* 11, 665, 1990.
[166] Roddy, E. S., Xu, H. W., and Ewing, A. G., Sample introduction techniques for microfabricated separation devices, *Electrophoresis* 25, 229, 2004.
[167] Wenclawiak, B. W. and Puschl, R., Sample injection for capillary electrophoresis on a micro fabricated device/on chip CE injection, *Anal. Lett.* 39, 3, 2006.
[168] Ermakov, S. V., Jacobson, S. C., and Ramsey, J. M., Computer simulations of electrokinetic injection techniques in microfluidic devices, *Anal. Chem.* 72, 3512, 2000.
[169] Lee, N. Y., Yamada, M., and Seki, M., Pressure-driven sample injection with quantitative liquid dispensing for on-chip electrophoresis, *Anal. Sci.* 20, 483, 2004.
[170] Vazquez, M., McKinley, G., Mitnik, L., Desmarais, S., Matsudaira, P., and Ehrlich, D., Electrophoretic injection within microdevices, *Anal. Chem.* 74, 1952, 2002.
[171] Ramseier, A., von Heeren, F., and Thormann, W., Analysis of fluorescein isothiocyanate derivatized amphetamine and analogs in human urine by capillary electrophoresis in chip-based and fused-silica capillary instrumentation, *Electrophoresis* 19, 2967, 1998.
[172] Shi, Y., Simpson, P. C., Scherer, J. R., Wexler, D., Skibola, C., Smith, M. T., and Mathies, R. A., Radial capillary array electrophoresis microplate and scanner for high-performance nucleic acid analysis, *Anal. Chem.* 71, 5354, 1999.
[173] Zhang, C. X. and Manz, A., Narrow sample channel injectors for capillary electrophoresis on microchips, *Anal. Chem.* 73, 2656, 2001.
[174] Schwarz, M. A. and Hauser, P. C., Recent Developments in Detection Methods for Microfabricated Analytical Devices, *Lab Chip* 1, 1, 2001.
[175] Vandaveer, W. R., Pasas, S. A., Martin, R. S., and Lunte, S. M., Recent developments in amperometric detection for microchip capillary electrophoresis, *Electrophoresis* 23, 3667, 2002.

[176] Mogensen, K. B., Klank, H., and Kutter, J. P., Recent developments in detection for microfluidic systems, *Electrophoresis* 25, 3498, 2004.
[177] Viskari, P. J. and Landers, J. P., Unconventional detection methods for microfluidic devices, *Electrophoresis* 27, 1797, 2006.
[178] Lu, H., Schmidt, M. A., and Jensen, K. F., Photochemical reactions and on-line UV detection in microfabricated reactors *Lab Chip* 1, 22, 2001.
[179] Mao, Q. and Pawlisyn, J., *Analyst* 124, 637, 1999.
[180] Cellar, N. A. and Kennedy, R. T., A capillary-PDMS hybrid chip for separations-based sensing of neurotransmitters in vivo, *Lab Chip* 6, 1205, 2006.
[181] De Montigny, P., Stobaugh, J. F., Givens, R. S., Carlson, R. G., Srinivasachar, K., Sternson, L. A., and Higuchi, T., Napthalene-2,3-dicarboxyaldehyde/cynaide ion: a rationally designed fluoregenic reagent for primary amines, *Anal. Chem.* 59, 1096, 1987.
[182] Ocvirk, G., Tang, T., and Harrison, D. J., Optimization of confocal epifluorescence microscopy for microchip-based miniaturized total analysis systems, *Analyst* 123 (7), 1429-1434, 1998.
[183] Gosch, M., Blom, H., Holm, J., Heino, T., and Rigler, R., Hydrodynamic flow profiling in microchannel structures by single molecule fluorescence correlation spectroscopy, *Anal. Chem.* 72, 3260, 2000.
[184] Webster, J. R., Burns, M. A., Burke, D. T., and Mastrangelo, C. H., Monolithic capillary electrophoresis device with integrated fluorescence detector, *Anal. Chem.* 73, 1622, 2001.
[185] Wang, J. and Pumera, M., Dual conductivity/amperometric detection system for microchip capillary electrophoresis, *Anal. Chem.* 74, 5919, 2002.
[186] Rossier, J. S., Roberts, M. A., Ferrigno, R., and Girault, H. H., Electrochemical detection in polymer microchannels, *Anal. Chem.* 71, 4294, 1999.
[187] Fritsch, I. and Aguilar, Z. P., *Anal. Bioanal. Chem.* 387, 159-163, 2007.
[188] Woolley, A. T., Lao, K. Q., Glazer, A. N., and Mathies, R. A., Capillary electrophoresis chips with integrated electrochemical detection, *Anal. Chem.* 70, 684, 1998.
[189] Baldwin, R. P., Roussel, T. J., Crain, M. M., Bathlagunda, V., Jackson, D. J., Gullapalli, J., Conklin, J. A., Pai, R., Naber, J. F., Walsh, K. M., and Keynton, R. S., Fully integrated on-chip electrochemical detection for capillary electrophoresis in a microfabricated device, *Anal. Chem.* 74, 3690, 2002.
[190] Dolnik, V., Liu, S., and Jovanovich, S., Capillary electrophoresis on microchip, *Electrophoresis* 21, 41, 2000.
[191] Bruin, G. J. M., Recent developments in electrokinetically driven analysis on microfabricated devices, *Electrophoresis* 21, 3931, 2000.
[192] Lapos, J. A., Manica, D. P., and Ewing, A. G., Dual fluorescence and electrochemical detection on an electrophoresis microchip, *Anal. Chem.* 74, 3348, 2002.
[193] Pumera, M., Wang, J., Opekar, F., Jelinek, I., Feldman, J., Lowe, H., and Hardt, S., Contactless conductivity detector for microchip capillary electrophoresis, *Anal. Chem.* 74, 1968, 2002.
[194] Tang, T., Badal, M. Y., Ocvirk, G., Lee, W. E., Bader, D. E., Bekkaoui, F., and Harrison, D. J., Integrated microfluidic electrophoresis system for analysis of genetic materials using signal amplification methods, *Anal. Chem.* 74, 725, 2002.

[195] Ramsey, R. S. and Ramsey, J. M., Generating Electrospray from Microchip Devices Using Electroosmotic Pumping, *Anal. Chem.* 69, 1174, 1997.
[196] Zhang, B., Foret, F., and Karger, B. L., A microdevice with integrated liquid junction for facile peptide and protein analysis by capillary electrophoresis/electrospray mass spectrometry, *Anal. Chem.* 72 1015, 2000.
[197] Xu, N. X., Lin, Y. H., Hofstadler, S. A., Matson, D., Call, C. J., and Smith, R. D., A microfabricated dialysis device for sample cleanup in electrospray ionization mass spectrometry, *Anal. Chem.* 70, 3553, 1998.
[198] Lazar, I. M., Trisiripisal, P., and Sarvaiya, H. A., Microfluidic liquid chromatography system for proteomic applications and biomarker screening, *Anal. Chem.* 78, 5513, 2006.
[199] Lazar, I. M., Grym, J., and Foret, F., Microfabricated devices: A new sample introduction approach to mass spectrometry, *Mass Spec. Rev.* 25, 573, 2006.
[200] Connatser, R. M., Riddle, R. A., and Sepaniak, M. J., Metal-polymer nanocomposites for integrated microfluidic separations and surface enhanced Raman spectroscopy detection, *J. Sep. Sci.* 27, 1545, 2004.
[201] Massin, C., Vincent, F., Homsy, A., Ehrmann, K., Boero, G., Besse, P. A., Daridon, A., Verpoorte, E., de Rooij, N. F., and Popovic, R. S., Planar microcoil-based microfluidic NMR probes, *J. Magn. Res.* 164, 242, 2003.
[202] Lion, N., Reymond, F., Girault, H. H., and Rossier, J. S., Why the move to microfluidics for protein analysis?, *Curr. Opin. Biotech.* 15, 31, 2004.
[203] Rios, A., Escarpa, A., Gonzalez, M. C., and Crevillen, A. G., Challenges of analytical microsystems, *Trends Anal. Chem.* 25, 467, 2006.
[204] Kamholz, A. E., Proliferation of microfluidics in literature and intellectual property, *Lab Chip* 4, 16N, 2004.
[205] Freemantle, M., Downsizing chemistry, *Chem. Eng. News* 77, 27, 1999.
[206] Tay, F. E. H., *Microfluidics and BioMEMS,* Kluwer Academic Pub, The Netherlands, 2002.
[207] Nguyen, N.-T., Huang, X., and Chuan, T. K., MEMS-Micropumps: A Review, *J. Fluids Eng.* 124 (6), 384-392, 2002.
[208] Rapp, R., Schomburg, W. K., Maas, D., Schulz, J., and Stark, W., LIGA micropump for gases and liquids, *Sens. Actuators A* 40, 57, 1994.
[209] Carrozza, M. C., Croce, N., Magnani, B., and Dario, P., A Piezoelectric-Driven Stereolithography-Fabricated Micropump, *J. Micromech. Microeng.* 5, 177, 1995.
[210] Tsai, J.-H. and Lin, L., Active microfluidic mixer and gas bubble filter driven by thermal bubble micropump, *Sens. Actuators A* 48, 665, 2002.
[211] Zengerle, R., Geiger, W., Richter, M., Ulrich, J., Kluge, S., and Richter, A., Transient measurements on miniaturized diaphragm pumps in microfluid systems, *Sens. Actuators A* 47, 557, 1995.
[212] Koch, M., Evans, A., and Brunnschweiler, A., *Microfluidic Technology and Applications* RSP Press, Bangor, UK, 2000.
[213] Xie, J., Shih, J., Lin, Q. A., Yang, B. Z., and Tai, Y. C., Surface micromachined electrostatically actuated micro peristaltic pump, *Lab Chip* 4, 495, 2004.
[214] Smits, J. G., Piezoelectric Micropump with Three Valves Working Peristaltically, *Sens. Actuators A* 36, 203, 1990.
[215] Truong, T. Q. and Nguyen, N. T., A polymeric piezoelectric micropump based on lamination technology, *J. Micromech. Microeng.* 14, 632, 2004.

[216] Nguyen, N. T. and Truong, T. Q., A fully polymeric micropump with piezoelectric actuator, *Sens. Actuators B* 97, 137, 2004.
[217] Anjanappa, M., Angara, R., and Si, L., Micro/MEMS Actuators for Microfluidic Applications, in *Proc. ISSS*, Bangalore, India, 2005.
[218] Zeng, S., Chen, C.-H., Mikkelsen, Jr. J. C., and Santiago, J. G., Fabrication and characterization of electroosmotic micropumps, *Sens. Actuators B* 79, 107, 2001.
[219] Jang, J. S. and Lee, S. S., Theoretical and experimental study of MHD (magnetohydrodynamic) micropump, *Sens. Actuators A* 80, 84, 2000.
[220] Neagu, C. R., Gardeniers, J. G. E., Elwenspoek, M., and Kelly, J. J., An electrochemical microactuator: Principle and first results, *J. Microelectromech. Syst.* 5, 2, 1996.
[221] Lazar, I. M. and Karger, B. L., Multiple Open-channel electroosmotic pumping system for microfluidic sample handling, *Anal. Chem.* 74, 6259, 2002.
[222] Edwards, J. M., Hamblin, M. N., Fuentes, H. V., Peeni, B. A., Lee, M. L., Woolley, A. T., and Hawkins, A. R., Thin film electroosmotic pumps for biomicrofluidic applications, *Biomicrofluidics.* 1 (014101), 1, 2007.
[223] Nie, F.-Q., Macka, M., Barron, L., Connolly, D., Kent, N., and Paull, B., Robust monolithic silica-based on-chip electro-osmotic micro-pump, *Analyst* 132, 417, 2007.
[224] Hua, S. Z., Sachs, F., Yang, D. X., and Chopra, D. H., Microfluidic Actuation Using Electrochemically Generated Bubbles, *Anal. Chem.* 74, 6392, 2002.
[225] Xie, J., Miao, Y. N., Shih, J., He, Q., Liu, J., Tai, Y. C., and Lee, T. D., An electrochemical pumping system for on-chip gradient generation, *Anal. Chem.* 76, 3756, 2004.
[226] Norman, M. A., Evans, C. E., Fuoco, A. R., Noble, R. D., and Koval, C. A., Characterization of a membrane-based, electrochemically driven pumping system using aqueous electrolyte solutions, *Anal. Chem.* 77, 6374, 2005.
[227] Bohm, S., Timmer, B., Olthuis, W., and Bergveld, P., A closed-loop controlled electrochemical actuated micro-dosing system, *J. Micromech. Microeng.* 10, 498, 2000.
[228] Okeefe, D., Oherlihy, C., Gross, Y., and Kelly, J. G., Patient-Controlled Analgesia Using a Miniature Electrochemically Driven Infusion-Pump, *Brit. J. Anaesth.* 73, 843, 1994.
[229] Furdui, V. I., Kariuki, J. K., and Harrison, D. J., Microfabricated electrolysis pump system for isolating rare cells in blood, *J. Micromech. Microeng.* 13, S164, 2003.
[230] Nyholm, L., Electrochemical techniques for lab-on-a-chip applications, *Analyst* 130, 599, 2005.
[231] Munyan, J. W., Fuentes, H. V., Draper, M., Kelly, R. T., and Woolley, A. T., Electrically actuated, pressure-driven microfluidic pumps, *Lab Chip* 3, 217, 2003.
[232] Xie, J., Miao, Y., Shih, J., Tai, Y.-C., and Lee, T. D., Microfluidic platform for liquid chromatography-tandem mass spectrometry analyses of complex peptide mixtures, *Anal. Chem.* 77, 6947, 2005.
[233] Fuentes, H. V. and Woolley, A. T., Electrically actuated, pressure-driven liquid chromatography separations in microfabricated devices, *Lab Chip* 7, 1524, 2007.
[234] Suzuki, H. and Yoneyama, R., Integrated microfluidic system with electrochemically actuated on-chip pumps and valves, *Sens. Actuators B* 96, 38, 2003.
[235] Sadek, P. C., *The HPLC Solvent Guide*, 2nd Ed., Wiley-Interscience, New York, 2002.
[236] Harris, C. M., Shrinking the LC landscape, *Anal. Chem.* 75, 64A, 2003.

[237] de Mello, A., On-chip chromatography: the last twenty years, *Lab Chip* 2, 48N, 2002.
[238] Serwe, M. and Ross, G. A., A comparison of CE-MS and LC-MS for peptide samples, *LC GC* 18, 46, 2000.
[239] Prado, M. S. A., Steppe, M., Tavares, M. F. M., Kedor-Hackmann, E. R. M., and Santoro, M. I. R. M., Comparison of capillary electrophoresis and reversed-phase liquid chromatography methodologies for determination of diazepam in pharmaceutical tablets, *J. Pharm. Biomed. Anal.* 37, 273, 2005.
[240] Snyder, L. R., Introduction to Modern Liquid Chromatography, *Wiley-Interscience, New York*, 1974.
[241] Ishii, D. and Ed., *Introduction to Microscale High-Performance Liquid Chromatography*, VCH Publishers, Weinheim, 1988.
[242] Chervet, J. P., Ursem, M., and Salzmann, J. B., Instrumental requirements for nanoscale liquid chromatography, *Anal. Chem.* 68, 1507, 1996.
[243] Szumski, M. and Buszewski, B., State of the art in miniaturized separation techniques, *Crit. Rev. Anal. Chem.* 32, 1, 2002.
[244] McEnery, M., Tan, A. M., Alderman, J., Patterson, J., O'Mathuna, S. C., and Glennon, J. D., Liquid chromatography on-chip: progression towards a micro total analysis system, *Analyst* 125, 25, 1999.
[245] O'Neill, A. P., O'Brien, P., Alderman, J., Hoffman, D., McEnery, M., Murrihy, J., and Glennon, J. D., On-chip definition of picolitre sample injection plugs for miniaturised liquid chromatography, *J. Chromatogr. A* 924, 259, 2001.
[246] Ericson, C., Holm, J., Ericson, T., and Hjerten, S., Electroosmosis- and pressure-driven chromatography in chips using continuous beds, *Anal. Chem.* 72, 81, 2000.
[247] Reichmuth, D. S., Shepodd, T. J., and Kirby, B. J., Microchip HPLC of peptides and proteins, *Anal. Chem.* 77, 2997, 2005.
[248] Stachowiak, T. B., Svec, F., and Frechet, J. M. J., Chip electrochromatography, *J. Chromatogr. A* 1044, 97, 2004.
[249] Unger, K. K., Huber, M., Walhagen, K., Hennessy, T. P., and Hearn, M. T. W., A critical appraisal of capillary electrochromatography., *Anal. Chem.* 74, 200A, 2002.
[250] Throckmorton, D. J., Shepodd, T. J., and Singh, A. K., Electrochromatography in microchips: Reversed-phase separation of peptides and amino acids using photopatterned rigid polymer monoliths, *Anal. Chem.* 74, 784, 2002.
[251] Yu, C., Svec, F., and Frechet, J. M. J., Towards stationary phases for chromatography on a microchip: Molded porous polymer monoliths prepared in capillaries by photoinitiated in situ polymerization as separation media for electrochromatography, *Electrophoresis* 21, 120, 2000.
[252] Jemere, A. B., Oleschuk, R. D., and Harrison, D. J., Microchip-based capillary electrochromatography using packed beds, *Electrophoresis* 24, 3018, 2003.
[253] Dulay, M. T., Quirino, J. P., Bennett, B. D., and Zare, R. N., Bonded-phase photopolymerized sol-gel monoliths for reversed phase capillary electrochromatography, *J. Sep. Sci.* 25, 3, 2002.
[254] Ceriotti, L., de Rooij, N. F., and Verpoorte, E., An integrated fritless column for on-chip capillary electrochromatography with conventional stationary phases, *Anal. Chem.* 74, 639, 2002.

[255] Grover, W. H., Skelley, A. M., Liu, C. N., Lagally, E. T., and Mathies, R. A., Monolithic membrane valves and diaphragm pumps for practical large-scale integration into glass microfluidic devices, *Sens. Actuators B* 89, 315, 2003.
[256] Chen, J. R., Dulay, M. T., Zare, R. N., Svec, F., and Peters, E., Macroporous photopolymer frits for capillary electrochromatography, *Anal. Chem.* 72, 1224-1227, 2000.
[257] Svec, F., Porous monoliths: The newest generation of stationary phases for HPLC and related methods, *LC GC Europe* 16, 24, 2003.
[258] Gu, B., Armenta, J. M., and Lee, M. L., Preparation and evaluation of poly(polyethylene glycol methyl ether acrylate-copolyetheylene glycol diacrylate) monolith for protein anlysis, *J. Chromatogr. A* (1079), 382, 2005.
[259] Tanaka, N., Kobayashi, H., Nakanishi, K., Minakuchi, H., and Ishizuka, N., Monolithic LC columns, *Anal. Chem.* 73, 420A, 2001.
[260] Merhar, M., Podgornik, A., Barut, M., Zigon, M., and Strancar, A., Methacrylate monoliths prepared from various hydrophobic and hydrophilic monomers - Structural and chromatographic characteristics, *J. Sep. Sci.* 26, 322, 2003.
[261] Svec, F., Peters, E. C., Sykora, D., and Frechet, J. M. J., Design of the monolithic polymers used in capillary electrochromatography columns, *J. Chromatogr. A* 887, 3, 2000.
[262] Gusev, I., Huang, X., and Horvath, C., Capillary columns with in situ formed porous monolithic packing for micro high-performance liquid chromatography and capillary electrochromatography, *J. Chromatogr. A* 855, 273, 1999.
[263] Cabrera, K., Lubda, D., Eggenweiler, H. M., Minakuchi, H., and Nakanishi, K., A new monolithic-type HPLC column for fast separations, *J. High Res. Chromatogr.* 23, 93, 2000.
[264] Tanaka, N., Nagayama, H., Kobayashi, H., Ikegami, T., Hosoya, K., Ishizuka, N., Minakuchi, H., Nakanishi, K., Cabrera, K., and Lubda, D., Monolithic silica columns for HPLC, micro-HPLC, and CEC, *J. High Res. Chromatogr.* 23, 111, 2000.
[265] Stachowiak, T. B., Rohr, T., Hilder, E. F., Peterson, D. S., Yi, M., Svec, F., and Fréchet, J. M. J., Fabrication of porous polymer monoliths covalently attached to the walls of channels in plastic microdevices, *Electrophoresis* 24, 3689, 2003.
[266] Swart, R., Kraak, J. C., and Poppe, H., Recent progress in open tubular liquid chromatography, *Trends Anal. Chem.* 16, 332, 1997.

2. ELECTRICALLY ACTUATED, PRESSURE-DRIVEN MICROFLUIDIC PUMPS*

2.1 INTRODUCTION

Miniaturization of chemical analysis using tools developed in the microelectronics industry offers significant advantages in terms of speed, throughput, and sample and reagent consumption. The potential benefits of miniaturization are perhaps best illustrated with microchip capillary electrophoresis,[1] where rapid, high-resolution, parallel analyses are readily performed.[2,3] However, analysis is but one of several operations including mixing and moving analytes through capillaries that must be miniaturized for the lab-on-a-chip concept to become a reality. Moreover, while electrically driven methods work well for analytes such as DNA,[4-6] miniaturizing pressure-driven chromatographic separations would greatly expand the versatility of microfluidic analysis. Thus, the development of a simple, easily integrated micropump system for use with microfluidic instrumentation would be very desirable.

Ideally, pumps should be miniaturized to reduce costs, facilitate their integration into microfluidic platforms, and eliminate the need for additional specialized or bulky equipment. Hence, pumps having small physical dimensions, but requiring connection to an external pressurized gas cylinder or vacuum system,[7,8] fall short of ideal characteristics. Microelectromechanical system (MEMS)-based micropumps with mechanical actuators and check valves[9-11] offer an elegant, though costly solution to

pumping. While MEMS-based micropumps typically can have the fluid outlet integrated on-chip, these systems lack flexibility in integration with a wide range of microfluidic substrates. Other non-MEMS micropumps demonstrated to date rely on electromagnetic[12,13] or electroosmotic[14-16] forces. However, these micropumps have the disadvantages of requiring bulky electromagnets, high voltages, charged samples, or charged microchannel wall surfaces. In particular, electrophoretic and electroosmotic micropumps are very sensitive to sample characteristics such as pH, ionic strength, and organic additives.[14]

While the concept of using gas from electrolysis to pump fluids is not new,[17] a facile way to interface this pumping approach with a wide range of planar microfluidic substrates has not been devised. Initial electrolysis-based pumping techniques used the generated gas to actuate a membrane and displace fluid;[17,18] however, these systems were intended primarily for ~10 mL drug delivery applications. Another early approach to the electrochemical pumping of liquids utilized electrolytic membranes;[19] a variant of this type of pump is available commercially (medecell.com), albeit with 5–10 mL pump volumes that vastly exceed the needs of planar microfluidic substrates. More recently, electrolysis gas membrane displacement has been adapted to a micromachined format; however, only membrane displacement and not fluid pumping was studied.[20] Microfabrication techniques have also been applied to the direct displacement of fluid by electrolysis gas generation.[21,22] While these micromachined pumps have outlets directly integrated on each device, the coupling of such pumps to different microfluidic substrates has not been demonstrated. Furthermore, although these systems are designed to allow pumping of a fluid different from the electrolysis solution, all results presented to date

have involved the pumping of aqueous KNO_3 electrolysis solution.[21,22] Thus, I was interested in developing low-cost micropumps that could be used to pump various types of liquids and could be integrated easily with different microfluidic substrates.

Here, I present a novel design for an electrically actuated pressure-driven electrochemical micropump. In this format, the build-up of electrolysis gases in an enclosed chamber provides pressure for pumping. The micropumps have a poly(dimethylsiloxane) (PDMS)[23] body, enabling them to be sealed reversibly over a microchannel reservoir, which facilitates integration with a variety of planar microfluidic substrates. Moreover, this pump design enables pumping of fluids different from the electrolyte solution. Other important features of this micropump configuration include construction from relatively inexpensive materials, use of low voltages, and facile ability to be interfaced with computer control. I tested a number of these devices in pumping experiments on microfluidic channels, studied their flow rate reproducibility, and compared the results with theoretical predictions.

2.2 EXPERIMENTAL METHODS

2.2.1 Micropump fabrication

The micropumps were constructed by embedding polypropylene (PP) interior components in a PDMS (Sylgard 184, Dow Corning, Midland, MI) matrix (**Figure 2.1**). Briefly, the micropumps consist of two electrodes (EL) in an electrolyte chamber (EC) with a snugly fitting cap (SC). A small opening in the upper side of the EC leads to the

bottom of the device *via* a connector tube (CT). This enables pressure generated within the EC to be applied to a microchannel reservoir sealed beneath the lower opening of the CT.

The first step in fabrication consisted of assembling the interior components. The EC was formed by removing the bottom conical portion of a 0.5 mL PP microcentrifuge tube and placing the cap from another microcentrifuge tube snugly in this opening to seal the bottom. A small hole was made near the top on the side of the microcentrifuge tube, into which the end of a 200 µL PP micropipette tip was inserted to form the CT. The EC was perforated with two additional holes, just large enough for the insertion of two platinum wire electrodes (32 gauge) wrapped around the stripped ends of insulated copper wire.

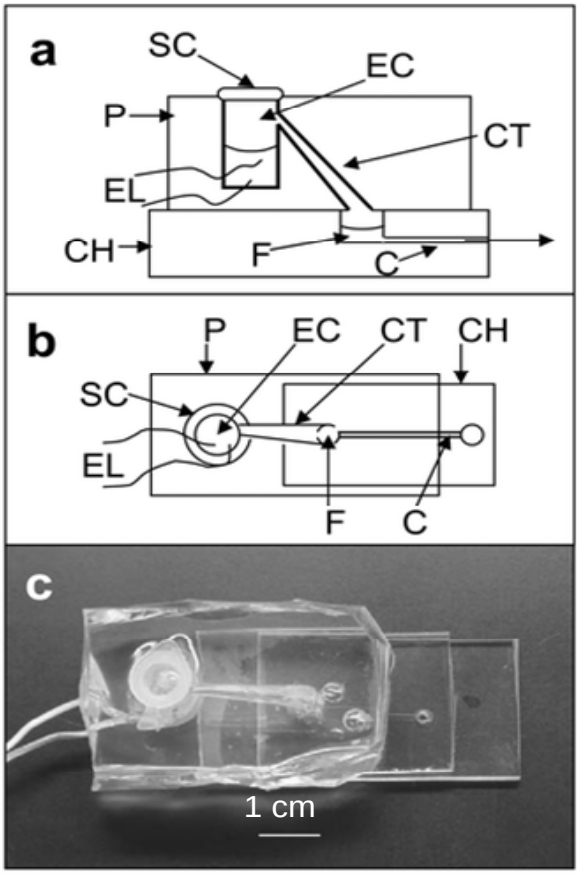

Figure. 2.1 Schematic drawing of a micropump attached to a channel. (a) Side view of assembly. (b) Top view of pump system. (c) Photograph of an assembled micropump and microchannel, scale bar is 1 cm. Legend: EL = electrodes, EC = electrolyte chamber, F = fluid to be pumped, C = channel, SC = snugly fitting cap on the electrolyte chamber, P = pump, CH = channel substrate, CT = connector tube. The micropumps had approximate dimensions of 5 cm × 3 cm × 2 cm. Two small air bubbles encased in the PMDS matrix during curing can be observed to the right of the CT in the pump body in (c).

In preparation for casting the PDMS micropump, a glass microscope slide was placed on top of a sheet of aluminium foil, which was then folded above the four sides of the glass, making an open box to serve as the mold. The insulated copper leads were wrapped around the glass to facilitate casting into PDMS, and the glass bottom plate also provided a flat lower surface for the micropump. After casting, the smooth and flat lower surface enabled the micropump to seal tightly with the top surface of the microchannel substrate. The assembled interior components on the microscope slide were placed carefully into the aluminium foil mold, and a 1/4”-diameter steel ball bearing was placed on top of the EC to prevent it from floating in the uncured PDMS mixture.

PDMS pre-polymer was mixed with curing agent at a 12:1 mass ratio. This mixture was degassed in a vacuum chamber and then poured into the mold to a level just above the top of the EC. Immediately after PDMS was poured into the mold, the assembly was placed into an oven, where it was cured at 90–130 °C for ~30 min until the device was firm to the touch. After the PDMS was fully cured, the aluminium foil, microscope slide, and excess cured PDMS were removed, including any elastomer at the bottom of the device blocking the lower opening of the CT.

2.2.2 Microchannel substrates

The microchannels used with the micropumps were fabricated according to an adaptation of a previously published procedure.[24] Briefly, a ¼”-thick poly(methyl methacrylate) (PMMA) piece (Plaskolite, Columbus, OH) was imprinted with a photolithographically patterned and chemically etched silicon template having an elevated channel feature 54 μm tall, 102 μm wide at half height, and 2 cm long. During imprinting the silicon

template and PMMA substrate were held together between glass microscope slides and aluminium blocks fastened with two 2” C-clamps for 30 min in a 140 °C oven. After imprinting, the silicon template and PMMA substrate were allowed to cool to room temperature and then were separated. The microchannel had reservoirs at both termini that were formed by drilling access holes at the ends of the microchannel in the imprinted substrate. The drilled, patterned PMMA sheet was bonded to an unimprinted ¼”-thick PMMA piece in a procedure similar to that of the imprinting. The substrates were clamped together, and the assembly was heated in an oven at 100 °C for 30 min, after which the setup was removed and allowed to cool to room temperature. Profilometry data and optical microscopy measurements indicate that the bonded PMMA microchannels were 54 μm tall and had respective top and base widths of 145 and 60 μm.

2.2.3 LabVIEW interface

An interface was created in National Instruments LabVIEW 6i (Austin, TX) running on a Dell (Round Rock, TX) computer with a PCI-6035E analog-to-digital/digital-to-analog converter card (National Instruments) for quantitative experiments with the micropumps. The LabVIEW program enabled setting a desired electrolysis voltage for a specified time. During pumping, a digital-to-analog line applied voltage to the device while an analog-to-digital line recorded current through the pump. After the voltage was applied for the indicated length of time, a file was created and saved with the data from that trial. The data file included the current readings, the total amount of time during which voltage was applied, and the time that elapsed before the user indicated the end of a trial, which

occurred when the volume of fluid had been pumped completely through the microchannel.

2.2.4 Pumping experiments

Multiple trials were conducted to evaluate micropump performance with several different combinations of micropumps and microchannels. Each experiment measured the time required to pump 5 μL of water from one of the reservoirs through a microchannel to the exit reservoir, and the pump times were used to determine flow rates. The SC on the pump was removed, 150 μL of aqueous 0.1 M KNO_3 was transferred with a micropipette into the EC, and then the SC was replaced. Next, the micropump was reversibly sealed to the microchannel substrate, with the opening at the bottom of the CT directly over the microchannel reservoir, as shown in **Figure 2.1**. Stripped ends from the insulated copper leads to the micropump were interfaced with the input/output card, and voltage settings were entered into the LabVIEW interface before pumping experiments started. Once the program was activated, voltage was applied to the micropump for the specified time duration. The pumping completion time could be entered manually into the program when all of the water had been pumped through the channel to the exit reservoir. This event was distinguished clearly by the passage of gas bubbles through the water in the exit reservoir. Between each pumping experiment, the 0.1 M KNO_3 solution was removed from the EC, the bottom of the micropump was wiped with ethanol, and the water was removed from the microchannel by vacuum suction.

2.3 RESULTS AND DISCUSSION

Preliminary pumping trials exhibited a broader range of flow rates than was desired (15–37 μL min^{-1}). Further experimentation revealed that much of this flow rate variability was due to the sequence of steps initially chosen for setup in pumping experiments. In these earlier trials, the micropump was sealed on the microchannel substrate before adding electrolyte solution to the EC. When the SC was replaced to seal the EC, a slight increase occurred in the pressure in the EC, which often caused fluid to flow before current was applied to the pump. The irregular occurrence of this premature fluid flow led to the broad range of measured flow values in these initial trials. Once this issue was identified, I changed the setup sequence to that described in Section 2.2.4, in all subsequent experiments such that the pump was sealed on the microchannel substrate only after the electrolyte solution had been added and the SC replaced. The revised experimental procedure greatly increased flow rate reproducibility (see **Table 2.1**). This premature fluid flow also explains the higher observed pumping rates in the initial experiments compared to the values reported in **Table 2.1**.

Table 2.1 lists the average results of ~150 pumping experiments using different pump and microchannel combinations. Importantly, the range of pumping rates decreased about four-fold, while the reproducibility improved substantially relative to the initial trials. Indeed, the relative standard deviations of flow rates were 4% or less for 12 of the 15 micropump-channel combinations, and as low as 1% in 5 of the 15 channel-pump pairs. This excellent reproducibility in flow rate should enable the application of these pumps in a number of microfluidic techniques.

Table 2.1 Average observed and predicted results from micropump trials using different pump and channel combinations.

Pump	Channel	# of trials	Observed flow rate ± s (μL/min)	Current ± s mA	Pressure kPa	Predicted flow rate (μL/min)
A	1	13	11.2 ± 0.4	12.1± 0.5	8.7	24
A	2	8	13 ± 3	11 ± 2	6.9	19
A	3	10	10.7 ± 0.8	11 ± 1	8.0	22
A	4	15	10.8 ± 0.3	12 ± 1	8.8	24
A	5	12	9.7 ± 0.3	10 ± 1	8.6	24
B	1	9	9.7 ± 0.4	10.9 ± 0.7	8.1	22
B	2	6	9.7 ± 0.5	12.8 ± 0.2	9.5	26
B	3	10	9.9 ± 0.5	12.8 ± 0.1	9.3	26
B	4	10	9.6 ± 0.3	12.7 ± 0.1	9.5	26
B	5	10	8.7 ± 0.2	12.7 ± 0.1	10.6	29
C	1	10	9.3 ± 0.1	8.9 ± 0.3	6.5	18
C	2	10	9.8 ± 0.1	8.8 ± 0.3	6.2	17
C	3	10	9.2 ± 0.1	8.5 ± 0.8	6.3	17
C	4	10	8.8 ± 0.1	8.3 ± 0.4	6.5	18
C	5	8	8.1 ± 0.1	8.2 ± 0.6	6.9	19

From the average current during experiments, the pressure within the micropump chamber was estimated. Multiplying the current by the duration of pumping time, and then dividing by Faraday's constant yielded the number of moles of electrons transported in the experiments. Then, the moles of electrons were multiplied by the appropriate stoichiometric ratios from the half-reactions (2 moles of electrons per mole of $H_{2(g)}$ and 4 moles of electrons per mole of $O_{2(g)}$) to determine the moles of gas produced. Finally, the ideal gas law was used to calculate the average pressure increase within the micropump chamber at room temperature, accounting for the interior volume of each pump. These calculated pressures are listed in Table 2.1.

The pressure-driven flow through a channel of circular cross-section can be calculated according to Equation 2.1:[25]

$$\nu = \frac{2\Delta P D^2}{f\,\mathrm{Re}\,L\eta} \qquad (2.1)$$

Here, ν is the predicted linear flow velocity, Δ*p* is the pressure difference between the two ends of the channel, *D* is the channel diameter, *f* is the friction factor, *Re* is the Reynolds number, *L* is the channel length, and η is the viscosity. The values of the friction factor and Reynolds number depend on the cross-sectional shape of the microchannel. I estimated *fRe* to be 56 for this channel geometry, based on tabulated values.[26] Also, because microchannels have a trapezoidal as opposed to circular cross-section, I can replace the diameter in equation 2.1 by the hydraulic diameter (D_h), as defined by equation 2.2**:**

$$D_h = \frac{4A}{P} \qquad (2.2)$$

In this equation, *A* is the cross-sectional area and *P* is the perimeter of the channel.[25] Substituting the channel parameters into **equation 2.2** yields a hydraulic diameter of 65 μm. Using the pressure data in **Table 2.1,** the calculated values of hydraulic diameter and *fRe*, the known channel length, and the viscosity for water, I calculated the predicted linear flow velocity for each pumping experiment. Multiplying the linear flow velocity by the channel cross-sectional area gave the volumetric flow rate for each pump–channel pair; these values are reported in the far-right column in **Table 2.1**. The measured flow rates are lower (on average) by a factor of 2.3 than the predicted flow rates, and range 1.5–3.3 times lower. This observation is consistent with the known permeability of PDMS to gases,[27,28] and probably indicates the loss of some electrolysis gases from the pump interior. Although the PP liners of the EC and CT were designed to reduce gas loss

through the PDMS, some leakage sites are likely still present. Another possible explanation for the difference in observed and calculated flow rates is the back reaction of H_2 with O_2 to form water. I believe this contribution to be less significant than diffusion through PDMS, since the platinum electrodes were submerged in solution, and the gaseous electrolysis products rapidly rose to the headspace above the electrolyte. I explored new pump designs that further reduced the amount of PDMS in contact with the pressurized electrolysis gases (results not included). However, it is important to note that the excellent flow rate reproducibility and reusable nature of these micropumps mean that the flow rate for a given pump can be determined empirically. This minimizes any impact from the difference between the observed and predicted flow rates on the application of these pumps in microfluidic experiments.

Small differences in flow rates for the same micropump with different channels are likely due to minor variations in the surfaces of the PMMA substrates. Because of the critical importance of the seal between the PDMS pump and the surface around the reservoir, even small differences in the flatness of the microchannel substrates can affect the pump-to-microchannel seal and, hence, the pressure and flow rate. Variations between the flow rates generated by different pumps on the same channel are probably caused by minor differences in pump characteristics, such as interior volumes, areas of exposed PDMS, and electrochemical cell resistance. The use of batch fabrication methods and alternate pump materials with lower gas permeability should improve pumping reproducibility even more.

To investigate further the general applicability of these micropumps, I performed additional experiments at lower flow rates and also determined the maximum pressure that could be sustained by these devices. Using pump B with channel 3, I applied 8 V instead of 10 V, and for four trials observed an average current of 7.9 mA and flow rate of 6.1 μL min^{-1}. These results indicate that I can adjust the flow rate in a microchannel simply by modifying the applied voltage. I also calculated the maximum internal pressure that a micropump could hold by sealing pump B on a planar glass substrate without a channel, and then operating the pump until gas leakage was observed, typically in the interface between the SC and EC. From the time and current measured in three replicate experiments, I determined a maximum pump pressure of ~300 kPa. Additional improvements in micropump design that eliminate the SC should enable even higher pressures to be attained, potentially making electrolysis-based, pressure-driven micropumps usable for liquid chromatography work.

The electrochemical micropumps that I have developed have several important advantages. First, they can operate with low applied voltages (<10 V) and, thus, are appropriate for interfacing with computer control. The small size of these micropumps (~30 cm^3), as well as the potential for even further miniaturization, makes them well suited for use in lab-on-a-chip analysis devices. The PDMS composition of the micropumps enables reversible sealability with different microchannel substrates, which allows repeated use on various microfluidic arrays. Moreover, these devices should be able to pump a range of liquids, since the mechanism of operation involves applied pressure only. Finally, the components of these micropumps are relatively inexpensive, so devices could be mass-produced with low cost.

2.4 CONCLUSIONS

I have demonstrated the successful development of novel electrically actuated integrated micropumps for microfluidic systems. With a 10 V applied potential, these micropumps can pump water through microchannels at rates of 8–13 μL min^{-1}, in approximate agreement with theory. Smaller flow rates can be achieved with lower applied voltages, and the maximum pressure the current device design can sustain is ~300 kPa. Future work with these devices will include evaluating materials with lower gas permeability, and testing the pumping of different types of liquids through microchannels, to explore the potential for chromatographic applications. These micropumps should provide simple, inexpensive, and easily integrated components for microfluidic analysis.

2.5 REFERENCES

[1] Reyes, D. R., Iossifidis, D., Auroux, P. A., and Manz, A., Micro Total Analysis Systems. 1. Introduction, Theory, and Technology, *Anal. Chem.* 74, 2623, 2002.

[2] Vandaveer, W. R., Pasas, S. A., Martin, R. S., and Lunte, S. M., Recent developments in amperometric detection for microchip capillary electrophoresis, *Electrophoresis* 23, 3667, 2002.

[3] Emrich, C. A., Tian, H. J., Medintz, I. L., and Mathies, R. A., Microfabricated 384-lane capillary array electrophoresis bioanalyzer for ultrahigh-throughput genetic analysis, *Anal. Chem.* 74, 5076, 2002.

[4] Dolnik, V., Liu, S., and Jovanovich, S., Capillary electrophoresis on microchip, *Electrophoresis* 21, 41, 2000.

[5] Mitnik, L., Novotny, M., Felten, C., Buonocore, S., Koutny, L., and Schmalzing, D., Recent Advances in DNA Sequencing by Capillary and Microdevice Electrophoresis *Electrophoresis* 22, 4104, 2001.

[6] Paegel, B. M., Blazej, R. G., and Mathies, R. A., Microfluidic devices for DNA sequencing: sample preparation and electrophoretic analysis, *Curr. Opin. Biotech.* 14, 42, 2003.

[7] Unger, M. A., Chou, H.-P., Thorsen, T., Scherer, A., and Quake, S. R., Monolithic Microfabricated Valves and Pumps by Multilayer Soft Lithography, *Science* 288, 113, 2000.
[8] Grover, W. H., Skelley, A. M., Liu, C. N., Lagally, E. T., and Mathies, R. A., Monolithic membrane valves and diaphragm pumps for practical large-scale integration into glass microfluidic devices, *Sens. Actuators B* 89, 315, 2003.
[9] Schabmueller, C. G. J., Koch, M., Mokhtari, M. E., Evans, A. G. R., Brunnschweiler, A., and Sehr, H., Self-aligning gas/liquid micropump, *J. Micromech. Microeng.* 12, 420, 2002.
[10] Park, J. -H., Yokota, S., and Yoshida, K., A piezoelectric micropump using resonance drive with high power density, *JSME Int. J. Ser. C-Mech. Syst. Mach. Elem. Manuf.* 45, 502, 2002.
[11] Nguyen, N.-T., Huang, X., and Chuan, T. K., MEMS-Micropumps: A Review, *J. Fluids Eng.* 124, 384, 2002.
[12] Hatch, A., Kamholz, A. E., Holman, G., Yager, P., and Bohringer, K. F., A ferrofluidic magnetic micropump, *J. Microelectromech. Syst.* 10, 215, 2001.
[13] Leventis, N. and Gao, X. R., Magnetohydrodynamic electrochemistry in the field of Nd-Fe-B magnets. Theory, experiment, and application in self-powered flow delivery systems, *Anal. Chem.* 73, 3981, 2001.
[14] Lazar, I. M. and Karger, B. L., Multiple open-channel electroosmotic pumping system for microfluidic sample handling, *Anal. Chem.* 74, 6259, 2002.
[15] Takamura, Y., Onoda, H., Inokuchi, H., Adachi, S., Oki, A., and Horiike, Y., Low-voltage electroosmosis pump for stand-alone microfluidics devices, *Electrophoresis* 24, 185, 2003.
[16] Selvaganapathy, P., Ki, Y. S. L., Renaud, P., and Mastrangelo, C. H., Bubble-free electrokinetic pumping, *J. Microelectromec .Syst.* 11, 448, 2002.
[17] Richter, G., U.S. Patent, 3,894,538, 1975.
[18] O'keefe, D., O'herlihy, C., Gross, Y., and Kelly, J. G., Patient-Controlled Analgesia Using a Miniature Electrochemically Driven Infusion-Pump, *Brit. J. Anaesth.* 73, 843, 1994.
[19] Maget, H. J. R., U.S. Patent, 4,402,817, 1983.
[20] Neagu, C. R., Gardeniers, J. G. E., Elwenspoek, M., and Kelly, J. J., An electrochemical microactuator: Principle and first results, *J. Microelectromech. Syst.* 5, 2, 1996.
[21] Böhm, S., Olthuis, W., and Bergveld, P., *Biomed. Microdevices* 1, 121, 1999.
[22] Böhm, S., Timmer, B., Olthuis, W., and Bergveld, P., A closed-loop controlled electrochemical actuated micro-dosing system, *J. Micromech. Microeng.* 10, 498, 2000.
[23] McDonald, J. C. and Whitesides, G. M., Poly(dimethylsiloxane) as a material for fabricating microfluidic devices, *Acc. Chem. Res.* 35, 491, 2002.
[24] Kelly, R. T. and Woolley, A. T., Thermal Bonding of Polymeric Capillary Electrophoresis Microdevices in Water, *Anal. Chem.* 75, 1941, 2003.
[25] Nguyen, N.-T. and Wereley, S. T., *Fundamentals and Applications of Microfluidics*, Artech House, Norwood, MA, 36, 2002.
[26] Sharp, K. V., Adrian, R. J., and Santiago, J. G., *in The MEMS Handbook,* Gad-el-Hak Ed., CRC Press, Boca Raton, FL, 2001.

[27] Merkel, T. C., Bondar, V. I., Nagai, K., Freeman, B. D., and Pinnau, I., Gas sorption, diffusion, and permeation in poly(dimethylsiloxane), *J. Pol. Sci.* 38, 415, 2000.
[28] Walker, G. M., Ozers, M. S., and Beebe, D. J., Insect cell culture in microfluidic channels, *Biomed. Microdevices* 4, 161, 2002.

3. ELECTRICALLY ACTUATED, PRESSURE-DRIVEN LIQUID CHROMATOGRAPHY SEPARATIONS IN MICROFABRICATED DEVICES*

3.1 INTRODUCTION

Miniaturization of analytical techniques holds great potential for performing a variety of sample-limited assays, especially because of the possibility of integrating multiple analysis steps in a single substrate.[1] Since first demonstrated in 1992,[2] capillary electrophoresis in microfabricated devices has seen significant advances, and numerous chemical and biological applications have been reported.[1,3,4] Electrically driven methods are well-suited for miniaturization, since electroosmotic flow (EOF) can be controlled without valves or external pumps. However, EOF pumping and fluid transport have inherent issues that may limit their broad application in miniaturized methods. For example, EOF typically requires high voltages (kV) and is affected by Joule heating; moreover, EOF is sensitive to the solution pH and column surface charge. Finally, electrophoretic techniques are optimal for charged analytes that can be exposed to an electric field.[5,6]

On the other hand, pressurized separation methods such as liquid chromatography (LC) are more general and broadly used. In 1990, Manz et al.[7] presented advantages of the miniaturization of LC; even though no experimental data were provided, this paper

showed that theoretically, the performance per unit time should be superior in microchips compared to conventional LC. Three critical elements for a fully miniaturized LC system are:[5,7,8] (i) integration of a pumping mechanism capable of generating pressure and flow compatible with microchannel dimensions; (ii) incorporation of a separation medium inside microchannels; and (iii) a minimal dead volume interface of the separation column with the pumping and injection mechanism. Despite the challenges it presents, the miniaturization of pressure-driven separation methods is of great interest;[5,7,8] however, most reports have focused on micromachining a separation column while maintaining an external pumping mechanism.[9-17] Thus, the full advantages of LC miniaturization were not realized. Two recent studies have made important progress in the development of miniaturized LC systems with integrated pumping and injection. Lazar et al.[18] fabricated an LC microdevice with integrated EOF micropumps for sample valving and separation. However, this approach required the use of relatively high electric fields (500 V/cm), was limited to solutions with low organic solvent concentrations, and was relatively slow (~40 min elution times). In other work, a hybrid silicon-parylene microfluidic chip with integrated electrochemical micropumps for sample injection and separation was used for the LC analysis of protein digests.[19] This report demonstrated the advantages of having a minimal dead volume between injection and separation, but again suffered from long analysis times (~1 h).

A variety of micropumps have been constructed for microfluidic applications.[20-23] Mechanical pumps[24,25] use moving parts, have relatively complex fabrication and often face challenges in integration with microfluidic systems in terms of materials

compatibility with solutions and samples. Non-mechanical pumps based on electroosmotic,[26] magnetohydrodynamic[27] or electrochemical actuation,[28] are thus appealing alternatives. Electroosmotic pumps, which generate pressure with EOF, are perhaps the most widely used micropumps in microfluidics applications.[26] However, to obtain appropriate flow rates, it is often necessary to apply high voltages (~kV) and make either packed small-diameter columns or microchannel network arrays,[29,30] which complicate the fabrication process. Moreover, electroosmotic pumps are only suitable for operation within a certain range of solution pH and conductance values.

Column technology for microchip LC is a key challenge.[8] Packing microchannels with particles as in conventional LC is difficult to achieve due to pressure constraints and difficulties in forming frits inside microchannels.[31] In 1998, Regnier et al.[32] demonstrated surface-modified micromachined posts, as a mimic of a packed microcolumn. While this approach was compatible with micromachining techniques, it was hindered by expensive fabrication protocols involving deep reactive ion etching. Moreover, non-uniform height of the microposts inside the channel prevented tight sealing of the microstructures. The possibility of performing separations in monolithic stationary phases or open tubular columns has given new opportunities for the development of miniaturized LC. The fabrication of monolithic structures inside microchannels has been demonstrated[33] and is becoming a promising approach, provided uniform monoliths in microchips with low back pressure are constructed.

The use of capillaries for open tubular liquid chromatography (OTLC) was first proposed by Jorgenson et al.[34] A key advantage of OTLC is lower back pressure than packed or monolithic columns, leading to faster analysis times. The main disadvantages of OTLC relative to packed column LC are slower mass transfer into the stationary phase and reduced sample capacity due to lower stationary phase volume. Importantly, micromachined systems can have small channel cross sections, increasing the mass transfer to the stationary phase. Theoretical work on OTLC has shown that band dispersion is lowest for microchannels with high aspect ratios.[35,36] Jacobson et al.[37] reported the use of high aspect ratio microchannels to perform open channel electrochromatography. Later, the same group determined that 5 μm channel depths were a good compromise between efficiency and ease of operation.[38] Although these devices were not tested for pressure-driven separations, the electrochromatography results indicate that open tubular microchannels are an attractive option for microchip chromatography.

In recent years, great interest has arisen in developing electrochemical systems for microchip pumping,[39] resulting in devices for valve actuation,[40] and dosing systems for applications in biology and medicine.[41,42] I have shown that the pressure caused by the build-up of electrolysis gases in an enclosed chamber can pump liquids in fluidic microchannels.[43] These electrochemical micropumps are integrated easily with microfluidics and can pump liquids with rates as high as ~10 μL/min. More recently, electrochemical actuation was demonstrated for sample delivery and solvent gradient generation in electrospray ionization mass spectrometry analysis.[44] Many features of

electrolysis, including simple instrumentation, rapid response time, low power consumption, and limited heat generation,[45] make it an attractive candidate for on-chip LC pumping. Moreover, a constant volume, electrolysis-based actuator can generate a maximum pressure of ~200 MPa.[46] Surprisingly, only one report[19] has appeared on the use of electrolysis-based micropumps in LC; while this initial work demonstrated feasibility, the separation time (~1 h) was not different from conventional LC.

In this paper, I describe the design, fabrication and characterization of electrically actuated micropumps for pressure-driven LC in microchips. Micropumps were made in glass and integrated with microfabricated channels in the same substrate. A pressure-balanced injection approach was implemented by controlling the electrolysis time and voltage applied to the mobile phase and sample micropumps. I studied parameters affecting the reproducibility of the system, and the effects of column coating, amount of sample injected and mobile phase composition on performance. Finally, these devices were evaluated in electrolysis-based injection and LC separation of fluorescently labeled amino acids.

3.2 EXPERIMENTAL

3.2.1 Chemicals

Amino acids were obtained from ICN Biomedicals (Aurora, OH). Fluorescein-5-isothiocyanate (FITC) was from Molecular Probes (Eugene, OR). Reagent-grade solvents including acetonitrile, methanol, acetone, and isopropanol were obtained from Fisher Scientific (Fair Lawn, NJ). Potassium nitrate, hydrogen peroxide and sulfuric acid were

from Sigma (St. Louis, MO). Buffer solutions were prepared using deionized (DI) water (18.3 MΩ·cm), which was obtained from an Easypure UV/UF purification system (Dubuque, IA).

3.2.2 Device fabrication

The integrated micropump-microchannel systems are composed of a three-layer glass sandwich as illustrated in **Figure 3.1**. The bottom layer contains microchannels for sample injection and separation. The middle layer contains through-holes which form the reservoirs for sample, eluent, and electrolyte solution. A pressure transfer tube (PT) on top of the middle layer connects one micropump with the sample reservoir (SR) and another micropump with the eluent reservoir (ER). Finally, access holes drilled in the top

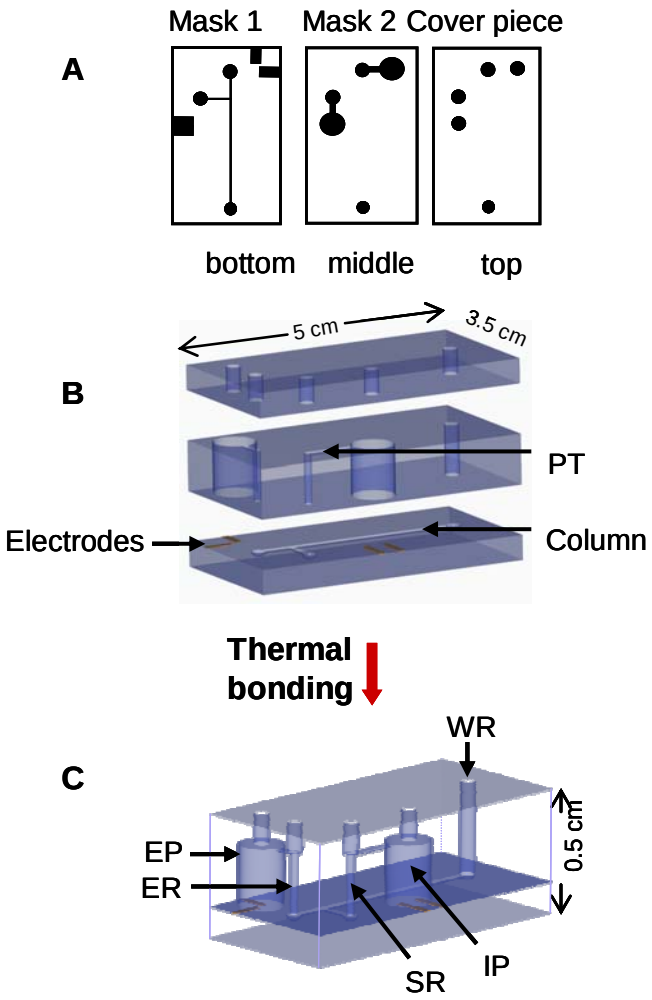

Figure 3.1. Schematics of the fabrication process to integrate micropumps with microchannels for microchip LC (*drawings not to scale, specific details in the text*). (A) Two masks are used to pattern the microchannels and micropumps in the bottom and middle layers. (B) Alignment of layers. (C) The final device containing sample and eluent pumps integrated with microchannels is formed by thermally bonding all the pieces together.

piece facilitate the introduction of sample, eluent and electrolyte solution into their respective reservoirs. Devices were made from microscopes slides (75 x 50 x 1 mm, Fisher). The fabrication process employed a combination of photolithography, wet-chemical etching, through-drilling with diamond-tipped bits (DiamondBurs.Net, Tucker, GA) and thermal bonding.

3.2.3 Substrate cleaning

Microscope slides were immersed in boiling piranha solution (H_2SO_4/H_2O_2, 3/1) for 10 min, rinsed with DI water and dried using nitrogen gas. Prior to photolithography, substrates were cleaned with acetone and isopropanol. Slides were then dehydrated in an Ultra-Clean 100 oven (Lab-Line Instruments, Melrose Park, IL) for 5 min at 120 ºC.

3.2.4 Photolithography

The glass slides were spin-coated with the adhesion promoter SurPass 4000 (Dischem, Ridgway, PA) at 4000 rpm for 45 s and baked on a hot plate at 90 ºC for 60 s. Then, substrates were coated with AZ 3330 positive photoresist (Clariant, Germany) and baked again for 60 s at 90 ºC.

The photoresist was exposed to UV radiation with a 250 W mercury source for 14 s through a patterning mask using a MA150 CC aligner (Karl Suss America, Waterbury Center, VT). The photomasks were drawn using mask layout software (WieWeb) and printed onto transparency film with a 3600 dpi printer at the BYU Print and Mail Production Center.

Two masks were used in microfabrication (**Figure 3.1A**). The first mask, which was used to pattern the bottom layer of the glass microdevices, contained a 3-cm-long separation column and two arms (1 cm each), one connected to the SR and the other to the ER. Channel linewidths in the mask were 100 μm. Four 1.5 x 9 mm rectangular features in this mask defined the areas for thermal deposition of the electrodes. The second mask was used to pattern the middle layer in the micropump-microchannel devices and contained two 1-cm-long x 200-μm-wide channels connecting the micropump chambers to either the SR or ER. Following exposure, the features from the photomask were developed in the photoresist by immersing the substrates in AZ 300 MIF developing solution (Clariant) for 45 s. After rinsing in DI water and drying by N_2 gas, the patterned substrates were hard baked at 115 ºC for 20 min.

3.2.5 Etching

Unprotected areas on the glass substrates were etched isotropically by submerging the slides in 10% buffered oxide etchant (BOE, Transene, Danvers, MA). The bottom layer was immersed in BOE for 6 min, and the middle layer was exposed for up to 18 min. During the etching process, substrates were removed from the BOE bath every 3 min and immersed in 1 M HCl for 10 min to remove any insoluble fluoride products formed.[47]

3.2.6 Electrode deposition

Gold electrodes (2500 Å atop a 200 Å Cr adhesion layer) were deposited thermally on the upper surface of the bottom layer using a CHA 600 thermal evaporator (CHA Industries,

Fremont, CA). To improve metal adhesion to the glass, substrates went through an oxygen plasma cleaning step for 15 s using a Sunbird plasma enhanced chemical vapor deposition system (SHS Equipment, Milpitas, CA), followed by a 15 s dip in BOE solution and a 15 s dip in 1 M HCl. During metal deposition, the microchannels were covered to keep Cr/Au out of the separation system. A lift-off process involving immersion of the glass slides in acetone for 15 min removed the photoresist, leaving patterned electrodes.

3.2.7 Reservoir drilling

Reservoirs for sample, eluent, and electrolyte solutions; and holes for electrode contacts were milled in the middle glass substrate with diamond-tipped bits using a bench-top drill press (Cameron Micro Drill Presses, Sonora, CA). This process was performed with the glass devices immersed in water to avoid thermal stress and breakage. Three 2.5-mm-diameter through-holes formed the ER, SR and waste reservoir (WR). Two 1.0-cm-diameter reservoirs were made to contain the electrolyte solution in the eluent pump (EP) and injection pump (IP). Five 1.5-mm-diameter holes were drilled in the cover piece for access to load sample, eluent and electrolyte solution into their respective reservoirs. Finally, four 1/32”-diameter holes were opened in the top layer to facilitate contacting the electrodes.

3.2.8 Bonding

Prior to bonding, the glass slides were trimmed to 50 x 35 mm. Then, the substrates were cleaned with acetone and isopropanol to remove particles, dust and organic

contamination. To increase the hydrophilicity of the glass surfaces, substrates (except the bottom layer containing gold electrodes) were immersed in boiling piranha solution for 10 min and soaked in concentrated sulfuric acid for 6 h. Finally, glass slides were rinsed with DI water under pressure for 5 min. Bonding was carried out by manually aligning the pieces as shown in **Figure 3.1B**. In some devices, we increased the volume of the micropumps and reservoirs by stacking three or four glass pieces with drilled holes as the middle layer. A few drops of water were added between the glass slides to help maintain alignment. The glass stack was sandwiched between polished quartz plates and held together using a high-temperature-alloy clamp. The assembly was placed inside a BF51800 furnace (Lindberg/Blue, Asheville, NC). The optimized bonding conditions involved ramping at 5 ºC/min to 620 ºC and holding for 5 h, followed by cooling to room temperature. Bonded devices had Nanoport reservoirs (Upchurch Scientific, Oak Harbor, WA) attached to the top surface, and electrical connections to the thin-film electrodes were made using Pt wires and conductive epoxy (Chemtronics, Kennesaw, GA).

3.2.9 Microchannel coating procedure

Octadecylsilane-coated microchannels were produced according to the method of Kutter et al.[38] Silanol groups were activated by pumping successively through the channels 1 M NaOH, DI water, 1 M HCl, DI water and methanol for 10 min each. Next, microdevices were dried at 110 ºC overnight, and the microchannels were purged with N_2 for 20 min at room temperature. The silane solution was prepared in dry toluene and contained 10% (w/w) chlorodimethyloctadecylsilane (Aldrich) with 50 μg/mL *n*-butylamine as a catalyst. After passing through a 0.45-μm filter (Pall, East Hills, NY), the coating

solution was aspirated via the WR through the separation channel for 12 h at room temperature, followed by rinses with toluene and methanol to remove any unreacted silane. Vacuum (as opposed to pressure) loading for surface derivatization prevented stationary phase deposition and analyte retention in the injection channel.

3.2.10 Sample preparation

FITC-labeled aspartic acid, glycine and phenylalanine were made according to a procedure described before.[48] Once prepared, aliquots of the FITC-tagged amino acids were combined and diluted to 0.5 μM in methanol or mobile phase.

3.2.11 Device operation

Pressure-balanced injection was performed by independently controlling the electrolysis time and voltage applied in the electrochemical micropumps (IP and EP) in the devices. A schematic diagram of the pressure-balanced injection approach is shown in **Figure 3.2**. For sample injection and separation, microchannels were filled by pipetting 20 μL of mobile phase via the Nanoports into the ER and SR, and applying vacuum to the WR. Then, 300 μL of electrolyte solution (0.1 M KNO_3) were loaded via the Nanoports into the IP and EP, after which they were capped using sealing nuts (Upchurch). Following this, the mobile phase in the SR was removed and replaced with ~10 μL of sample, and if needed, the ER was re-filled with mobile phase. Both the SR and ER Nanoports were then sealed in a manner similar to the micropumps. To equilibrate a device (**Figure 3.2B**), 20 V were applied to the EP for ~5 s until the microchannels were bubble-free and entirely filled with mobile phase. Then, for injection (**Figure 3.2C**), 20 V were applied to

the IP while the voltage at the EP was turned off. After a time empirically optimized for each device (5-8 s), which allowed a plug of sample to be transferred to the microchannel intersection, the IP was turned off and 25 V were applied to the EP to pump the injected sample through the separation column, as shown in **Figure 3.2D**.

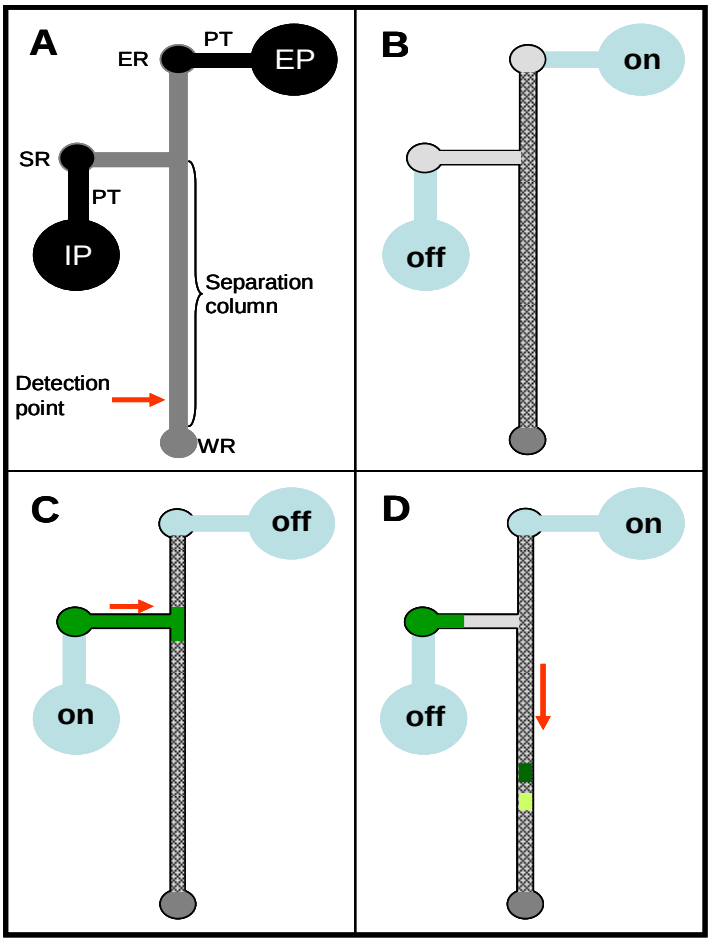

Figure 3.2. Schematic representation of the pressure-balanced injection approach. (A) Device layout. (B) Equilibration; microchannels are filled with eluent; the EP is on and the IP is off. (C) Injection; a sample plug is transferred to the microchannel intersection with the EP off and the IP on. (D) Separation; the EP is on and the IP is off.

The pressure-balanced injection mode was optimized with fluorescein and FITC-labeled glycine. Then, a 0.5 μM mixture of three FITC-labeled amino acids was injected and

separated. For all experiments, laser-induced fluorescence detection was conducted in the separation channel at a 2.5-cm distance from the injection intersection. The detection system has been described elsewhere;[49] briefly, the 488 nm line from an argon ion laser was focused ~5 mm from the end of the separation channel. Fluorescence was collected with the same objective, spectrally and spatially filtered, and detected by a photomultiplier tube.

3.3. RESULTS AND DISCUSSION

Figure 3.3A shows a microchannel-reservoir intersection after etching at room temperature for 18 min in BOE. The etching rate under my experimental conditions was 0.8 μm/min, which is similar to the value of 0.9 μm/min obtained by Lin et al.[47] The glass substrates containing the separation column were etched for 6 min to produce ~5 μm deep microchannels. **Figure 3.3B** shows a cross-sectional electron micrograph of a microchannel after bonding of a cover plate. Separation channel widths after wet chemical isotropic etching were 105-110 μm. As seen in **Figure 3.3B**, the thermal enclosure protocol produced well-bonded devices since there is no visible interface between the two plates. **Figure 3.3C** shows a photograph of a completed device, and a close up of a pump/reservoir (with Nanoports and electrical connections) is shown in **Figure 3.3D.**

Microdevices with one intermediate layer only pumped for short (10-15 s) periods. Thus, I made multilayer microdevices with larger electrolyte reservoir volumes as described in Section 3.2.8 The average reservoir volume in single- and four-intermediate-layer devices was determined to be 120 μL ($n = 3$) and 460 μL ($n = 6$), with relative standard

deviations (RSDs) of 6% and 10%, respectively. These minor variations in volume had little effect on device-to-device injection and separation reproducibility.

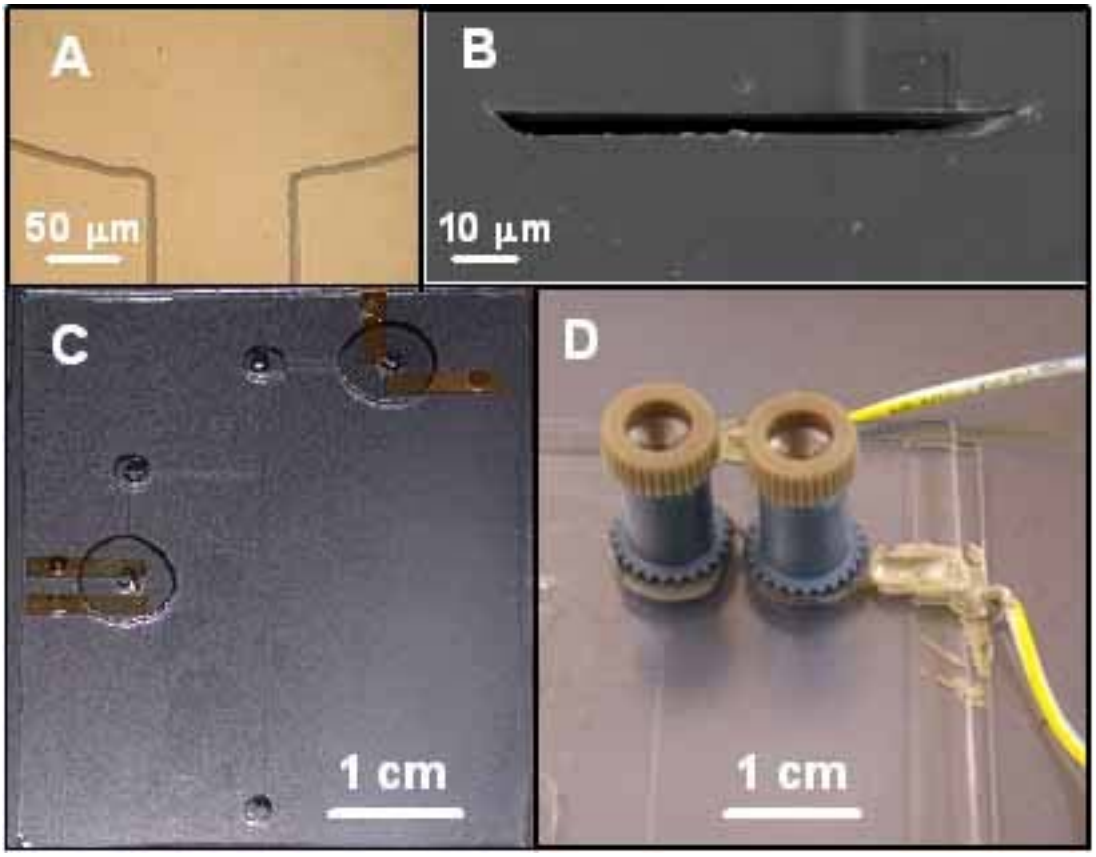

Figure 3.3 Device images. (A) Photograph of the intersection of a microchannel and reservoir etched 18 min in BOE. (B) Electron micrograph of the microchannel cross sectional area. (C) Photograph of a bonded device. (D) Image of a microchip with attached Nanoports that facilitate introduction of eluent and electrolyte solution.

To characterize pumping rates, a ruler was attached to the bottom of a microdevice and a colored solution was pumped through the microchannel from the ER to the WR by electrochemical actuation. A flow rate of 210 nL/min (7.1 mm/s) was observed for an electrolysis potential of 15 V. The RSD for the flow rate measurement was 4.2% (n = 5). The ability of the micropumps to operate against elevated back pressure was evaluated by connecting a gas cylinder with a pressure regulator to the WR via the Nanoport. Pumping

of the colored solution was performed as above, but in this case against 100 psi. A flow rate of 86 nL/min, (RSD = 7.9%, n = 5) was measured for this experiment, which is comparable to published results for electrochemically driven pumping[44] and is suitable for microchip LC.[50]

Due to the oxidizing character of the KNO_3 electrolyte solution and the voltage applied through the micropumps, gold electrodes typically lasted for 15-20 runs. Device lifetime could be extended with similar performance using Pt wires inserted through drilled holes in the bottom of the pump reservoirs and sealed with epoxy.

I first evaluated and optimized the pressure-balanced injection approach using 5 μM fluorescein. Multiple injections were made to find the optimal injection time, determined as the time at which the fluorescent sample plug reached the microchannel intersection. For most experiments (performed in seven different devices) this time was 5-8 s. Importantly, for this injection protocol, the amount of sample loaded can be controlled by the pumping time of the IP, which defines the length of the injected sample plug. For an injection time of 6 s, the plug length (measured at the full width at half maximum) was estimated to be 90-100 μm, corresponding to an injection volume of ~50 pL, which is in the desirable range for microchip LC.[51]

To characterize the reproducibility of the pressure-balanced injection protocol for sample introduction, I studied the injection and detection of a single analyte. For non-optimal mobile phase compositions and pH values, I obtained broad peaks (results not shown). I

optimized the mobile phase composition and pH, since these parameters have been shown to affect the efficiency of separation of similar, phenylisothiocyanate-derivatized amino acids.[52,53] I was able to obtain relatively narrow, well-defined peaks using 70/30 acetonitrile/50 mM acetate buffer (pH 5.45) as the mobile phase.

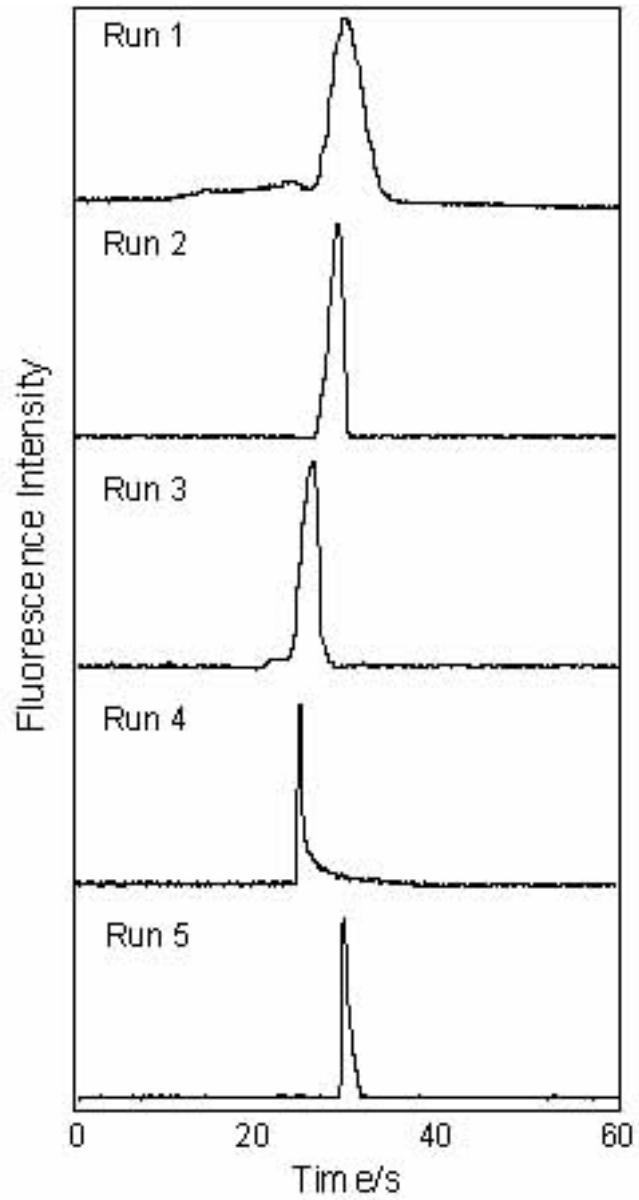

Figure 3.4. Pressure-balanced injection of 1 µM FITC-derivatized glycine. Mobile phase: 70% acetonitrile/30% 50 mM acetate (pH 5.45). Injection: IP on for 6 *s* at 20 V. Elution: IP off after 6 *s* and EP on at 25 V.

Figure 3.4 shows the results obtained for repetitive injections of FITC-labeled glycine with detection at a point 2.5 cm downstream. The reproducibility of the retention time of the FITC-glycine peak is promising but not optimal (7.2% RSD). I hypothesized that stochastic bubble formation at the surface of the electrodes caused variations in the current and, hence, pressure for pumping. Thus, I recorded the current across the micropump during electrolysis of the KNO_3 solution, and **Figure 3.5** indicates that the current varied between runs. In some experiments, the current changed by

less than a few percent, while in others greater deviations were observed. **Figure 3.5** also shows that larger current changes were experienced with increased electrolysis time, and current typically decreased over time for constant voltage operation. A 24% RSD in current was observed after 120 s, whereas after only 30 s, a much smaller 5.5% RSD was measured. Importantly, this latter value is close to the retention time RSD for the FITC-glycine peak, which eluted at ~30 s. These results lend strong support to my hypothesis that partial current interruption by the presence of bubbles on the electrode surface was the main source of retention time variability. I also note that this pumping system is best suited for relatively fast (<1 min) microchip LC analysis.

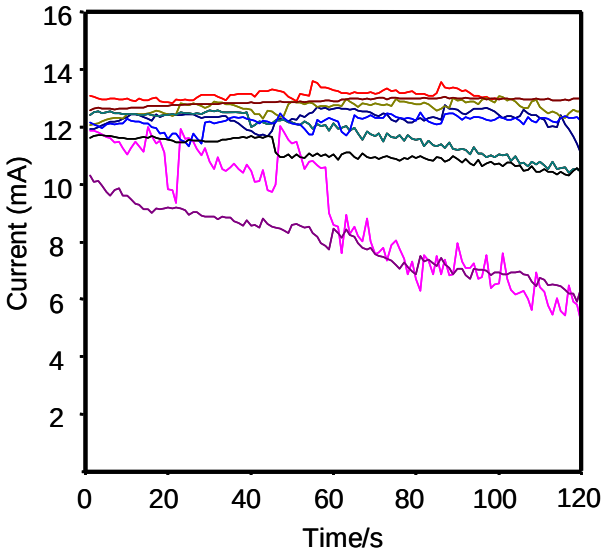

Figure 3.5. Variation of the current in the electrolysis chamber as a function of time. The current in the same pump was monitored during nine consecutive runs.

The performance of the LC microdevices was further evaluated in separation of three FITC-labeled amino acids. For these experiments, I used the analysis conditions described before, which were optimized for the injection of a single peak. **Figure 3.6** presents chromatograms of three replicate electrolysis-based pressure-driven LC microchip separations of aspartic acid, glycine and phenylalanine in ~35 s. Peak identities were determined by the elution times of individually injected amino acids and are consistent with analyte polarities. I observed that the reproducibility of the retention time decreased with

increasing retention time. The RSD for the retention time of the first peak was 2.2%, compared to 7.7% for the last peak. An efficiency (*N)* of 3350 theoretical plates was obtained for the aspartic acid peak, which corresponds to a plate height *(H)* of 7.5 μm for the 2.5 cm separation channel. This value improves over prior plate heights (12-50 μm) reported for microchip OTLC without integrated pumping.[54]

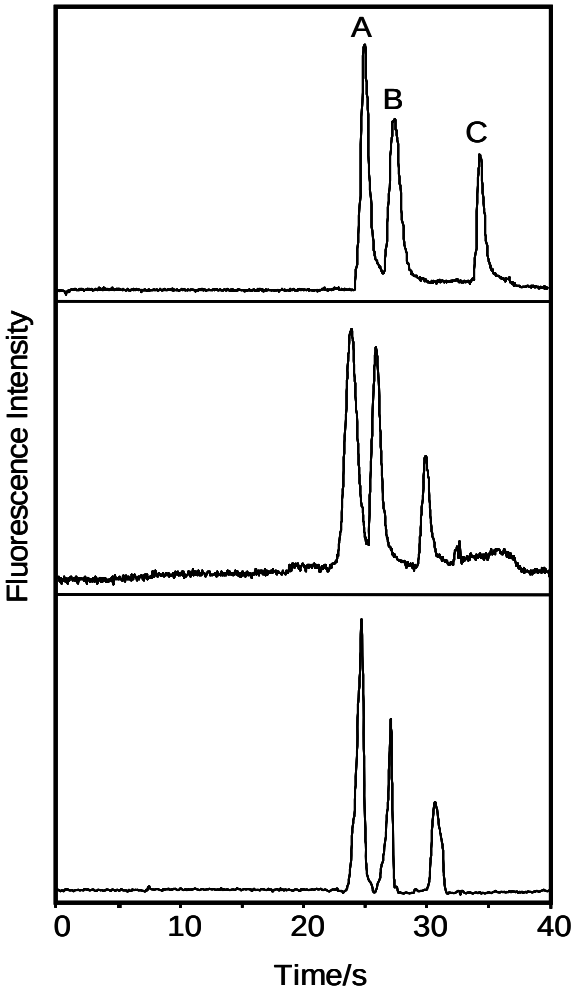

Figure 3.6. Chromatographic separation of a mixture of 0.5 μM FITC-derivatized amino acids in an electrochemically pumped 2.5 cm x 100 μm x 5 μm LC microchip column. Peaks are: (A) aspartic acid, (B) glycine and (C) phenylalanine. Mobile phase was 70% acetonitrile/30% 50 mM acetate (pH 5.45).

The higher efficiency of my system is likely due to smaller injected volumes and the use of shallower channels. Microchannel geometry influences the efficiency in pressure-driven LC separations,[35] and large aspect ratio (e.g., shallow) channels should reduce analyte dispersion effects from less efficient mass transfer to the stationary phase.[55,56] Importantly, these channel dimensions are in the range predicted for optimal OTLC separations.[7,9] Another key advantage of my system is that it allows the injection of pL-range samples with no dead volume between the injector and column, which is critical for high-efficiency microchip LC.

The peaks in **Figure 3.6** were either baseline or nearly baseline separated, and the resolution between aspartic acid and glycine was 1.2 (RSD = 8.0%, n = 3). This value is lower compared to that for the same peaks in conventional HPLC (~24),[57] which uses both gradient elution and longer columns. However, improved resolution could be achieved in my device by incorporating another EP to deliver a second mobile phase in the system, enabling gradient elution. Importantly, the separations obtained are ~20 fold faster than those achieved by conventional LC.[53] Furthermore, the separation efficiency of my devices could be improved by using microchannels with a double-etched profile near the column sidewalls to reduce band dispersion, as proposed by Dutta et al.[55,56]

3.4 CONCLUSIONS

Here, I demonstrate rapid microchip LC analysis with integrated electrolysis-based pumping. I have developed a straightforward microfabrication strategy for interfacing microfluidic channels with electrically actuated micropumps in a single substrate. A pressure-balanced sample injection approach was devised for microchip LC, allowing the introduction of pL-range sample volumes without valves or other components that are difficult to integrate in microdevices. On-chip LC separation of amino acids was carried out successfully in <40 s with good efficiency (3350 theoretical plates). Current stability in the micropumps represented the main limitation in analysis reproducibility. Improved electrode designs with greater surface area and feedback loop current control of the micropumps should improve results. The approach presented holds great potential for the miniaturization of pressure-driven separations or other pumping applications in which nL/min - μL/min volumes must be delivered in a simple and compact format.

3.5. REFERENCES

[1] Dittrich, P. S., Tachikawa, K., and Manz, A., Micro total analysis systems. Latest advancements and trends, *Anal. Chem.* 78, 3887, 2006.

[2] Manz, A., Harrison, D. J., Verpoorte, E. M. J., Fettinger, J. C., Paulus, A., Ludi, H., and Widmer, H. M., Planar Chips Technology for Miniaturization and Integration of Separation Techniques into Monitoring Systems - Capillary Electrophoresis on a Chip, *J. Chromatogr.* 593, 253, 1992.

[3] Jin, L. J., Ferrance, J., and Landers, J. P., Miniaturized electrophoresis: An evolving role in laboratory medicine, *Biotechniques* 31, 1332, 2001.

[4] Liu, Y., Garcia, C. D., and Henry, C. S., Recent progress in the development of mu TAS for clinical analysis, *Analyst* 128, 1002, 2003.

[5] Harris, C. M., Shrinking the LC landscape, *Anal. Chem.* 75, 64A, 2003.

[6] Sato, K., Hibara, A., Tokeshi, M., Hisamoto, H., and Kitamori, T., Integration of chemical and biochemical analysis systems into a glass microchip, *Anal. Sci.* 19, 15, 2003.

[7] Manz, A., Miyahara, Y., Miura, J., Watanabe, Y., Miyagi, H., and Sato, K., Design of an Open-Tubular Column Liquid Chromatograph Using Silicon Chip Technology, *Sens. Actuators B* 1, 249, 1990.

[8] de Mello, A., On-chip chromatography: the last twenty years, *Lab Chip* 2, 48n, 2002.

[9] Ocvirk, G., Verpoorte, E., Manz, A., Grasserbauer, M., and Widmer, H. M., High-Performance Liquid-Chromatography Partially Integrated onto a Silicon Chip, *Anal. Meth. Instr.* 2, 74, 1995.

[10] Murrihy, J. P., Breadmore, M. C., Tan, A. M., McEnery, M., Alderman, J., O'Mathuna, C., O'Neill, A. P., O'Brien, P., Advoldvic, N., Haddad, P. R., and Glennon, J. D., Ion chromatography on-chip, *J. Chromatogr. A* 924, 233, 2001.

[11] McEnery, M. M., Glennon, J. D., Alderman, J., and O'Mathuna, S. C., Liquid Chromatography on-chip, *Biomed. Chromatogr.* 14, 44, 2000.

[12] McEnery, M., Tan, A. M., Alderman, J., Patterson, J., O'Mathuna, S. C., and Glennon, J. D., Liquid chromatography on-chip: progression towards a micro total analysis system, *Analyst* 125, 25, 1999.

[13] Ericson, C., Holm, J., Ericson, T., and Hjerten, S., Electroosmosis- and pressure-driven chromatography in chips using continuous beds, *Anal. Chem.* 72, 81, 2000.

[14] Yin, H., Killeen, K., Brennen, R., Sobek, D., Werlich, M., and van de Goor, T., Microfluidic Chip for Peptide Analysis with an Integrated HPLC Column, Sample Enrichment Column, and Nanoelectrospray Tip, *Anal. Chem.* 77, 527, 2005.

[15] Reichmuth, D. S., Shepodd, T. J., and Kirby, B. J., Microchip HPLC of peptides and proteins, *Anal Chem* 77, 2997, 2005.

[16] Ishida, A., Yoshikawa, T., Natsume, M., and Kamidate, T., Reversed-phase liquid chromatography on a microchip with sample injector and monolithic silica column, *J. Chromatogr. A* 1132, 90, 2006.

[17] Shintani, Y., Hirako, K., Motokawa, M., Iwano, T., Zhou, X. J., Takano, Y., Furuno, M., Minakuchi, H., and Ueda, M., Development of miniaturized multi-channel high-performance liquid chromatography for high-throughput analysis, *J. Chromatogr. A* 1073, 17, 2005.

[18] Lazar, I. M., Trisiripisal, P., and Sarvaiya, H. A., Microfluidic liquid chromatography system for proteomic applications and biomarker screening, *Anal. Chem.* 78, 5513, 2006.
[19] Xie, J., Miao, Y., Shih, J., Tai, Y.-C., and Lee, T. D., Microfluidic platform for liquid chromatography-tandem mass spectrometry analyses of complex peptide mixtures, *Anal. Chem.* 77, 6947, 2005.
[20] Nguyen, N.-T., Huang, X., and Chuan, T. K., MEMS-Micropumps: A Review, *J. Fluids Eng.* 124, 384, 2002.
[21] Tay, F. E. H., *Microfluidics and BioMEMS*, Kluwer Academic Pub., New York, 2002.
[22] Chou, H. P., Unge, M. A., and Quake, S. R., A microfabricated rotary pump, *Biomed. Microdevices* 3, 323, 2001.
[23] Bardell, R. L., Sharma, N. R., Forster, F. K., Afromowitz, M. A., and Penney, R. J., Designing High Performance micropumps base on no moving parts and valves, *MEMS* 354, 47, 1997.
[24] Tsai, J. H. and Lin, L. W., Active microfluidic mixer and gas bubble filter driven by thermal bubble micropump, *Sens. Actuators A* 97-8, 665, 2002.
[25] Carrozza, M. C., Croce, N., Magnani, B., and Dario, P., A Piezoelectric-Driven Stereolithography-Fabricated Micropump, *J. Micromech. Microeng.* 5, 177, 1995.
[26] Zeng, S. L., Chen, C. H., Mikkelsen, J. C., and Santiago, J. G., Fabrication and characterization of electroosmotic micropumps, *Sens. Actuators B* 79, 107, 2001.
[27] Jang, J. S. and Lee, S. S., Theoretical and experimental study of MHD (magnetohydrodynamic) micropump, *Sens. Actuators A* 80, 84, 2000.
[28] Neagu, C. R., Gardeniers, J. G. E., Elwenspoek, M., and Kelly, J. J., An electrochemical microactuator: Principle and first results, *J. Microelectromech Syst.* 5, 2, 1996.
[29] Lazar, I. M. and Karger, B. L., Multiple open-channel electroosmotic pumping system for microfluidic sample handling, *Anal. Chem.* 74, 6259, 2002.
[30] Nie, F.-Q., Macka, M., Barron, L., Connolly, D., Kent, N., and Paull, B., Robust monolithic silica-based on-chip electro-osmotic micro-pump, *Analyst* 132, 417, 2007.
[31] Oleschuk, R. D., Shultz-Lockyear, L. L., Ning, Y. B., and Harrison, D. J., Trapping of bead-based reagents within microfluidic systems: On-chip solid-phase extraction and electrochromatography, *Anal. Chem.* 72, 585, 2000.
[32] He, B., Tait, N., and Regnier, F., Fabrication of nanocolumns for liquid chromatography, *Anal. Chem.* 70, 3790, 1998.
[33] Rohr, T., Yu, C., Davey, M. H., Svec, F., and Frechet, J. M. J., Porous polymer monoliths: Simple and efficient mixers prepared by direct polymerization in the channels of microfluidic chips, *Electrophoresis* 22, 3959, 2001.
[34] Jorgenson, J. W. and Guthrie, E. J., Liquid-Chromatography in Open-Tubular Columns - Theory of Column Optimization with Limited Pressure and Analysis Time, and Fabrication of Chemically Bonded Reversed-Phase Columns on Etched Borosilicate Glass-Capillaries, *J. Chromatogr.* 255, 335, 1983.
[35] Dutta, D., Ramachandran, A., and Leighton, D. T., Effect of channel geometry on solute dispersion in pressure-driven microfluidic systems, *Microfluidics Nanofluidics* 2, 275, 2006.
[36] Dutta, D. and Leighton, D. T., Dispersion reduction in open-channel liquid electrochromatographic columns via pressure-driven back flow, *Anal. Chem.* 75, 3352, 2003.

[37] Jacobson, S. C., Hergenroder, R., Koutny, L. B., and Ramsey, J. M., Open-Channel Electrochromatography on a Microchip, *Anal. Chem.* 66, 2369, 1994.
[38] Kutter, J. P., Jacobson, S. C., Matsubara, N., and Ramsey, J. M., Solvent-programmed microchip open-channel electrochromatography, *Anal. Chem.* 70, 3291, 1998.
[39] Nyholm, L., Electrochemical techniques for lab-on-a-chip applications, *Analyst* 130, 599, 2005.
[40] Suzuki, H. and Yoneyama, R., Integrated microfluidic system with electrochemically actuated on-chip pumps and valves, *Sens. Actuators B* 96, 38, 2003.
[41] O'Keefe, D., O'Herlihy, C., Gross, Y., and Kelly, J. G., Patient-controlled analgesia using a miniature electrochemically driven infusion pump., *Br. J. Anaesthesia* 73, 843, 1994.
[42] Bohm, S., Timmer, B., Olthuis, W., and Bergveld, P., A closed-loop controlled electrochemical actuated micro-dosing system, *J. Micromech. Microeng.* 10, 498, 2000.
[43] Munyan, J. W., Fuentes, H. V., Draper, M., Kelly, R. T., and Woolley, A. T., Electrically actuated, pressure-driven microfluidic pumps, *Lab Chip* 3, 217, 2003.
[44] Xie, J., Miao, Y. N., Shih, J., He, Q., Liu, J., Tai, Y. C., and Lee, T. D., An electrochemical pumping system for on-chip gradient generation, *Anal. Chem.* 76, 3756, 2004.
[45] Neagu, C., Jansen, H., Gardeniers, H., and Elwenspoek, M., The electrolysis of water: an actuation principle for MEMS with a big opportunity, *Mechatronics* 10, 571, 2000.
[46] Cameron, C. G. and Freund, M. S., Electrolytic actuators: Alternative, high-performance, material-based devices, *Proc. Natl. Acad. Sci. USA* 99, 7827, 2002.
[47] Lin, C. H., Lee, G. B., Lin, Y. H., and Chang, G. L., A fast prototyping process for fabrication of microfluidic systems on soda-lime glass, *J. Micromech. Microeng.* 11, 726, 2001.
[48] Kelly, R. T., Pan, T., and Woolley, A. T., Phase changing sacrificial materials for solvent bonding of high-performance polymeric capillary electrophoresis microchips, *Anal. Chem.* 77, 3536, 2005.
[49] Kelly, R. T. and Woolley, A. T., Thermal bonding of polymeric capillary electrophoresis microdevices in water, *Anal. Chem.* 75, 1941, 2003.
[50] Chervet, J. P., Ursem, M., and Salzmann, J. B., Instrumental requirements for nanoscale liquid chromatography, *Anal. Chem.* 68, 1507, 1996.
[51] O'Neill, A. P., O'Brien, P., Alderman, J., Hoffman, D., McEnery, M., Murrihy, J., and Glennon, J. D., On-chip definition of picolitre sample injection plugs for miniaturised liquid chromatography, *J. Chromatogr. A* 924, 259, 2001.
[52] Morvai, M., Fabian, V., and Molnarperl, I., Buffer and pH-Dependence of the Retention of Phenylthiocarbamylamino Acids in Reversed-Phase High-Performance Liquid-Chromatography, *J. Chromatogr.* 600, 87, 1992.
[53] Heinrikson, R. L. and Meredith, S. C., Amino-Acid-Analysis by Reverse-Phase High-Performance Liquid-Chromatography - Precolumn Derivatization with Phenylisothiocyanate, *Anal. Biochem.* 136, 65, 1984.
[54] Vahey, P. G., Park, S. H., Marquardt, B. J., Xia, Y. N., Burgess, L. W., and Synovec, R. E., Development of a positive pressure driven micro-fabricated liquid chromatographic analyzer through rapid-prototyping with poly(dimethylsiloxane) - Optimizing chromatographic efficiency with sub-nanoliter injections, *Talanta* 51, 1205, 2000.

[55] Dutta, D. and Leighton, D. T., Dispersion reduction in pressure driven flow through microetched channels, *Anal. Chem.* 73, 504, 2001.
[56] Dutta, D. and Leighton, D. T., Dispersion in large aspect ratio microchannels for open-channel liquid chromatography, *Anal. Chem.* 75, 57, 2003.
[57] Boyd, B. W., Witowski, S. R., and Kennedy, R. T., Trace-level amino acid analysis by capillary liquid chromatography and application to in vivo microdialysis sampling with 10-s temporal resolution, *Anal. Chem.* 72, 865, 2000.

4. USING PHASE-CHANGING SACRIFICIAL MATERIALS TO FABRICATE MICRODEVICES FOR CHEMICAL ANALYSIS*

4.1. INTRODUCTION

Polymer microchips are expected to contribute significantly to biological analysis in the postgenome era, especially in the field of proteomics.[1,2] Considerable research has already focused on separations, the use of new materials, and transferring conventional analysis methods to a microchip platform; however, more work remains to enable the exploitation of the full potential of plastic microdevices. In particular, the use of conventional device bonding techniques has limited the broad application of polymer microchips.

Solvent bonding is an attractive alternative to conventional thermal bonding.[3-7] In principle, solvent bonding of polymer substrates should produce robustly enclosed microchannels due to the strong molecular interaction between the surfaces. However, the use of this technique has been limited due to the ease with which microchannels can be blocked by dissolved polymer, or swelling or softening of the substrate. Recently, Shah et al.[6] reported the enclosure of polymer microfluidic devices by inducing a flow of solvent through a microfabricated channel via capillary action. This approach was simple to implement, but the bond strength of the microdevices was low (80 psi), which would limit applications that require pumping of viscous gels or chromatographic stationary phases into microchannels under pressure. Therefore, the development of fabrication

* This Chapter is modified from Chapter 51 in: *Handbook of Capillary and Microchip Electrophoresis and Associated Microtechniques*, 3rd Edition, Landers, J.P., Ed; Copyright CRC Press, 2007

protocols that more fully realize the advantages of solvent bonding are warranted.

This chapter describes the theory, methodology and application of a microfabrication process that uses phase-changing sacrificial layers (PCSLs) as intermediates to protect microchannel features during bonding or hydrogel polymerization. The content focuses on key process details associated with the fabrication of microchips, and the application of PCSL-formed microfluidic devices in CE separations and other electric field-based analysis methods. Finally, I provide a brief overview of potential future trends and applications of PCSL fabrication methods in microfluidics.

4.2. BACKGROUND AND THEORY

In the past 15 years, the use of microfluidic devices for chemical analysis has increased tremendously. Indeed, a broad range of chromatographic and electrophoretic separation methods have been implemented in microchips.[8] However, for widespread utilization of microfabricated devices in analysis applications, particularly in the field of proteomics, further efforts are needed to develop simple fabrication techniques that achieve functional integration of multiple tasks in a single device.[9] In this section, I describe the fabrication of microdevices using sacrificial materials and discuss some of the advantages of this approach over conventional microfabrication methods.

4.2.1 Sacrificial materials

Microfabrication using sacrificial layers is well-developed in the field of micro electro mechanical systems (MEMS). Reports include the fabrication of micro- and

nanomechanical components,[10] electroosmotic micropumps in silicon and glass substrates,[11] and nano-[12] or microchannels[13,14] with potential applications in biology.[15] Unlike bonding protocols, in which a cover plate is affixed to a patterned substrate to seal microchannels, sacrificial layer methods can obviate the bonding step, making this approach very attractive.[16,17]

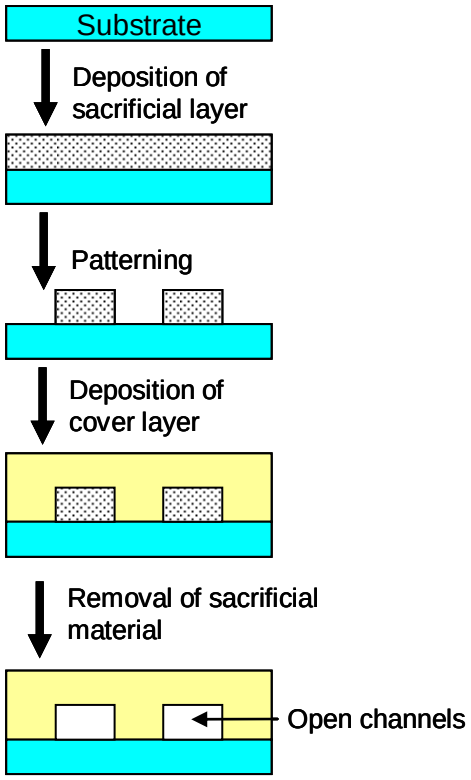

Figure 4.1. Schematic diagram of the general processing steps involved in the fabrication of microchannel structures using sacrificial materials.

Figure 4.1 provides a general overview of the process for making microfluidic systems using sacrificial materials. Briefly, a sacrificial layer is deposited on a substrate by spin coating, vapor deposition or some other method. Then, using photolithography, the sacrificial material is patterned and serves as a temporary "placeholder," which defines the channel geometry. After deposition of a top layer, the sacrificial material is removed, leaving behind open tubular features between the substrate and the cover layer.[16]

There are a variety of materials that can be used as sacrificial cores. Inorganic sacrificial materials include SiO_2[18] and metals such as aluminum,[19] titanium,[20] and nickel.[21] Polymers such as polyimide,[22] poly(methyl methacrylate) (PMMA),[10] polycarbonate (PC)[13] and photoresist[23] have also been used as

sacrificial materials. After deposition of the cover film, removal of the sacrificial layer can be achieved by dissolution,[24] etching,[11,19,25] or thermal degradation.[26,27] These removal methods each have benefits and drawbacks; selection of the optimal approach is specific to particular combinations of substrate, sacrificial layer and cover film.[18,28] Recently, Whitesides et al.[29] implemented a fabrication method using water-soluble sacrificial cores. Poly(acrylic acid) and dextran proved to be effective sacrificial layers that could be dissolved in water or aqueous NaCl, for making metallic microstructures by nickel electrodeposition.

Importantly, microfabrication using sacrificial cores is a versatile technique. First, there are no limitations in the size or flatness of the channel substrate, since no bonding is involved.[26] Second, the choice of sacrificial material can influence the geometry of the resulting microchannels; for example, Peeni et al.[19] used aluminum/photoresist, SU-8 and aluminum to obtain semicircular, rectangular and trapezoidal geometries, respectively. In addition, even though glass[11,19] and silicon[30,31] are the two most common substrates for microfabrication using sacrificial layers, the surface properties of microfluidic vias can be adapted to specific applications by depositing selected materials beneath and on top of the sacrificial layer. Moreover, sacrificial approaches facilitate the formation of three-dimensional fluidic systems through sequential deposition of layers.[12,32] Finally, the fabrication of microchannels *in-situ* should enable the integration of fluidic and electronic components in microdevices.

4.2.2 Sacrificial layer fabricated microfluidic devices

4.2.2.1 Silica and glass materials

Sacrificial etching methods have been used widely in the microelectronics industry for years; however, only a few examples of separations in sacrificially formed microfluidic systems have been demonstrated. Craighead and coworkers used thin-film deposition and wet chemical etching to define ~100-nm-dimension nanochannels, which were utilized to measure the electrophoretic mobilities of two different lengths of DNA.[33] More recently, the same group fabricated submicrometer-dimension fluidic channels for the analysis of <100 fg of DNA.[25] Hawkins' group fabricated a microdevice using thin-film techniques, and used it to perform single-molecule detection.[34] Peeni et al.[19] showed CE separations of fluorescently labeled amino acids in a 9-mm long microchannel fabricated by thin-film deposition of silicon dioxide over a photoresist/aluminum sacrificial layer. Subsequent optimization also enabled peptide separations to be carried out in these devices.[35] These studies demonstrate the potential for performing separations in microdevices fabricated using sacrificial layer techniques, but further work remains.

Despite the successful construction of microchips using sacrificial layer methods, several issues must still be addressed with the fabrication process and the resulting devices. First, fabrication requires cleanroom facilities, costly instrumentation for thin-film deposition and patterning, and expertise to use such equipment, all of which make this approach inaccessible to some researchers. In addition, there are several constraints on the types of substrates, sacrificial layers and overlayers that can be used.[13,30] For example, the sacrificial material must produce a high-quality and uniform film of several micrometers

thickness.[18] In addition, the sacrificial layer must adhere well to the substrate and not react with the covering film. Ideally, the sacrificial layer will be removed completely, leaving a smooth inner surface in the microchannel. Moreover, neither the substrate nor the cover layer must be affected during the sacrificial layer removal step.[13] Unfortunately, the removal of the sacrificial material can take hours to days, which limits the mass production of microchips by this method. Solubility can be a concern, especially when a polymer is used as the cover layer with a photoresist-based sacrificial material. In this case, the solvent present in the coating polymer solution can attack the sacrificial photoresist and compromise microchannel integrity.[13] Similarly, if a thermally decomposable polymer is used as a sacrificial layer, complete decomposition should occur in a narrow temperature range, which must be compatible with the other materials and components on the substrate.[36]

Structural strength is another important consideration in the fabrication of microchannels for fluid handling. In the sacrificial layer fabrication approach, microchannels are generated by deposition of a thin film on top of a patterned material, and the resulting structures are generally weaker than those made by standard bonding methods. Hubbard et al.[28] investigated possible causes of channel wall failure during fabrication with an aluminum sacrificial layer and silicon dioxide overcoating. Elevated internal pressure from gas generated during the etching of aluminum was found to be the main cause of microchannel wall failure during fabrication. A finite element model showed that channel width and film thickness were the most critical parameters to optimize in avoiding device failure.

In summary, sacrificial fabrication of microfluidic devices in glass and silicon overcomes some limitations of conventional manufacturing methods. Important benefits include the ability to fabricate nanometer- to several micrometer-dimension structures and the elimination of a bonding step. Nevertheless, several problems with sacrificial fabrication have limited the implementation of this technique in making microfluidic devices. First, the fabrication protocols are not generally easy to carry out and require sophisticated instrumentation. Second, device materials are limited to glass and silicon, the substrates most compatible with the manufacturing methods. Finally, fabrication yield and reproducibility still need improvement. Thus, further work is essential to develop sacrificial fabrication techniques.

4.2.2.2 Polymeric materials

Woolley's group has been interested in applying sacrificial layer methods for making polymer microfluidic systems. Kelly et al.[37] carried out ground-breaking studies in this area in 2005, inspired by work that utilized the solid-liquid phase change of waxes at their melting point to form actuators such as valves in fluidic microchips.[38-41] This phase transition offers a promising approach for filling (as a liquid) and protecting (as a solid) microchannels during device processing steps.

In brief, PCSL microfabrication involves heating a solid sacrificial material to a temperature above its melting point and using it to fill a microchannel imprinted in a polymeric substrate. After cooling, the sacrificial material solidifies and protects the microchannel from solvent and dissolved polymer during bonding. Next, solvent is

spread on top of the PCSL-protected channels, and a polymeric cover layer containing access reservoirs is aligned and held in contact with the imprinted substrate until a robust bond is obtained, resulting in enclosed PCSL-filled channels. Finally, the device is heated above the melting temperature of the sacrificial material, and vacuum is applied to remove the melted PCSL, leaving open microchannels. Indeed, a paraffin wax PCSL was recently used to construct microfluidic devices; the combination of PCSLs and solvent bonding enabled polymer microchips to be fabricated and evaluated in μCE analysis of amino acids and peptides.[37]

PCSL microfabrication is an attractive alternative for making robustly enclosed microchannels by solvent bonding, while protecting microchannel integrity using a sacrificial material. This technique does not require sophisticated thin-film deposition instrumentation and should be easy to implement by microfluidics researchers. In Section 4.3, I provide guidelines for the fabrication of polymer microfluidic systems using PCSLs.

4.3 FABRICATION TECHNIQUES AND METHOD DEVELOPMENT

Because of the many advantages of polymer microchips, there is a tremendous need for alternative fabrication processes to allow the realization of their full potential.[9,42] Thus, this section describes the steps to follow to make polymer microdevices using PCSL and solvent bonding techniques. Because of its good optical properties and well-known patterning procedures, PMMA is used frequently for the fabrication of microfluidic

chips.[43-45] As a result, the PCSL microfabrication method will be detailed for PMMA microchip fabrication. However, constructing microdevices from different polymers using the PCSL method should be straightforward, if the appropriate combination of substrate, sacrificial material and solvent are selected. A schematic overview of the PCSL fabrication approach is depicted in **Figure 4.2**.

4.3.1 Template fabrication and microchannel imprinting

Polymer microfluidic systems for chemical analysis are normally fabricated by transferring a patterned microstructure from a template to a substrate (**Figure 4.2A-C**).[44] Micromachined silicon templates created by standard photolithographic and etching methods[46] are normally used to imprint elevated features in PMMA substrates, forming microchannels (see **Sections 1.1.2.3** and **1.1.2.4**).

Although the silicon micromachining process is well developed, extensive use of costly cleanroom instrumentation is required. Thus, alternative and simpler template construction approaches are being pursued. One such method utilizes SU-8, an epoxy-based negative photoresist, which has excellent chemical resistance and mechanical properties. Patterned SU-8 is being applied increasingly in making microstructures for templates in microchip production.[47-49]

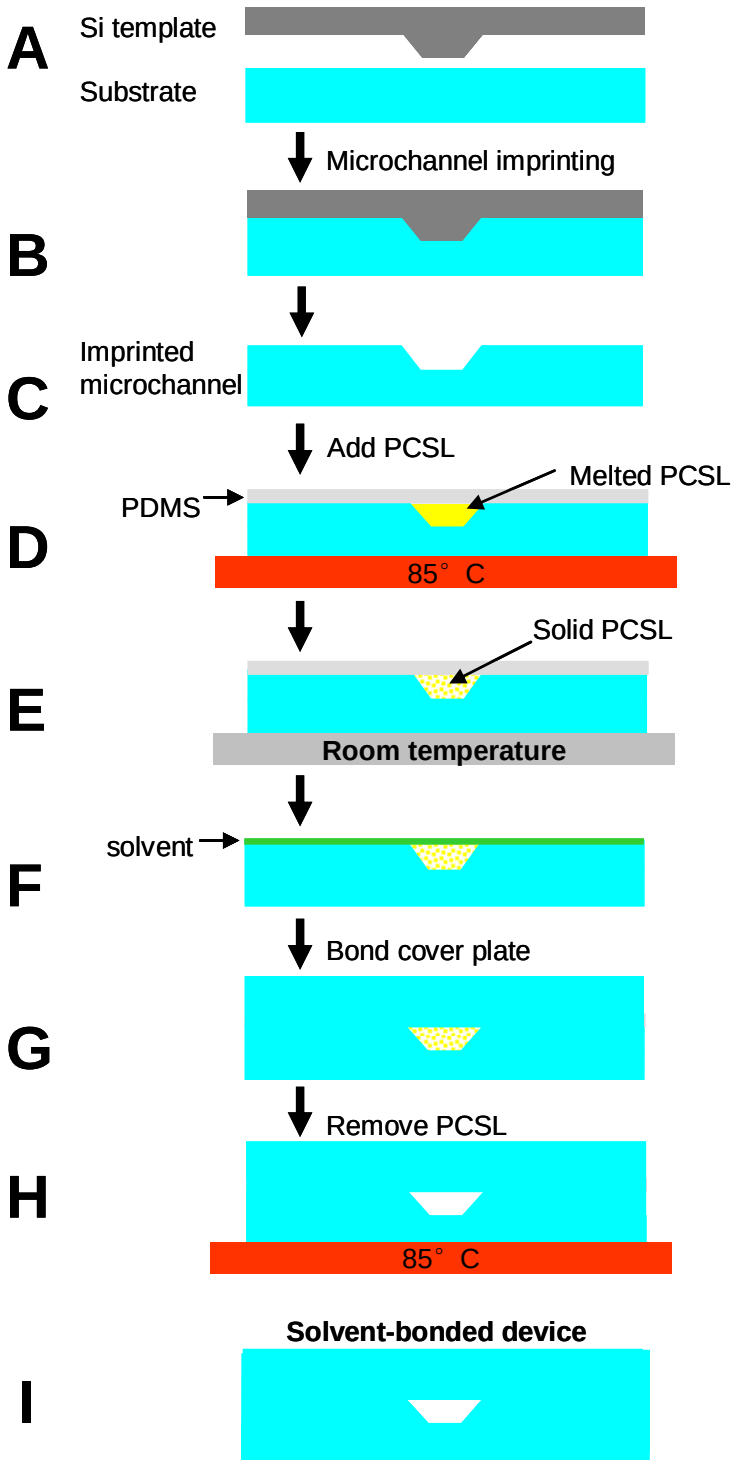

Figure 4.2. Fabrication of microchannels in a polymer substrate using PCSLs and solvent bonding (*additional details are in the text*).

4.3.2 Filling microchannels with PCSL

Prior to solvent bonding, the microchannels must be filled with PCSL. Some practical considerations for selecting a material for a sacrificial layer are: (1) it should have a lower melting point than the substrate itself; (2) it must be resistant to the bonding solvent; (3) it should not react with the polymer substrate; (4) it should form a smooth surface after solidification; and (5) it must be easy to remove from the microchannel after bonding.

The following is a short overview of the process for depositing a PCSL into imprinted features. A PMMA piece having imprinted microchannels (formed as described in Section 4.3.1) is sealed reversibly to a ~1-mm-thick PDMS film, which has small holes that correspond to the channel ends. This temporarily enclosed PMMA-PDMS structure is placed on a hot plate at 85 ºC, heated paraffin wax is added to all but one of the channel access holes in the PDMS film, and vacuum is applied at the unfilled opening, causing liquid PCSL to fill the entire microchannel network (**Figure 4.2D**). Cooling the assembly to room temperature produces a solid PCSL, protecting the microchannels as indicated in **Figure 4.2E**.

Occasionally, some PCSL solidifies outside the microchannel region, and this excess wax must be removed for proper bonding. Two solutions to this issue have been developed. First, if the paraffin wax PCSL is left in contact with PDMS for 1-2 hours, the PCSL outside the channels dissolves into the PDMS.[37] A second solution is to add the liquid paraffin wax to the device without applying vacuum; in this case, the PCSL enters the

microchannels by capillary action, and more uniform filling is observed. Once well-defined microchannels loaded with solid sacrificial material are obtained, the PDMS film is removed carefully, and the PCSL-filled device is ready for bonding.

4.3.3 Microdevice bonding

To form enclosed microchannels, the PCSL-protected PMMA piece must be bonded to a cover plate having channel access holes. To this end, solvent is added on top of the imprinted substrate (**Figure 4.2F**), a polymer top piece is aligned with the PCSL-protected microstructure, and pressure is applied for ~2 min to complete microdevice bonding (**Figure 4.2G**). The solvent bonding step must be performed quickly such that the solvent does not evaporate or dissolve the substrate extensively, which could affect channel integrity. In practice, it was found that bringing the two PMMA pieces together at an angle allowed air bubbles to escape out the side, leading to higher-quality microdevice bonding. Finally, it is important for the cover PMMA piece to be about the same size as the imprinted substrate.

The amount of solvent added also affects the quality of the bonded devices. Sufficient solvent must be added to cover the entire PCSL-protected surface without leaving bubbles or unwetted areas. On the other hand, if an excess of solvent is applied, it flows outside the bonding interface and can compromise the optical quality of the surface of the resulting device. To overcome this problem, PDMS films can be placed on the non-bonding sides of the PMMA to keep the solvent from damaging the microchip exterior surfaces. Using masking tape to protect the PMMA surfaces has also been successful.

4.3.4 Sacrificial layer removal

The final step in PCSL fabrication of microfluidic systems is removal of the sacrificial material to yield clean, smooth microchannel inner surfaces. Paraffin wax PCSL is removed by heating the microdevice to 85 ºC and applying vacuum to a reservoir in the PMMA cover piece to aspirate the liquid PCSL (**Figure 4.2H**). Non-polar organic solvents such as hexane or cyclohexane can be used subsequently to dissolve and remove residual sacrificial material from inside the channel. With PMMA microdevices, complete removal of the PCSL (**Figure 4.2I**) is verified by an absence of air bubbles in the channels upon filling with water.

4.3.5 Microchip evaluation

Several aspects of the microchips can be characterized after bonding is completed. For instance, the microchannel shape can be indicative of the effectiveness of the sacrificial material in protecting the microchannel during solvent bonding. Edge-on photomicrographs allow measurement of the cross-sectional areas of features, both before and after bonding. As an example, **Figure 4.3** shows cross-sectional views of a microchannel at several stages of the fabrication process. As is visible in **Figure 4.3B**, the paraffin wax PCSL appears to undergo a small amount of shrinkage upon solidification. Importantly, this minor shrinkage does not compromise microchannel usefulness, even with structures having depths as small as 7 μm.[37]

Another important parameter to evaluate in PCSL-fabricated microchips is the bond strength. Several techniques have been reported to determine the bonding strength of microfluidic chips; for example, by measuring the tensile force in pulling pieces apart[50] or by evaluating the shear force at the bonding interface of chips.[51] These methods normally use epoxy to attach a device to an external force; thus, the bond strength determination may be limited by the strength of the epoxy rather than the microchip itself. Kelly et al.[37] developed an approach for determining the maximum internal pressure that can be sustained in PCSL solvent-bonded devices. Briefly, an appropriately threaded PMMA piece (which can be connected to a N_2 cylinder via 1/16-in copper tubing) was bonded to a second PMMA substrate utilizing the same conditions (solvent, applied pressure and time) as for microchips. Once this assembly is connected to a gas cylinder, the applied pressure can be increased until either the device fails or the maximum cylinder value (~2200 psi) is reached. Using this approach, it was determined that PMMA bonded using acetonitrile

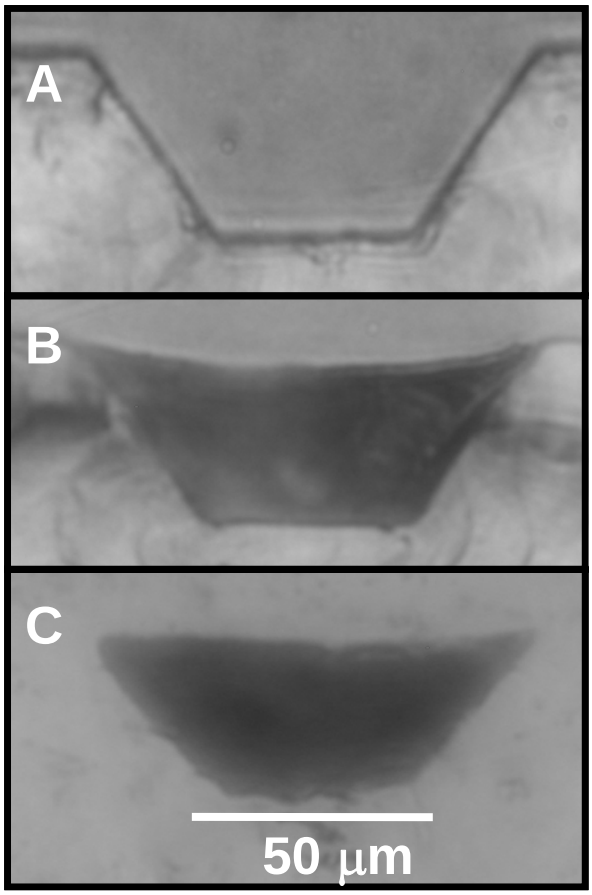

Figure 4.3 Edge-on photomicrographs of channel cross-sections at different fabrication stages. (A) Imprinted channel. (B) Imprinted channel filled with solidified PCSL. (C) Bonded device after PCSL removal. *Reprinted with permission from ref. 37; copyright 2005, American Chemical Society.*

under selected conditions was stable to at least 2200 psi internal pressure.[37] To more precisely measure the bond strength, one could appropriately connect PMMA substrates to a high-pressure liquid chromatography pump and measure the maximum pressure obtained before breakage. As with all high-pressure device failure determination methods, it is necessary to take proper safety precautions to avoid injury from PMMA projectiles that may be produced when failure occurs.

4.4 PRACTICAL APPLICATIONS

4.4.1 Microchip capillary electrophoresis

CE in polymer microfluidic devices was first demonstrated 10 years ago, in both PDMS[52,53] and PMMA.[44] The analysis of amino acids and peptides by μCE is a well-established procedure.[37,46,54] The operational parameters for injection and separation in μCE were presented in **Section 1.2.4.** A typical approach involves sample injection using the pinched injection mode[55] and detection by laser induced fluorescence to measure the signal of fluorescently labeled amino acids.[46,56] In this section, I describe the application of PCSL-formed PMMA microchips to the μCE analysis of amino acids and peptides.

4.4.1.1 Amino acid and peptide analysis

The PCSL techniques described in **Section 4.3** were used to fabricate PMMA microchips for μCE analysis. **Figure 4.4** shows an electropherogram of four FITC-labeled amino acids separated in a PCSL-formed solvent-bonded microchip. Importantly, these PCSL-fabricated microdevices are able to withstand applied electric fields of at least 1500 V/cm, which is the highest reported field strength for μCE in polymeric devices. The use

of high electric fields provided separation efficiencies of over 40,000 theoretical plates, which are comparable to values obtained in glass microchips.[54,57] **Figure 4.5** shows an electropherogram of seven FITC-labeled peptides separated in a PMMA microchip constructed using solvent bonding with PCSLs. The separation efficiency in the analysis of FITC-labeled peptides was similar to that for the analysis of amino acids. The ability to carry out high-performance μCE of peptides indicates that PCSL-formed devices have potential for proteomic analysis. In addition, PCSL-fabricated microchips were used to perform >300 μCE runs over a 3 month period with no degradation of separation performance. These results demonstrate the excellent potential for using PCSL solvent bonding in the fabrication of robust, low-cost microchips for high-quality and rapid electrophoretic analysis of biomolecules.

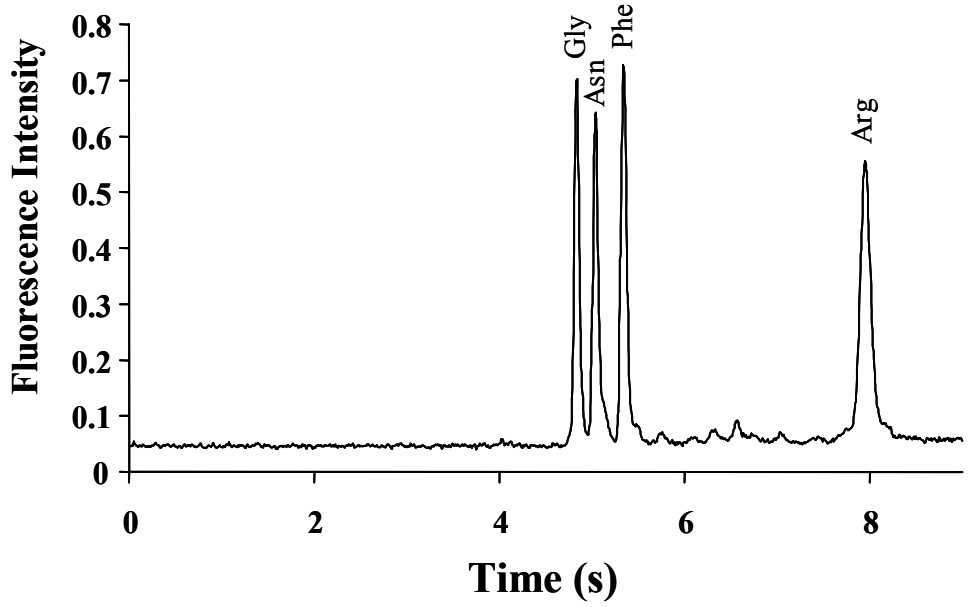

Figure 4.4 Separation of FITC-labeled amino acids (75 nM) in 10 mM carbonate buffer, pH 9.2. The injection voltage was +800 V, and the separation voltage was +3.0 kV. ***Reprinted with permission from ref. 37; copyright 2005, American Chemical Society.***

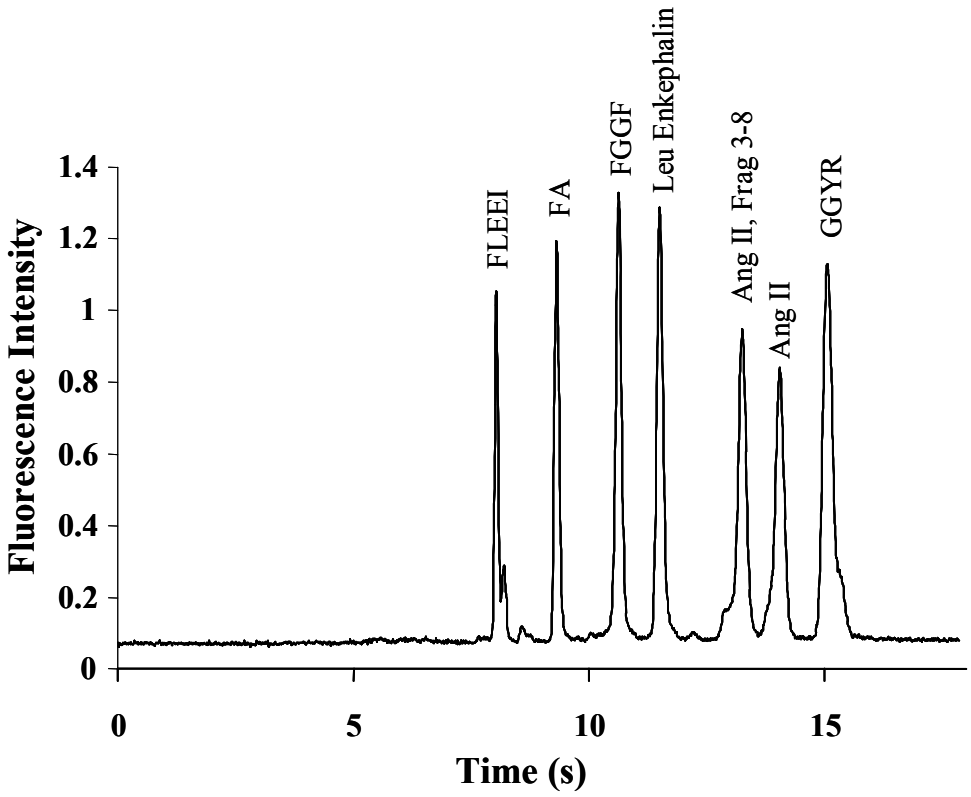

Figure 4.5 Separation of 110 nM FITC-labeled peptides; μCE separation conditions were the same as in Figure 4.4. ***Reprinted with permission from ref. 37; copyright 2005, American Chemical Society.***

4.4.2 PCSLs for integrating membranes with microfluidics

4.4.2.1 Fabrication

PCSLs offer a straightforward approach for incorporating additional components in-situ during the fabrication of microchips. For example, **Figure 4.6** shows a fabrication scheme for integrating an ion-permeable membrane with a microfabricated channel using PCSLs.[58] First, a PCSL-protected microchannel substrate is bonded to a PMMA cover piece having one or more reservoirs for membrane formation (**Figure 4.6A**). Next, prepolymer solution is poured into the membrane reservoir and UV polymerized while

maintaining the whole assembly at 4 ºC to avoid melting the PCSL (**Figure 4.6B-C**). Finally, the microchip is heated to allow facile removal of the liquefied PCSL, leaving a membrane-integrated microchannel in the device (**Figure 4.6D**). In addition to the characteristics noted in **Section 4.3.2,** PCSLs for the integration of membranes with microchannels must not react with or dissolve in either the membrane monomer solution or the polymerized hydrogel.

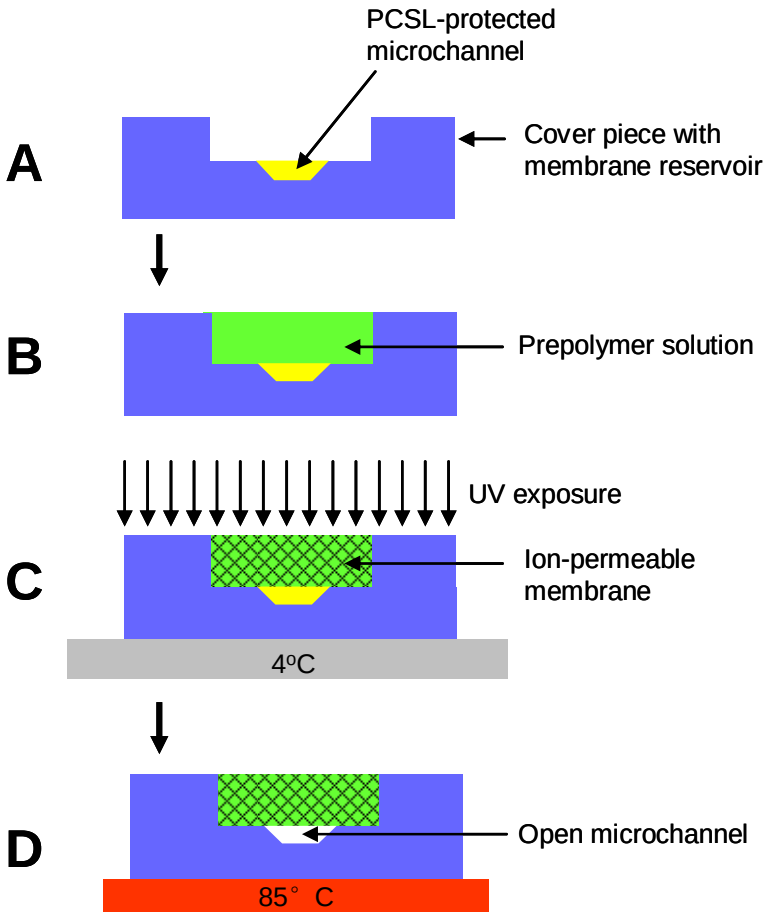

Figure 4.6 Schematic diagram of using PCSLs to interface microfluidics with ion-permeable membranes. (A) A PCSL-protected microchannel substrate is bonded to a PMMA cover piece having a membrane reservoir. (B) Prepolymer solution (green) is poured into the membrane reservoir. (C) An ion-permeable hydrogel is photopolymerized. (D) The PCSL is melted and removed from the channel. ***Adapted with permission from ref. 58; copyright 2006, American Chemical Society*****.**

4.4.2.2 Application to electric field gradient focusing

Electric field gradient focusing (EFGF) is an equilibrium-gradient separation method[59] in which analytes are focused at different equilibrium positions in an electric field gradient.[60,61] In EFGF, the electrophoretic motion of charged molecules in an electric field gradient in a column is opposed by hydrodynamic flow. The result is that each analyte will focus (stop) at an equilibrium position where the electrophoretic and laminar flow velocities are opposite and equal. The principle of EFGF has been studied theoretically and experimentally.[60-64]

Perhaps the simplest way to do EFGF is to interface an open column of constant cross-sectional area with a semipermeable membrane of changing cross-sectional area.[65] The ion-permeable membrane allows free flow of small buffer ions, but proteins are constrained to the open column, and the changing cross-sectional area of the semipermeable copolymer creates an electric field gradient. Interfacing an open column with an ion-permeable membrane is challenging using conventional methods,[65] but is a task that is ideally suited for PCSL fabrication.

Woolley's group has fabricated EFGF microchips using the PCSL approach.[58] In these devices, the membrane reservoir was a shaped region (for generating an electric field gradient) in the PMMA cover piece, and the open channel in the patterned substrate was protected with PCSL during membrane polymerization. The performance of PCSL-fabricated EFGF microchips was compared to that in capillary-based EFGF devices by analyzing two natively fluorescent proteins, R-phycoerythrin (R-PE) and green

fluorescent protein (GFP), in both systems. The results indicated a 4-fold reduction in peak width and a 3-fold improvement in resolution for PCSL-fabricated EFGF systems compared to capillary devices. Moreover, resolution for the analysis of peptides in microchip EFGF devices was comparable to that in μCE, but sample was concentrated 150-fold in the EFGF system.[58]

Using PCSLs to integrate microfabricated channels with ion-permeable membranes improves EFGF experiments. The smaller cross-sectional channel dimensions in the microchip EFGF devices reduce bandwidth and improve the resolution of protein peaks. Importantly, the fabrication protocols are flexible and easy to adapt as needed for different device designs.

4.4.2.3 Application to protein preconcentration

The same PCSL fabrication protocols for interfacing microfluidics and membranes in EFGF can also be used for on-chip protein preconcentration and separation.[58,66] A PCSL-filled microchannel imprinted in PMMA was affixed to a cover plate containing a membrane reservoir, and hydrogel was polymerized as described above.[58] To concentrate protein samples at the membrane, a voltage was applied between the sample and membrane reservoirs. Concentration factors as high as 10,000-fold for a model protein (R-PE) were observed.[58] Preconcentrated proteins were separated electrophoretically by applying a potential between the membrane reservoir and the reservoir at the end of the channel. A protein mixture containing R-PE and GFP was concentrated and separated electrophoretically in a membrane-integrated device.[66] These experiments verify the

power of the PCSL approach in making microchips for integrated sample enrichment and separation.

4.5 CONCLUDING REMARKS AND FUTURE TRENDS

In this chapter, I presented phase-changing sacrificial layers as enabling tools for making a variety of microfluidic devices in polymers. Several successful uses of PCSLs in biological analysis were discussed, which should motivate the pursuit of new developments and applications of this approach.

In the future, I anticipate the generalization of PCSL fabrication methods to polymers in addition to PMMA. **Table 4.1** summarizes the key considerations for selecting the substrate, sacrificial material and solvent in PCSL fabrication.[67] Some promising results have been obtained in extending the PCSL technique to other polymeric substrates, including PC, PET and COC.[67]

Table 4.1 PCSL solvent bonding method development considerations.

	Requirements
Substrate	Easily imprinted with template Inexpensive Seals to elastomer Doesn't interfere with chemical analysis
Sacrificial Material	Transitions from solid to liquid near room temperature Doesn't interact with polymer/elastomer Appropriate viscosity Forms smooth, even channels Solubility differs from substrate
Solvent	Dissolves substrate but not sacrificial layer Appropriate rate for dissolving substrate

In addition to the possibility of using PCSLs to construct microfluidics in various polymeric materials, this approach could also facilitate the implementation of new analysis techniques in a microchip format. For example, applications that require high pressures, such as for loading viscous sieving polymers for DNA separation or for packing small-diameter-particle stationary phases for chromatography, may become feasible in PCSL-fabricated polymer microchips, because of their high pressure stability.

4.5.1 Fabrication of multilayer microfluidic arrays

Interestingly, most research efforts with polymer microfluidic structures have focused on applying the same planar two-dimensional layouts of glass microchips in plastic devices. However, multilayer microstructures, wherein multiple channels can cross over one another without contamination, would significantly increase the operational flexibility in miniaturized analysis. Multilayer microfluidics have been fabricated in glass,[68] PDMS[69,70] and PDMS/glass hybrid microchips.[71] However, this design has not been implemented in easy-to-fabricate thermoplastic (rigid) polymers. Importantly, thermal bonding is problematic in the fabrication of multilayer structures because the heat and pressure often deform the surface, making it difficult to bond subsequent layers; moreover, microchannels can be constricted or blocked as a result of repeated heating steps. In contrast, PCSL fabrication protocols are simple and straightforward to implement, which would be advantageous for making multilayer polymer microchips. Indeed, using PCSL microfabrication, multiple substrates can be bonded together successfully without affecting the previous layers.

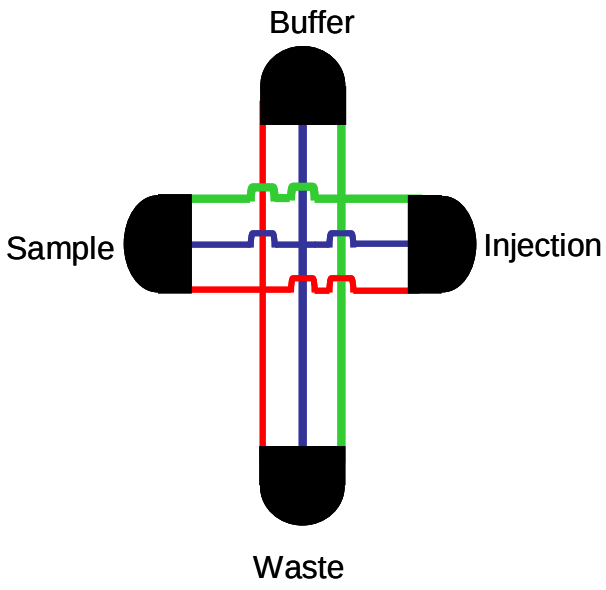

Figure 4.7 Layout of a multilayer microdevice for parallel, simultaneous analysis of a single sample in three channels.

Important new applications could be developed in multilayer polymer microfluidic systems. For example, multiple replicate analyses of a sample in a single reservoir could be performed in parallel on a single device. **Figure 4.7** shows a schematic diagram of a multilayer microdevice with channels crossing over each other. This device could be used to separate a sample in three microchannels using a single input, which would allow parallel, replicate analyses of the same specimen. Additional designs could be formed with parallel channels having different surface properties or separation media, to implement orthogonal separation mechanisms. Such layouts could then be used in parallel analysis of the same sample under different conditions. Finally, multilayer structures with crossing channels would facilitate the integration of end-column fluorescent or other labeling techniques in μCE.

4.6 REFERENCES

[1] Lion, N., Reymond, F., Girault, H. H., and Rossier, J. S., Why the move to microfluidics for protein analysis?, *Curr. Opin. Biotechnol.* 15, 31, 2004.
[2] Marko-Varga, G., Nilsson, J., and Laurell, T., New directions of miniaturization within the proteomics research area, *Electrophoresis* 24, 3521, 2003.
[3] Griebel, A., Rund, S., Schonfeld, F., Dorner, W., Konrad, R., and Hardt, S., Integrated polymer chip for two-dimensional capillary gel electrophoresis, *Lab Chip* 4, 18, 2004.

[4] Wang, J., Pumera, M., Chatrathi, M. P., Escarpa, A., Konrad, R., Griebel, A., Dorner, W., and Lowe, H., Towards disposable lab-on-a-chip: poly(methylmethacrylate) microchip electrophoresis device with electrochemical detection, *Electrophoresis* 23, 596, 2002.
[5] Brown, L., Koerner, T., Horton, J. H., and Oleschuk, R. D., Fabrication and characterization of poly(methylmethacrylate) microfluidic devices bonded using surface modifications and solvents, *Lab Chip* 6, 66, 2006.
[6] Shah, J. J., Geist, J., Locascio, L. E., Gaitan, M., Rao, M. V., and Vreeland, W. N., Capillarity induced solvent-actuated bonding of polymeric microfluidic devices, *Anal. Chem.* 78, 3348, 2006.
[7] Kricka, L. J., Fortina, P., Panaro, N. J., Wilding, P., Alonso-Amigo, G., and Becker, H., Fabrication of plastic microchips by hot embossing, *Lab Chip* 2, 1, 2002.
[8] Dittrich, P. S., Tachikawa, K., and Manz, A., Micro total analysis systems. Latest advancements and trends, *Anal. Chem.* 78, 3887, 2006.
[9] Stone, H. A. and Kim, S., Microfluidics: Basic issues, applications and challenges, *AICHE J.* 47, 1250, 2001.
[10] Teh, W. H. and Smith, C. G., Fabrication of quasi-three-dimensional micro/nanomechanical components using electron beam cross-linked poly(methyl methacrylate) resist, *J. Vac. Sci. Tech. B* 21, 3007, 2003.
[11] Edwards, J. M., Hamblin, M. N., Fuentes, H. V., Peeni, B. A., Lee, M. L., Woolley, A. T., and Hawkins, A. R., Thin film electroosmotic pumps for biomicrofluidic applications, *Biomicrofluidics* 1, 014101, 2007.
[12] Reano, R. M. and Pang, S. W., Sealed three-dimensional nanochannels, *J. Vac. Sci. Tech. B,* 23, 2995, 2005.
[13] Reed, H. A., White, C. E., Rao, V., Allen, S. A. B., Henderson, C. L., and Kohl, P. A., Fabrication of microchannels using polycarbonates as sacrificial materials, *J. Micromech. Microeng.* 11, 733, 2001.
[14] Wu, X. Q., Reed, H. A., Wang, Y., Rhodes, L. F., Elce, E., Ravikiran, R., Shick, R. A., Henderson, C. L., Allen, S. A. B., and Kohl, P. A., Fabrication of microchannels using polynorbornene photosensitive sacrificial materials, *J. Electrochem. Soc.* 150, H205, 2003.
[15] Li, W. L., Tegenfeldt, J. O., Chen, L., Austin, R. H., Chou, S. Y., Kohl, P. A., Krotine, J., and Sturm, J. C., Sacrificial polymers for nanofluidic channels in biological applications, *Nanotechnology* 14, 578, 2003.
[16] Home, R., Surface micromachining for microsensors and microactuators, *J. Vac. Sci. Tech. B,* 16, 1809, 1998.
[17] Harnett, C. K., Coates, G. W., and Craighead, H. G., Heat-depolymerizable polycarbonates as electrom beam patternable sacrificial layers for nanofluidics, *J. Vac. Sci. Technol. B* 19, 2842, 2001.
[18] Sharma, S., Buchholz, K., Luber, S. M., Rant, U., Tornow, M., and Abstreiter, G., Silicon-on-insulator microfluidic device with monolithic sensor integration for μTAS applications, *J. Micromech. Syst.* 15, 308, 2006.
[19] Peeni, B. A., Conkey, D. B., Barber, J. P., Kelly, R. T., Lee, M. L., Woolley, A. T., and Hawkins, A. R., Planar thin film device for capillary electrophoresis, *Lab Chip* 5, 501, 2005.

[20] Burbaum, C., Mohr, J., Bley, P., and Ehrfeld, W., Fabrication of Capacitive Acceleration Sensors by the LIGA Technique, *Sens. Actuators A* 27, 559, 1991.
[21] Maciossek, A., Lochel, B., Quenzer, H. J., Wagner, B., Schulze, S., and Noetzel, J., Galvanoplating and Sacrificial Layers for Surface Micromachining, *Microelectron. Eng.* 27, 503, 1995.
[22] Bagolini, A., Pakula, L., Scholtes, T. L. M., Pham, H. T. M., French, P. J., and Sarro, P. M., Polyimide sacrificial layer and novel materials for post-processing surface micromachining, *J. Micromech. Microeng.* 12, 385, 2002.
[23] Song, I. H. and Ajmera, P. K., Use of a photoresist sacrificial layer with SU-8 electroplating mould in MEMS fabrication, *J. Micromech. Microeng.* 13, 816, 2003.
[24] Chan, K. and Gleason, K. K., Air-gap fabrication using a sacrificial polymeric thin film synthesized via initiated chemical vapor deposition, *J. Electrochem. Soc.* 153, C223, 2006.
[25] Foquet, M., Korlach, J., Zipfel, W., Webb, W. W., and Craighead, H. G., DNA fragment sizing by single molecule detection in submicrometer-sized closed fluidic channels, *Anal. Chem.* 74, 1415, 2002.
[26] Wu, X. Q., Reed, H. A., Rhodes, L. F., Elce, E., Ravikiran, R., Shick, R. A., Henderson, C. L., Allen, S. A. B., and Kohl, P. A., Photoinitiation systems and thermal decomposition of photodefinable sacrificial materials, *J. Appl. Polym. Sci.* 88, 1186, 2003.
[27] Metz, S., Jiguet, S., Bertsch, A., and Renaud, P., Polyimide and SU-8 microfluidic devices manufactured by heat-depolymerizable sacrificial material technique, *Lab Chip* 4, 114, 2004.
[28] Hubbard, N. B., Howell, L. L., Barber, J. P., Conkey, D. B., Hawkins, A. R., and Schmidt, H., Structural models and design rules for on-chip micro-channels with sacrificial cores, *J. Micromech. Microeng.* 15, 720, 2005.
[29] Linder, V., Gates, B. D., Ryan, D., Parviz, B. A., and Whitesides, G. M., Water-soluble sacrificial layers for surface micromachining, *Small* 1, 730, 2005.
[30] Esinenco, D., Psoma, S. D., Kusko, M., Schneider, A., and Muller, R., SU-8 micro-mosensor based on Mach-Zehnder interferometer, *Rev. Adv. Mater. Sci.* 10, 295, 2005.
[31] Nam, W. J., Bae, S., Kalkan, A. K., and Fonash, S. J., Nano- and microchannel fabrication using column/void network deposited silicon, *J. Vac. Sci. Technol. A* 19, 1229, 2001.
[32] Bhusari, D., Reed, H. A., Wedlake, M., Padovani, A. M., Allen, S. A. B., and Kohl, P. A., Fabrication of air-channel structures for microfluidic, microelectromechanical, and microelectronic applications, *J. Microelectromech. Syst.* 10, 400, 2001.
[33] Turner, S. W., Perez, A. M., Lopez, A., and Craighead, H. G., Monolithic nanofluid sieving structures for DNA manipulation, *J. Vac. Sci. Technol. B* 16, 3835, 1998.
[34] Yin, D. L., Deamer, D. W., Schmidt, H., Barber, J. P., and Hawkins, A. R., Single-molecule detection sensitivity using planar integrated optics on a chip, *Opt. Lett.* 31, 2136, 2006.
[35] Peeni, B. A., Lee, M. L., Hawkins, A. R., and Woolley, A. T., Sacrificial layer microfluidic device fabrication methods, *Electrophoresis* 27, 4888, 2006.
[36] Jayachandran, J. P., Reed, H. A., Zhen, H. S., Rhodes, L. F., Henderson, C. L., Allen, S. A. B., and Kohl, P. A., Air-channel fabrication for microelectromechanical systems via sacrificial photosensitive polycarbonates, *J. Microelectromech. Syst.* 12, 147, 2003.

[37] Kelly, R. T., Pan, T., and Woolley, A. T., Phase-changing sacrificial materials for solvent bonding of high-performance polymeric capillary electrophoresis microchips, *Anal. Chem.* 77, 3536, 2005.
[38] Liu, R. H. and Grodzinski, P., Development of integrated microfluidic system for genetic analysis, *J.Microlith. Microfab.* 2, 340, 2003.
[39] Klintberg, L. and Suedberg, M., Fabrication of a paraffin actuator using hot embossing of polycarbonate, *Sens. Actuators A* 103, 307, 2003.
[40] Sethu, P. and Mastrangelo, C. H., Polyethylene glycol (PEG)-based actuator for nozzle-diffuser pumps in plastic microfluidic systems, *Sens. Actuators A* 104, 283, 2003.
[41] Pal, R., Yang, M., Johnson, B. N., Burke, D. T., and Burns, M. A., Phase change microvalve for integrated devices, *Anal. Chem.* 76, 3740, 2004.
[42] Verpoorte, E., Microfluidic chips for clinical and forensic analysis, *Electrophoresis* 23, 677, 2002.
[43] Qi, S., Liu, X., Ford, S., Barrows, J., Thomas, G., Kelly, K., McCandless, A., Lian, K., Goettert, J., and Soper, S. A., Microfluidic devices fabricated in poly(methyl methacrylate) using hot-embossing with integrated sampling capillary and fiber optics for fluorescence detection, *Lab Chip* 2, 88, 2002.
[44] Martynova, L., Locascio, L. E., Gaitan, M., Kramer, G. W., Christensen, R. G., and MacCrehan, W. A., Fabrication of plastic microfluid channels by imprinting methods, *Anal. Chem.* 69, 4783, 1997.
[45] McCormick, R. M., Nelson, R. J., Alonso-Amigo, M. G., Benvegnu, D. J., and Hooper, H. H., Microchannel electrophoretic separations of DNA in injection-molded substrates, *Anal. Chem.* 69, 2626, 1997.
[46] Kelly, R. T. and Woolley, A. T., Thermal bonding of polymeric capillary electrophoresis microdevices in water, *Anal. Chem.* 75, 1941, 2003.
[47] Jackman, R. J., Floyd, T. M., Ghodssi, R., Schmidt, M. A., and Jensen, K. F., Microfluidic systems with on-line UV detection fabricated in photodefinable epoxy, *J. Micromech. Microeng.* 11, 263, 2001.
[48] Huang, F. C., Liao, C. S., and Lee, G. B., An integrated microfluidic chip for DNA/RNA amplification, electrophoresis separation and on-line optical detection, *Electrophoresis* 27, 3297, 2006.
[49] Huang, C., Huang, S., and Lee, G., Pneumatic micropumps with serially connected actuation chambers, *J. Micromech. Microeng.* 16, 2265, 2006.
[50] Takeshi, I., Kazuharu, S., and Seishiro, O., Water glass bonding for micro-total analysis system, *Sens. Actuators B* 81, 187, 2002.
[51] Zhuang, G., Jin, Q., Liu, J., Cong, H., Liu, K., Zhao, J., Yang, M., and Wang, H., A low temperature bonding of quartz microfluidic chip for serum lipoproteins analysis, *Biomed. Microdevices* 8, 255, 2006.
[52] Duffy, D. C., McDonald, J. C., Schueller, O. J. A., and Whitesides, G. M., Rapid Prototyping of Microfluidic Systems in Poly(dimethylsiloxane), *Anal. Chem.* 70, 4974, 1998.
[53] Effenhauser, C. S., Bruin, G. J. M., Paulus, A., and Ehrat, M., Integrated capillary electrophoresis on flexible silicone microdevices: Analysis of DNA restriction fragments and detection of single DNA molecules on microchips, *Anal. Chem.* 69, 3451, 1997.

[54] Ramsey, J. D., Jacobson, S. C., Culbertson, C. T., and Ramsey, J. M., High-efficiency, two-dimensional separations of protein digests on microfluidic devices, *Anal. Chem.* 75, 3758, 2003.
[55] Jacobson, S. C., Hergenroder, R., Koutny, L. B., Warmack, R. J., and Ramsey, J. M., Effects of Injection Schemes and Column Geometry on the Performance of Microchip Electrophoresis Devices, *Anal. Chem.* 66, 1107, 1994.
[56] Monnig, C. A. and Jorgenson, J. W., On-column sample gating for high-speed capillary zone electrophoresis, *Anal. Chem.* 63, 802, 1991.
[57] Rocklin, R. D., Ramsey, R. S., and Ramsey, J. M., A microfabricated fluidic device for performing two-dimensional liquid-phase separations, *Anal. Chem.* 72, 5244, 2000.
[58] Kelly, R. T., Li, Y., and Woolley, A. T., Phase-changing sacrificial materials for interfacing microfluidics with ion-permeable membranes to create on-chip preconcentrators and electric field gradient focusing microchips, *Anal. Chem.* 78, 2565, 2006.
[59] Giddings, J. C., Resolution and peak capacity in equilibrium-gradient methods of separation, *Sep. Sci.* 6, 345, 1971.
[60] Tolley, H. D., Wang, Q., LeFebre, D. A., and Lee, M. L., Equilibrium Gradient Methods with Nonlinear Field Intensity Gradient: A Theoretical Approach, *Anal. Chem.* 74, 4456, 2002.
[61] Koegler, W. S. and Ivory, C. F., Focusing proteins in an electric field gradient, *J. Chromatogr. A* 726, 229, 1996.
[62] Ivory, C. F., A Brief Review of Alternative Electrofocusing Techniques, *Sep. Sci. Technol.* 35, 1777, 2000.
[63] Wang, Q., Tolley, H. D., LeFebre, D. A., and Lee, M. L., Analytical equilibrium gradient methods, *Anal. Bioanal. Chem.* 373, 125, 2002.
[64] Petsev, D. N., Lopez, G. P., Ivory, C. F., and Sibbett, S. S., Microchannel protein separation by electric field gradient focusing, *Lab Chip* 5, 587, 2005.
[65] Humble, P. H., Kelly, R. T., Woolley, A. T., Tolley, H. D., and Lee, M. L., Electric field gradient focusing of proteins based on shaped ionically conductive acrylic polymer, *Anal. Chem.* 76, 5641, 2004.
[66] Li, Y., Membrane-based protein preconcentration devices, *MSc. Thesis, Brigham Young University*, 2006.
[67] Draper, M., Solvent bonding of microfluidic devices, *Honors Thesis, Brigham Young University*, 2005.
[68] Verpoorte, E. M. J., van der Schoot, B. H., Jeanneret, S., Manz, A., Widmer, H. M., and de Rooij, N. F., Three-Dimensional Micro Flow Manifolds for Miniaturized Chemical Analysis Systems, *J. Micromech. Microeng.* 4, 246, 1994.
[69] Thorsen, T., Maerkl, S. J., and Quake, S. R., Microfluidic Large-Scale Integration, *Science* 298, 580, 2002.
[70] Kuo, T. C., Cannon, D. M., Chen, Y. N., Tulock, J. J., Shannon, M. A., Sweedler, J. V., and Bohn, P. W., Gateable nanofluidic interconnects for multilayered microfluidic separation systems, *Anal. Chem.* 75, 1861, 2003.
[71] Grover, W. H., Skelley, A. M., Liu, C. N., Lagally, E. T., and Mathies, R. A., Monolithic membrane valves and diaphragm pumps for practical large-scale integration into glass microfluidic devices, *Sens. Actuators B* 89, 315, 2003.

5. PHASE-CHANGING SACRIFICIAL LAYER FABRICATION OF MULTILAYER POLYMER MICROFLUIDIC DEVICES*

5.1 INTRODUCTION

In recent years, the use of micromachining to fabricate microfluidic structures for chemical analysis has emerged as a promising technology with potential application in bioanalytical chemistry.[1-4] Chip-based capillary electrophoresis (μCE) highlights many of the advantages of miniaturized devices relative to their macroscale counterparts.[5,6] However, constructing a true micro-total analysis system (μTAS)[7] in which sample pretreatment, mixing, separation and detection are performed in a single miniaturized platform remains a challenging task.

Polymers offer several advantages over glass for making microfluidic chips.[8,9] The ease of fabrication, low cost and availability of a broad range of polymeric substrates are key considerations that have motivated researchers to evaluate polymer-based microfluidic devices.[8,10] Materials such as poly(dimethylsiloxane) (PDMS),[11] poly(methyl methacrylate) (PMMA),[12] polycarbonate (PC),[13] and cyclic olefin copolymer[14,15] have been used increasingly in fabricating microfluidic systems.

Although polymers provide some benefits, glass microdevices also continue to be used broadly.[16,17] One important limiting factor in the wider application of polymer microchips appears to be the use of conventional microfabrication techniques. Indeed, the two-

* This chapter is reproduced with permission from *Anal. Chem.,* 2007, (*in press*). Copyright 2007, American Chemical Society.

dimensional nature of planar microchip systems, in which fluid flow is limited to a single plane, is one of the bottlenecks slowing the realization of true μTAS platforms. Therefore, the development of fabrication methods to meet the requirements for highly integrated and miniaturized devices is a critical research area.

A logical approach to increase design flexibility and functionality in microfluidic chips is the fabrication of multilayer systems in which fluidic paths proceed in multiple levels instead of remaining on a single layer. The development of multilayer devices has proven to be challenging due to difficulties in aligning and bonding individual layers; however, some progress has been made. Three-dimensional, layered microfluidic manifolds have been fabricated in PDMS,[18-21] SU-8[22] and glass.[23,24] PDMS multilayer systems are relatively easy to manufacture by replica molding or soft-lithography,[11,21] but are also subject to several weaknesses.[25,26] For instance, microstructures can be damaged readily during release from the mold, and bonded devices are sometimes delaminated under applied pressure or voltage. Additionally, applications in PDMS microdevices are limited by the compatibility of PDMS with many analytes.[27] Despite these challenges, PDMS-based multilayer systems have seen some success. Separated bands have been transferred between microchannels,[28] and gated sample injections have been performed by transferring sample from an injection channel into a separation channel via a nanocapillary array.[29] Quake et al.[30] demonstrated that multilayer systems can provide higher levels of integration, allowing complex fluid manipulations with a minimal number of controlled inputs.[19,30] Compared to PDMS, glass-based multilayer microdevices are attractive because of their chemical stability, well-known surface

chemistry and established micromachining protocols.[31] However, making multilayer microdevices in glass is a difficult task, requiring repeated thermal bonding steps that are time consuming.

Due to these challenges with glass and PDMS, fabricating multilayer systems in thermoplastic materials is attractive and could facilitate the development of sophisticated analytical microdevices. Fettinger et al.[32] machined a multilayer system in PMMA having millimeter-dimension channel or chamber structures in each level interconnected by through-holes. Although this initial work demonstrated that liquid flow in multilayer systems was possible for millimeter-scale fluidics, the feasibility of constructing multilayer hard polymer microfluidic platforms and utilizing them for multi-analyte separations has not yet been shown. Importantly, conventional thermal bonding techniques are problematic for fabricating multilayer systems having micrometer-dimension structures because heating a material to near its glass transition temperature in repetitive bonding steps typically distorts patterned features. Moreover, the low bond strength and electrical field resistance of thermally bonded devices may limit potential applications.

Some progress has been made in fabricating multilayer microfluidic devices in hard polymers using alternative bonding methods. Flachsbart et al.[33] used adhesives to enclose multilayer PMMA/PC microfluidics and were able to inject and detect a single protein. However, they found that the adhesive could block microchannels and interfere with electroosmotic flow. Weigl et al.[34] also used adhesive bonding to assemble multilayer polymer microchips with laser-machined features. However, the smallest channel

dimensions feasible with this method (50-100 μm) were in the range of large microfluidics, such that they would be non-ideal for separations. Mensing et al.[35] used liquid-phase photopolymerization to construct multilayer devices. Although this approach avoided adhesive for bonding, the microchannels were several hundred micrometers in cross-section, making them unsuitable for high-performance electrophoretic applications. In summary, advances have been made in assembling multilayer polymer microfluidic structures, but further fabrication improvements are needed to enable broad use in chemical separations.

Woolley's group recently developed a microfabrication method using a combination of phase-changing sacrificial layers (PCSLs) and solvent bonding to make polymer microfluidic chips for μCE analysis.[36] Furthermore, the PCSL approach was applied in the fabrication of microchannels integrated with ion-permeable hydrogels for analyte preconcentration[37] and electric field gradient focusing.[38] The simplicity of the PCSL fabrication technique, the robustness of the constructed microsystems, and the quality of the separations obtained indicate that PCSLs may be valuable for making multilayer systems in thermoplastic polymers.[39]

Herein, I report the fabrication, characterization and utilization of multilayer microfluidic chips made in PMMA using PCSLs and solvent bonding. Individual substrates with PCSL-filled microchannels and through-holes were aligned and solvent bonded to produce multilayer structures in which microchannels can cross one another. I evaluated the bonding strength, the fluidic and electrical independence of channels, μCE analysis,

and the effects of fluid flow and applied potentials in crossing channels on separation efficiency in these devices.

5.2 EXPERIMENTAL SECTION

5.2.1 Materials and reagents

Paraffin wax (melting point 65ºC; Service Assets, Newport Beach, CA) was used as the PCSL. Glycine, asparagine, phenylalanine and arginine were purchased from ICN Biomedicals (Aurora, OH). Fluorescein-5-isothiocyanate (FITC) came from Molecular Probes (Eugene, OR). Deionized (DI) water (18.3 MΩ·cm) obtained from an Easypure UV/UF water purification system (Dubuque, IA) was used to prepare all solutions. Carbonate and Tris buffer solutions were adjusted to set pH values with 0.1 M NaOH or HCl. Reagent-grade solvents (acetonitrile, hexane, acetone, and isopropanol) were purchased from Fisher Scientific (Fair Lawn, NJ). Masking and adhesive tape were Scotch brand (3M, St. Paul, MN).

5.2.2 Device fabrication

Construction of the microdevices involved five steps: (i) chip design, (ii) photolithographic patterning and micromachining of silicon templates, (iii) substrate imprinting and reservoir fabrication, (iv) protecting features with sacrificial material, and (v) alignment and solvent-assisted bonding. These processes are described in detail in the following paragraphs.

5.2.2.1 Chip design

A schematic of the microchip layout is shown in **Figure 5.1A**. In our three-layer design, fluidic manifolds are obtained by aligning the top and bottom microchannel-containing layers with the interconnecting through-holes in the middle piece (**Figure 5.1B**). The bottom layer has features for two independent electrophoretic systems positioned perpendicular to each other. The main separation path is defined in the bottom layer, and most of the second separation channel is also patterned on the bottom piece, but this structure overpasses the main fluidic path via through-holes bridged with a microchannel in the lower surface of the top layer. Channel linewidths were 40 μm, depths were 30 μm, lengths from reservoirs 1-3 to the injection intersection were 0.5 cm, and the separation channel was 2.5-cm long from the injection region to reservoir 4. The layouts for the bottom and top masks included marks for alignment of the substrates during the bonding step.

5.2.2.2 Silicon template preparation

Two photomasks with the features of the bottom and top layers in **Figure 5.1A** were drawn using mask layout software (WieWeb) and converted to chromium-coated 5" glass plates using an Electromask TRE Cris-Cross Pattern Generator (Woodland Hills, CA). The features in the mask were then transferred to a silicon template using conventional photolithography and wet chemical etching as described previously.[40]

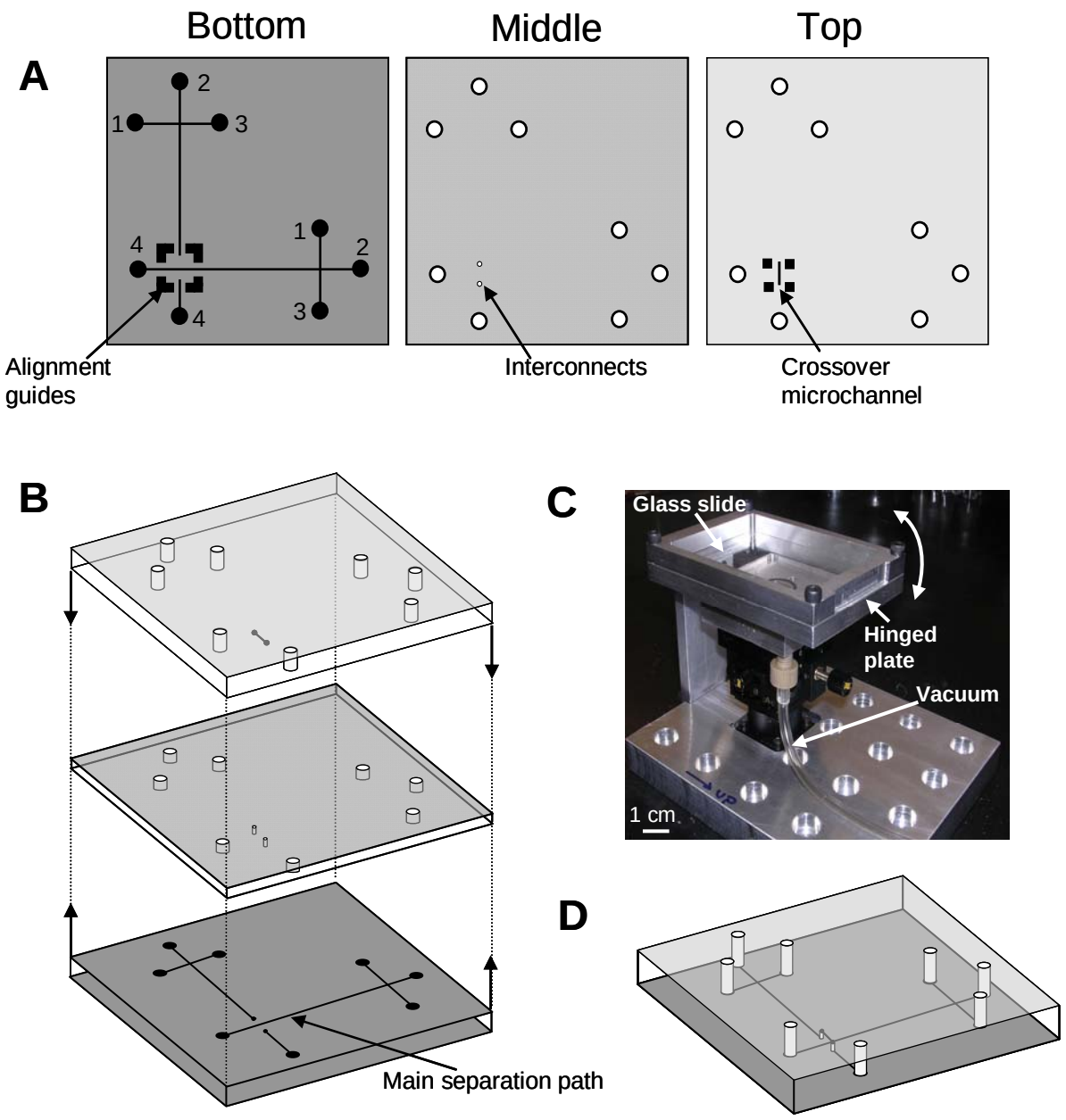

Figure 5.1. (A) Schematic of the three layers for the fabrication of microchannels in multilayer microdevices. Reservoirs are: (1) analyte, (2) buffer, (3) injection waste, and (4) waste. (B) Exploded view of the three layers. (C) Photograph of the alignment and bonding station. (D) Schematic of a completed microchip formed by successive alignment and bonding of the individual layers. A final device is 4 cm on each side and 4.5 mm tall.

5.2.2.3 Substrate imprinting and reservoir fabrication

Using a procedure reported by Locascio et al.,[41] I embossed the elevated features in the silicon template into 1/16-in-thick PMMA substrates (Acrylite OP-3, Cyro, Rockaway, NJ) in a convection oven at 140 ºC. I affixed a microscope slide to the back of the template to reinforce it to avoid breakage during imprinting. To prevent the Si template from sticking to the PMMA, I sprayed the surface with silicone lubricant (Stoner, Quarryville, PA) before imprinting the substrates. A CO_2 laser cutter (C-200, Universal Laser Systems, Scottsdale, AZ) was used to create 2-mm-diameter reservoirs in the middle and top layers for sample and buffer loading. Finally, two 280-μm-diameter through-holes were made in the middle layer to serve as interconnects.

5.2.2.4 Filling with sacrificial material

The main fluidic path in the bottom layer was filled with PCSL using the approach reported by Kelly et al.[36] Filling non-continuous channels in the bottom layer, interconnecting holes in the middle piece and the crossover channel in the top layer required a modified approach. To deposit sacrificial material in discontinuous channels, solid paraffin wax was placed in the patterned reservoir area at one end of each channel. Then, the substrate was placed on a hotplate at 85ºC to melt the sacrificial material and fill the microchannels by capillary action. To avoid overflow of sacrificial material, the amount of paraffin used in this step was selected to cover ~50% of the reservoir area. To fill the crossover microchannels, which did not have patterned reservoir areas at either end, an opening the approximate length of the microchannel was defined on a piece of adhesive tape using the laser cutting system. Then, the surface was covered with the

patterned tape, aligning the opening with the microchannel underneath. After this, a small piece of solid paraffin wax was placed on top of the tape and melted to fill the microchannel. Through-holes in the middle layer were also filled with PCSL using this patterned adhesive tape approach.

5.2.2.5 Alignment and solvent-assisted bonding

Individual layers were aligned as shown in **Figure 5.1B.** I designed and assembled an alignment and bonding station using translation and rotation stages (Melles Griot, Carlsbad, CA) integrated in a custom-machined stand (**Figure 5.1C**). The station was designed to allow alignment and bonding steps to be performed sequentially by means of three moving parts: (1) a lower x-y-z translation stage (resolution: 1.5 μm), (2) a rotating plate attached on top of the translation stage (angular resolution: 5′), and (3) a microscope slide attached to a top hinged plate, which could be lifted or lowered.

For alignment, the bottom PMMA substrate with PCSL-filled microchannels was held in place on the rotating plate by vacuum. Next, the middle layer was reversibly attached to the microscope slide on the hinged plate using a ~100-μm-thick PDMS film (Sylgard 184, Dow Corning, Midland, MI). Following this, the aligner was placed under a Leica semiconductor inspection microscope (Wetzlar, Germany), and the interconnects in the middle piece were aligned with the two ends of the discontinuous microchannel in the bottom layer. Once the two pieces were aligned, the hinged plate was lifted and 280 μL of acetonitrile were spread on the upper surface of the bottom substrate. Finally, the hinged plate was lowered quickly and the two layers were held together for 2 min to

effect bonding. This sequence of alignment and bonding steps was repeated to seal the top substrate and obtain a fluidic routing manifold with independent crossing microchannels (**Figure 5.1D**).

5.2.3 Microdevice characterization

I evaluated bonding strength, fluid flow in the crossover channel, fluidic integrity, and electrical independence of the flow paths in PCSL-fabricated multilayer microdevices. For these studies, a modified microchip was fabricated in which reservoirs 1 and 3 were eliminated in the crossover channel and the spacing between reservoirs 2 and 4 was decreased to 1.5 cm, with either a 5.0 or 0.8 mm gap for the crossover. Bonding strength was determined by affixing Nanoport reservoirs (Upchurch Scientific, Oak Harbor, WA) on top of the openings at both ends of the crossover channel. After filling the main path with orange dye solution and the crossover with green dye, one Nanoport was capped while the other was connected via appropriate fittings to an N_2 cylinder at various pressures, and the microdevices were inspected for solution leaks or delamination of the layers. The colored solutions facilitated visual inspection and easy determination of any leaks. The ability of the devices to handle fluid flow in both channels was tested by filling with buffer solution and examining for bubbles inside the microchannels and the crossover section. Complete filling of the crossover channel was verified by measuring the current as a function of applied voltage. I also studied the electrical independence of the flow paths by taking current measurements under applied voltages in the separation channel while various potentials were applied in the crossing channel.

5.2.4 Electrophoretic analysis of amino acids

I tested the ability of our PCSL-fabricated multilayer microdevices to perform μCE. In addition, I studied the effects of both pressure and potential applied in the crossover on the separation performance of fluorescently labeled amino acids dissolved in 10 mM carbonate buffer, pH 9.2. Each amino acid was tagged using FITC as described previously.[36] Microchannels and reservoirs were filled with buffer, and 15 μL of sample were added to reservoir 1. To reduce electroosmotic flow, 0.5% (w/v) hydroxypropyl cellulose (100 kDa average MW, Sigma-Aldrich) was added to the running buffer.[42] Sample was loaded using "pinched" injection[43] for 20 s with +1.0 kV applied at reservoir 3, while keeping the other reservoirs grounded. For separation, reservoir 2 was grounded, reservoirs 1 and 3 were held at +1.0 kV and a potential of +3.5 kV was applied at reservoir 4. Separated amino acids were detected by laser-induced fluorescence using the 488-nm line from an air-cooled Ar ion laser, as described before.[40] Briefly, I focused the laser ~800 μm from the end of the main separation path using a 20x, 0.45 NA objective. Fluorescence was collected with the same objective and detected at a photomultiplier tube after spectral and spatial filtering.

Fluidic integrity during separation was determined by filling the crossover with 0.5 μM fluorescein solution and detecting a μCE separation (in the main path) of two amino acids at a point 2 mm before and 2 mm after the crossover channel. Additionally, I studied the effect of pressurized buffer flow in the crossover on the separation of FITC-labeled amino acids in the main path. Finally, electrical independence during separation was

evaluated by applying a potential along the crossover channel and monitoring its effect on μCE of FITC-labeled amino acids in the main path.

5.3 RESULTS AND DISCUSSION

Figure 5.2A-B shows pictures of the crossover region of an imprinted PMMA microdevice before and after filling the channels with PCSL. By flowing the sacrificial material into the microchannels by using capillary action as opposed to vacuum, I was able to obtain well-filled features without PCSL deposition outside the microchannels.[36] **Figure 5.2C** shows a photograph of a completed PCSL-fabricated multilayer microdevice with a 0.8-mm-long crossover.

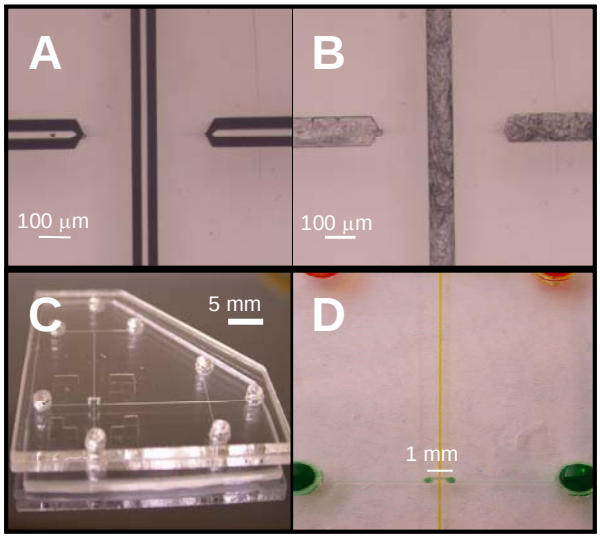

Figure 5.2 Microdevice photographs. (A) Image of the crossover region of an imprinted device showing two channel ends. (B) Photograph of the crossover area in the same device after filling with sacrificial material. (C) Photo of a PCSL-fabricated multilayer microdevice with an 0.8-mm-long microchannel crossing over the main separation path. (D) Close-up picture of a crossover in a multilayer microdevice; channels have been filled with colored dye solution to enhance contrast.

During each bonding step, the non-bonding sides of the substrates were covered with masking tape to prevent solvent from contacting the device exterior. In multilayer systems with interconnecting channels, alignment between layers is crucial to ensure fluidic continuity. Although the translational resolution of the *x*-*y*-*z* stage in the alignment station was 1.5

μm, the alignment precision was 26 μm (RSD = 3.5%, *n* = 10). I attribute this experimental variation to positioning uncertainty in the hinged plate. However, given the larger diameter of the interconnects (280 μm) relative to the microchannels, I was readily able to obtain adequate fluidic continuity between microchannels and interconnects. Ideally, the crossover channel should be as short as possible. The gap between the two ends of the crossover in **Figure 5.2A** is ~600 μm; however, laser cutting of through-holes was problematic with this spacing. An 800-μm gap enabled robust crossover fabrication and was the shortest distance for which reliable results were obtained. The volume of these crossover channels was ~0.45 nL, corresponding to <0.4% of the total crossover volume of ~125 nL; the remainder of the crossover volume was contributed by the through-holes.

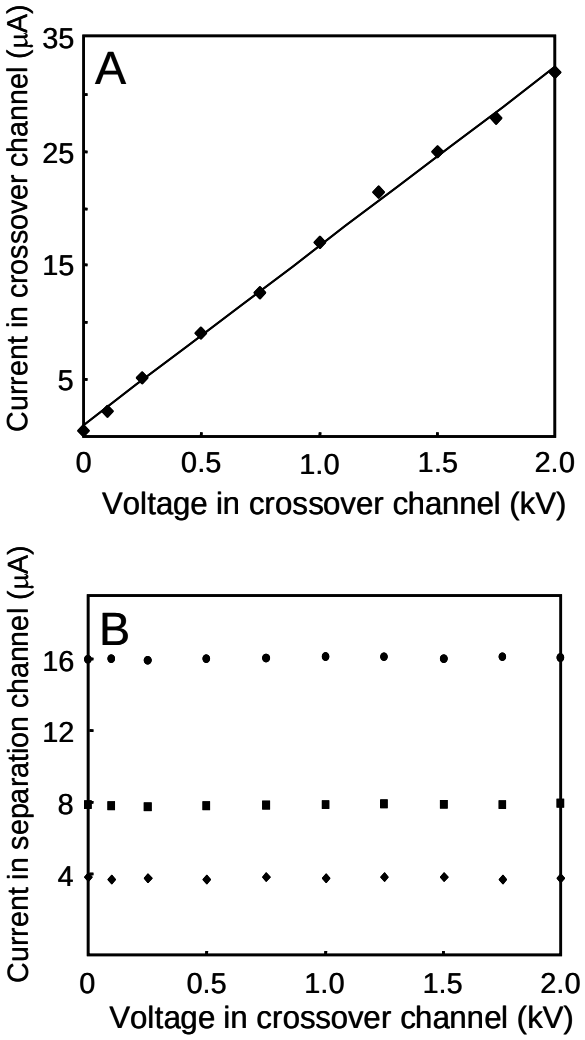

Figure 5.3 Study of the electrical independence of microchannels in PCSL-fabricated multilayer microdevices. (A) Current vs. voltage relationship in the crossover channel (mA = 0.0157V + 0.982; r^2 = 0.998). (B) Current in the main separation path at three different potentials (◆: 0.5 kV, ■: 1.0 kV, ●: 2.0 kV) in the presence of the indicated voltages on the crossover channel (*additional details are in the text*).

Figure 5.2D shows a close-up of the crossover region in a multilayer microdevice. The two colored solutions demonstrate independent fluid flow through the microchannels. When the crossover was pressurized at up to 300 psi, no discernable leaks were observed in microchannels and no delamination of PMMA layers occurred; however, seals between the Nanoports and reservoirs typically failed at ~300 psi, hindering our assessment at higher pressures. Should the need arise for greater pressures in crossover channels, it may be possible to evaluate device integrity at higher pressures by creating threaded reservoir openings.[36] Importantly, our results demonstrate that robust PMMA multilayer microfluidic devices can be fabricated using PCSLs.

Figure 5.3A shows a current vs. voltage plot obtained in a crossover channel filled with 10 mM Tris buffer, pH 8.1. The linear relationship observed (r^2 = 0.998) indicates that the crossover channel was bubble free and Joule heating was not a problem even at the highest potential applied (2.0 kV). **Figure 5.3B** shows current measurements for three applied voltages in the separation channel in the presence of a range of applied potentials in the crossover channel. For all voltages in the crossover, current measurements in the separation channel at 0.5, 1.0 and 2.0 kV were relatively constant (RSD: 0.2-1.0%). Furthermore, the linear current vs. voltage relationships (r^2 = 0.998-0.999) in the separation channel at all applied potentials in the crossover channel indicate the absence of Joule heating. These observations demonstrate that a potential in the crossover channel has no measurable effect on the electrical characteristics of the separation channel.

To further confirm the fluidic and electrical independence of the microchannels in PCSL-fabricated multilayer devices, I studied the effects on μCE of flow and applied potentials in the crossing channel. Separations of amino acids in the main path of multilayer microdevices (e.g., **Figure 5.4A**) were similar to those obtained in standard designs without crossover channels.

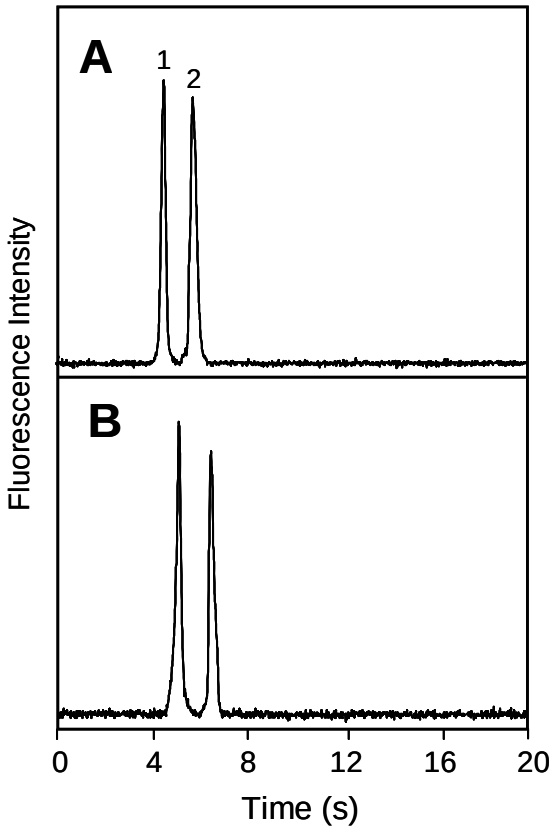

Figure 5.4 Microchip CE of FITC-labeled amino acids for evaluating the fluidic independence of microchannels in multilayer microdevices. Separation and detection were performed in the main (non-crossover) separation path, and the crossover channel was filled with 0.5-μM fluorescein. Detection was (A) 2 mm before and (B) 2 mm after the crossover region. Peaks are: (1) glycine and (2) asparagine.

To study the fluidic independence of the separation and crossover channels, a crossover with a 0.8-mm-long section bridging over the main separation path was filled with 0.5 μM fluorescein solution, and μCE of two FITC-tagged amino acids was performed in the separation channel. Peaks detected 2 mm before (**Figure 5.4A**) and 2 mm after (**Figure 5.4B**) the crossover channel maintained their shape and baseline integrity. The small shift in migration time was due to detection at different positions in the separation channel.

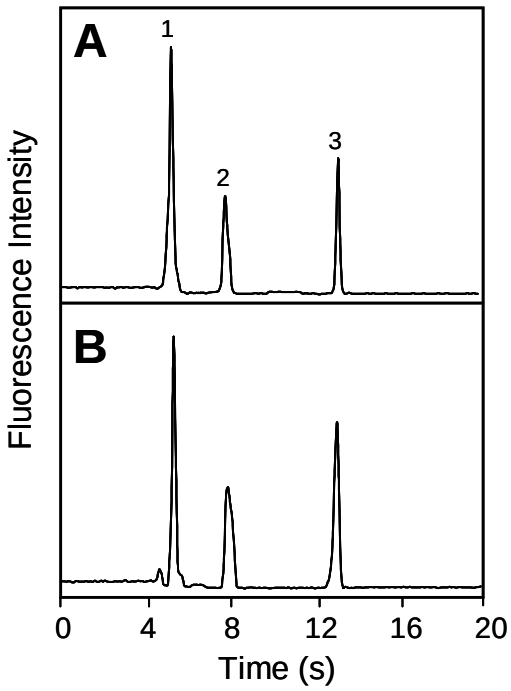

Figure 5.5 Microchip CE of FITC-tagged amino acids in the main separation path in the (A) absence and (B) presence of pressurized 1.5 mL/min buffer flow in the crossover channel. Peaks are: (1) glycine, (2) phenylalanine and (3) arginine.

Microchannel fluidic independence was further studied by pumping 10 mM Tris buffer (pH 8.1) through the crossover channel during μCE in the main path. The electrophoretic analysis of three FITC-tagged amino acids in **Figure 5.5A** was essentially the same as when the separation was performed with a 1.5 μL/min buffer flow in the crossover channel (**Figure 5.5B**). These results clearly demonstrate that microchannels in PCSL-fabricated multilayer devices are fluidically independent. I evaluated the electrical independence of microchannels in our multilayer systems by probing the effects of voltage applied in the crossover channel on separation in the main channel. **Figure 5.6A-B** shows μCE analysis of three fluorescently labeled amino acids in a multilayer microdevice with a 5.0-mm-long crossover. **Figure 5.6C-D** shows μCE of four fluorescently labeled amino acids in a multilayer microdevice with a 0.8-mm-long crossover. Electropherograms with 250 V/cm applied in the crossover channel (**Figure 5.6B,D)** are indistinguishable from those in **Figure 5.6A,C** with no applied potential. Separation efficiency for phenylalanine in ten consecutive runs with and without voltage in the crossover was 10,400 theoretical plates (RSD = 3.7%),

indicating that the voltage in the crossover has no significant effect on separation efficiency in the main path.

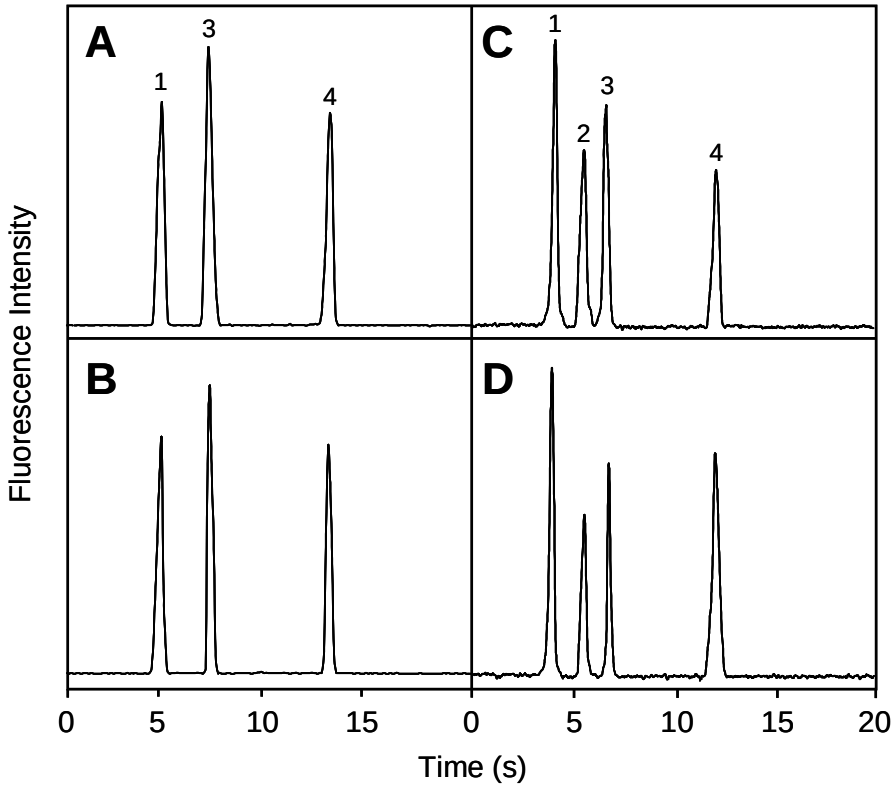

Figure 5.6 CE analysis of FITC-labeled amino acids for evaluating the electrical independence of microchannels in multilayer microdevices. (A-B) Microchip with a 5.0-mm-long crossover channel. (C-D) Microdevice with a 0.8-mm-long crossover channel. (A,C) Separation and detection in the main separation path; (B,D) same as (A,C) but with 250 V/cm applied in the crossover channel. Peaks are: (1) glycine, (2) asparagine, (3) phenylalanine and (4) arginine.

These results demonstrate that crossover channels in PCSL-fabricated multilayer systems are electrically independent. This should allow simultaneous microchip separations in both the main fluidic path and a crossover channel, although the large laser-cut through-holes occupy a much greater volume relative to the channels, which currently precludes high-performance μCE in crossover channels.

Importantly, even in the present format, applications can be envisioned in which multiple separation paths are maintained in a single layer (so separation quality is sufficient), whereas other fluid manipulations are performed in crossover channels, to reduce the total number of reservoirs needed in a device. For instance, one injection reservoir could be interfaced with many separation channels, by using crossovers only in the injection channels. This would enable the parallel analysis of samples by multiple methods (zone electrophoresis, denaturing or native gel electrophoresis, micellar electrokinetic chromatography, etc.). Moreover, with crossover channels, a single sample labeling reservoir could be connected to parallel separation channels (that lack crossovers) to simplify end-column labeling. Crossover volumes could also be reduced; for example, a 250-μm-thick middle layer would decrease the crossover volume six-fold. Alternative hole forming methods could shrink the dead volume further. A heated ~100-μm-diameter wire could form smaller openings in these films than is feasible with laser cutting. Micromachined posts with ~50-μm-diameters could provide through-holes for a middle layer made from a cast or polymerized ~50-μm-thick film; these vias would have a dead volume of ~100 pL, a decrease of three orders of magnitude over the current format. Such volume reductions would enable high-performance separations in channels with crossovers; Chapter 6 explores this exciting possibility.

5.4 CONCLUSIONS

I have presented a novel method for fabricating multilayer polymeric microchips using paraffin wax as a phase-changing sacrificial material during solvent bonding. I demonstrated that PCSL-fabricated crossover microchannels are fluidically and

electrically independent; moreover, efficient μCE separations can be performed in the presence of pressure-driven flow or an applied potential in the crossover channel. This work represents a significant advance in the construction of multilayered microfluidic chips in thermoplastic polymers. Fabrication is easier and faster compared to glass micromachining, and the resulting devices should be suitable for analyses not feasible in previous microchips. PCSL-fabricated multilayer microdevices have potential to increase design flexibility with the integration of additional layers or microchannels for multiplexed and parallel analysis.

5.5 REFERENCES

[1] Reyes, D. R., Iossifidis, D., Auroux, P. A., and Manz, A., Micro Total Analysis Systems. 1. Introduction, Theory, and Technology, *Anal. Chem.* 74, 2623, 2002.
[2] Khandurina, J. and Guttman, A., Bioanalysis in microfluidic devices, *J. Chromatogr. A* 943, 159, 2002.
[3] Sia, S. K. and Whitesides, G. M., Microfluidic devices fabricated in poly(dimethylsiloxane) for biological studies, *Electrophoresis* 24, 3563, 2003.
[4] Roman, G. T., Chen, Y. L., Viberg, P., Culbertson, A. H., and Culbertson, C. T., Single-cell manipulation and analysis using microfluidic devices, *Anal. Bioanal. Chem.*. 387, 9, 2007.
[5] Dolnik, V., Liu, S., and Jovanovich, S., Capillary electrophoresis on microchip, *Electrophoresis* 21, 41, 2000.
[6] Dolnik, V. and Liu, S. R., Applications of capillary electrophoresis on microchip, *J. Sep. Sci.* 28, 1994, 2005.
[7] Manz, A., Graber, N., and Widmer, H. M., Miniaturized Total Chemical-Analysis Systems - a Novel Concept for Chemical Sensing, *Sens. Actuators B* 1, 244, 1990.
[8] Soper, S. A., Ford, S. M., Qi, S., McCarley, R. L., Kelly, K., and Murphy, M. C., Polymeric microelectromechanical systems, *Anal. Chem.* 72, 642A, 2000.
[9] Becker, H. and Locascio, L. E., Polymer microfluidic devices, *Talanta* 56, 267, 2002.
[10] Boone, T. D., Hugh Fan, Z., Hooper, H. H., Ricco, A. J., Tan, H., and Williams, S. J., Plastic advances microfluidic devices, *Anal. Chem.* 74, 78A, 2002.
[11] McDonald, J. C., Duffy, D. C., Anderson, J. R., Chiu, D. T., Wu, H., Schueller, O. J. A., and Whitesides, G. M., Fabrication of microfluidic systems in poly(dimethylsiloxane), *Electrophoresis* 21, 27, 2000.
[12] Qi, S. Z., Liu, X. Z., Ford, S., Barrows, J., Thomas, G., Kelly, K., McCandless, A., Lian, K., Goettert, J., and Soper, S. A., Microfluidic devices fabricated in poly(methyl

methacrylate) using hot-embossing with integrated sampling capillary and fiber optics for fluorescence detection, *Lab Chip* 2, 88, 2002.
[13] Liu, Y., Ganser, D., Schneider, A., Liu, R., Grodzinski, P., and Kroutchinina, N., Microfabricated Polycarbonate CE Devices for DNA Analysis, *Anal. Chem.* 73, 4196, 2001.
[14] Kameoka, J., Craighead, H. G., Zhang, H. W., and Henion, J., A polymeric microfluidic chip for CE/MS determination of small molecules, *Anal. Chem.* 73, 1935, 2001.
[15] Stachowiak, T. B., Mair, D. A., Holden, T. G., Lee, L. J., Svec, F., and Frechet, J. M. J., Hydrophilic Surface Modification of Cyclic Olefin Copolymer Microfluidic Chips Using Sequential Photografting, *J. Sep. Sci.* 30, 1088, 2007.
[16] Dittrich, P. S., Tachikawa, K., and Manz, A., Micro total analysis systems. Latest advancements and trends, *Anal. chem.* 78, 3887, 2006.
[17] Rodriguez, I., Spicar-Mihalic, P., Kuyper, C. L., Fiorini, G. S., and Chiu, D. T., Rapid prototyping of glass microchannels, *Anal. Chim. Acta* 496, 205, 2003.
[18] Grover, W. H., Skelley, A. M., Liu, C. N., Lagally, E. T., and Mathies, R. A., Monolithic membrane valves and diaphragm pumps for practical large-scale integration into glass microfluidic devices, *Sens. Actuators B* 89, 315, 2003.
[19] Liu, J., Hansen, C., and Quake, S. R., Solving the "world-to-chip" interface problem with a microfluidic matrix, *Anal. Chem.* 75, 4718, 2003.
[20] Kim, J. Y., Baek, J. Y., Lee, K. A., and Lee, S. H., Automatic aligning and bonding system of PDMS layer for the fabrication of 3D microfluidic channels, *Sens. Actuators A* 119, 593, 2005.
[21] Unger, M. A., Chou, H.-P., Thorsen, T., Scherer, A., and Quake, S. R., Monolithic Microfabricated Valves and Pumps by Multilayer Soft Lithography, *Science* 288, 113, 2000.
[22] Agirregabiria, M., Blanco, F. J., Berganzo, J., Arroyo, M. T., Fullaondo, A., Mayora, K., and Ruano-Lopez, J. M., Fabrication of SU-8 multilayer microstructures based on successive CMOS compatible adhesive bonding and releasing steps, *Lab Chip* 5, 545, 2005.
[23] Verpoorte, E. M. J., van der Schoot, B. H., Jeanneret, S., Manz, A., Widmer, H. M., and de Rooij, N. F., Three-Dimensional Micro Flow Manifolds for Miniaturized Chemical Analysis Systems, *J. Micromech. Microeng.* 4, 246, 1994.
[24] Daridon, A., Fascio, V., Lichtenberg, J., Wutrich, R., Langen, H., Verpoorte, E., and de Rooij, N. F., Multi-layer microfluidic glass chips for microanalytical applications, *Fres. J. Anal. Chem.* 371, 261, 2001.
[25] Ocvirk, G., Munroe, M., Tang, T., Oleschuk, R., Westra, K., and Harrison, D. J., Electrokinetic control of fluid flow in native poly(dimethylsiloxane) capillary electrophoresis devices, *Electrophoresis* 21, 107, 2000.
[26] Baltussen, E., Sandra, P., David, F., Janssen, H. G., and Cramers, C., Study into the equilibrium mechanism between water and poly(dimethylsiloxane) for very apolar solutes: Adsorption or sorption?, *Anal. Chem.* 71, 5213, 1999.
[27] Ren, X. Q., Bachman, M., Sims, C., Li, G. P., and Allbritton, N., Electroosmotic properties of microfluidic channels composed of poly(dimethylsiloxane), *J. Chromatogr. B* 762, 117, 2001.

[28] Kuo, T. C., Cannon, D. M., Chen, Y. N., Tulock, J. J., Shannon, M. A., Sweedler, J. V., and Bohn, P. W., Gateable nanofluidic interconnects for multilayered microfluidic separation systems, *Anal. Chem.* 75, 1861, 2003.
[29] Cannon, D. M., Kuo, T. C., Bohn, P. W., and Sweedler, J. V., Nanocapillary array interconnects for gated analyte injections and electrophoretic separations in multilayer microfluidic architectures, *Anal. Chem.* 75, 2224, 2003.
[30] Thorsen, T., Maerkl, S. J., and Quake, S. R., Microfluidic large-scale integration, *Science* 298, 580, 2002.
[31] Simpson, P. C., Woolley, A. T., and Mathies, R. A., Microfabrication Technology for the Production of Array Electrophoresis Chips, *J. Biomed. Microdevices* 1, 7, 1998.
[32] Fettinger, J. C., Manz, A., Ludi, H., and Widmer, H. M., Stacked modules for microflow systems in chemical analysis: concept and studies using an enlarged model *Sens. Actuators B* 17, 19-25, 1993.
[33] Flachsbart, B. R., Wong, K., Iannacone, J. M., Abante, E. N., Vlach, R. L., Rauchfuss, P. A., Bohn, P. W., Sweedler, J. V., and Shannon, M. A., Design and fabrication of a multilayered polymer microfluidic chip with nanofluidic interconnects via adhesive contact printing, *Lab Chip* 6, 667, 2006.
[34] Weigl, B. H., Bardell, R., Schulte, T., Battrell, F., and Hayenga, J., Design and rapid prototyping of thin-film laminate-based microfluidic devices, *Biomed. Microdevices* 3, 267, 2001.
[35] Mensing, G., Pearce, T., and Beebe, D. J., An ultrarapid method of creating 3d channels and microstructures, *J. Assoc. Lab. Autom.* 10 , 24, 2005.
[36] Kelly, R. T., Pan, T., and Woolley, A. T., Phase-changing sacrificial materials for solvent bonding of high-performance polymeric capillary electrophoresis microchips, *Anal. Chem.* 77, 3536, 2005.
[37] Kelly, R. T., Li, Y., and Woolley, A. T., Phase-changing sacrificial materials for interfacing microfluidics with ion-permeable membranes to create on-chip preconcentrators and electric field gradient focusing microchips *Anal. Chem.* 78, 2565, 2006.
[38] Kelly, R. T. and Woolley, A. T., Electric field gradient focusing, *J. Sep. Sci.* 28, 1985, 2005.
[39] Fuentes, H. V. and Woolley, A. T., Using Sacrificial Materials to Fabricate Polymeric Microfluidic Devices, in *Handbook of Capillary and Microchip Electrophoresis and Associated Microtechniques*, Landers, J. P. Ed. CRC, Boca Raton, FL, 2007.
[40] Kelly, R. T. and Woolley, A. T., Thermal bonding of polymeric capillary electrophoresis microdevices in Water, *Anal. Chem.* 75, 1941, 2003.
[41] Martynova, L., Locascio, L. E., Gaitan, M., Kramer, G. W., Christensen, R. G., and MacCrehan, W. A., Fabrication of plastic microfluid channels by imprinting methods, *Anal. Chem.* 69, 4783, 1997.
[42] Sanders, J. C., Breadmore, M. C., Kwok, Y. C., Horsman, K. M., and Landers, J. P., Hydroxypropyl cellulose as an adsorptive coating sieving matrix for DNA separations: Artificial neural network optimization for microchip analysis, *Anal. Chem.* 75, 986, 2003.
[43] Jacobson, S. C., Hergenroder, R., Koutny, L. B., Warmack, R. J., and Ramsey, J. M., Effects of injection schemes and column geometry on the performance of microchip electrophoresis devices, *Anal. Chem.* 66, 1107, 1994.

6. MULTIPLEXED SEPARATIONS IN MULTILAYER MICROFLUIDIC DEVICES WITH CROSSOVER CHANNELS

6.1. INTRODUCTION

Recent advances in genomics and proteomics have increased the demand for high-throughput analytical tools capable of analyzing multiple samples in parallel. Multiplexed capillary electrophoresis (CE) was key for the completion of the Human Genome Project years before the estimated finishing deadline.[1] Today, multiplexed CE separations are routine for DNA sequencing, genotyping and characterizing libraries of compounds for drug discovery.[2]

Miniaturization has become a central issue in the area of chemical separations with a growing number of applications in chemical and biological analyses.[3] One of the most attractive features associated with microfluidic platforms is their potential to integrate multiple fluid manifolds in a single substrate using micromachining techniques. An outstanding illustration of multiplexed separations on-chip has been reported by Mathies et al.[4] for the analysis of DNA in 384 microchannel arrays. Microfluidic devices for parallel separations have been utilized for genetic analysis,[5,6] immunoassays,[7] enzyme assays,[8] clinical diagnostics,[9] and multiplexed on-chip electrospray mass spectrometry.[10]

Whereas these applications have demonstrated the advantages of multiplexing microfluidic channels or manifolds, fabrication protocols and device operation are normally labor intensive due to the large number of reservoirs that need to be made and utilized. Indeed, as the number of channels (N) increases, it becomes more challenging to control sample introduction and electrical inputs. In a planar two-dimensional layout, 3N + 1 reservoirs and electrical connections are needed to operate a microdevice.[5] Moreover, the number of channel networks and reservoirs that can be integrated in a device is limited due to spatial restrictions on a device footprint.[11] Finally, loading of samples and reagents, as well as making electrical connections to multiple reservoirs, is usually time consuming.

The two-dimensional nature of many microfluidics platforms does not allow complex fluid and electrical connections since microchannels cannot cross each other without interaction. Therefore, generating three-dimensional (3D) structures in which independent microchannels can cross one another should allow the realization of more sophisticated multiplexed systems with minimal control inputs.[12,13] Using phase changing sacrificial layers (PCSLs) and solvent bonding,[14] I recently developed a method to fabricate multilayer polymeric microfluidic systems, as reported in Chapter 5.[15] These devices have microchannels that can cross one another without electrical or fluidic interference.

In this chapter, I report the design, fabrication and evaluation of multilayer polymer microfluidic chips with crossover channels for electrophoretic separations and

multiplexed analysis. Compared to the devices in Chapter 5,[15] the crossover volume was reduced at least fifty-fold by using a 250-μm-thick intermediate PMMA film with <100-μm-diameter through-holes. Finally, multichannel multilayer microchips were evaluated for the multiplexed, parallel separation of two fluorescently labeled peptides.

6.2. MATERIALS AND METHODS

6.2.1 Chemicals

Peptides, Phe-Leu-Glu-Glu-Ile (FLEEI) and Ala-Leu-Ala-Leu (ALAL), were from Sigma (St. Louis, MO), and amino acids including glycine, phenylalanine and arginine were purchased from ICN Biomedicals (Aurora, OH). Buffer solutions were prepared with deionized water (18.3 MΩ·cm) from an Easypure UV/UF purification system (Dubuque, IA). Fluorescein-5-isothiocyanate (FITC) came from Molecular Probes (Eugene, OR). All solvents used (acetonitrile, hexane, acetone, and isopropanol) were reagent-grade and were purchased from Fisher Scientific (Fair Lawn, NJ). Paraffin wax (melting point, 65ºC; Service Assets, Newport Beach, CA) was used as the sacrificial material during solvent bonding.

6.2.2 Description of the fabrication protocol

Multilayer microdevices having crossover microchannels were fabricated in poly(methyl methacrylate) (PMMA, Cyro, Rockaway, NJ) using a methodology described in Chapter 4-5.[15,16] Microchannels were imprinted in 1/16-in-thick PMMA layers using photolitographically patterned and chemically etched silicon templates.[17] Fluidic paths in the top and bottom layers were interconnected via through-holes in a 250-μm-thick

intermediate PMMA film (Goodfellow, Oakdale, CA). Access holes for sample and buffer solutions, as well as interconnects in the middle layer, were created using a CO_2 laser cutting system (C-200, Universal Laser Systems, Scottsdale, AZ). To facilitate bonding of the middle layer, the thin PMMA film was attached to a microscope slide (Fisher, trimmed to 35 x 35 mm) using double-sided tape (Scotch, 3M, St. Paul, MN) and bonded to the bottom layer. Following this, the top layer was sealed as described in Section 5.2.2.5[15] (**Figure 6.1**).

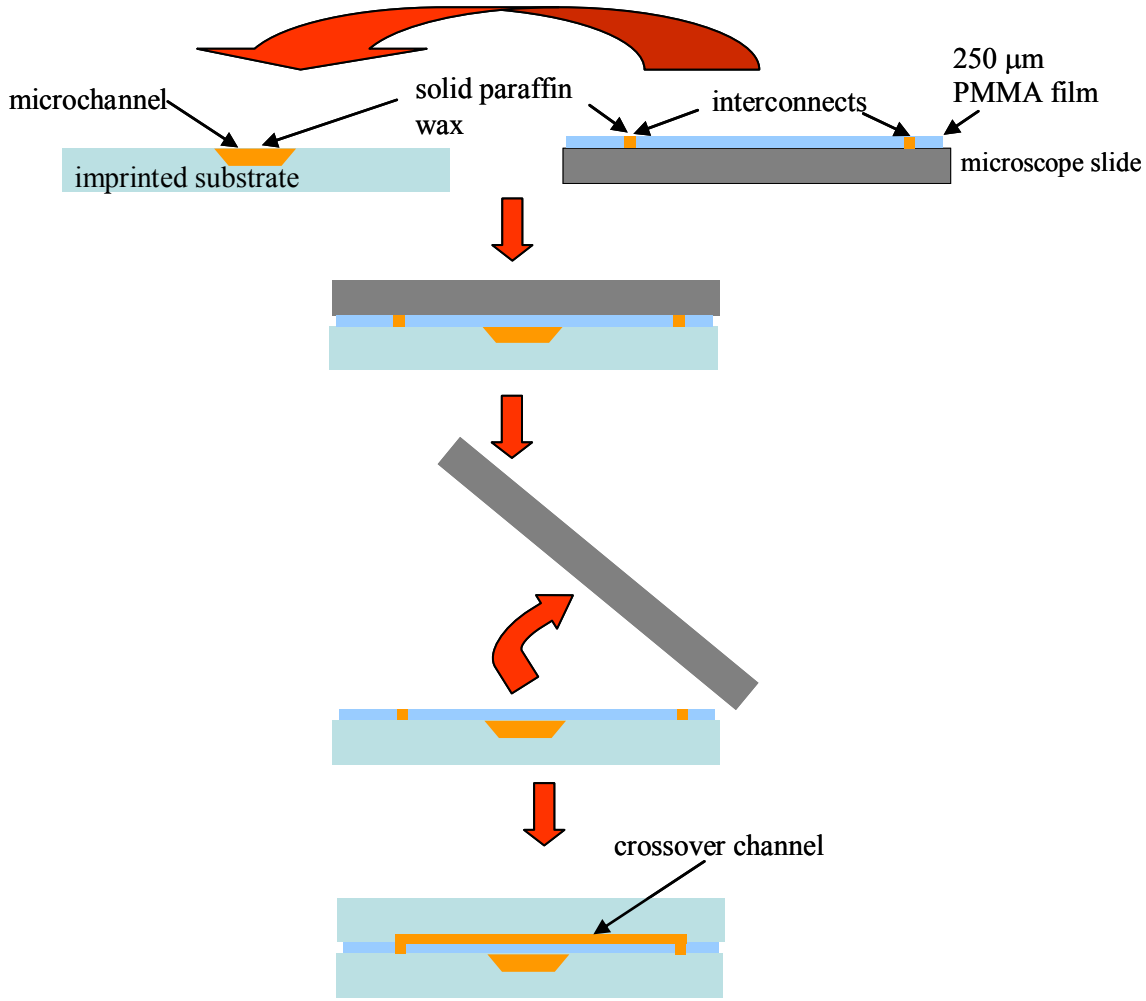

Figure 6.1 Schematic of the fabrication of multilayer microfluidic devices with a thin intermediate layer.

6.2.3 Device fabrication

I used a microchip design similar to that described in Section 5.2.2.1 to evaluate the feasibility of fabricating multilayer microdevices with a thin intermediate layer. **Figure 6.2A** illustrates the microchip layout in which the separation path has a gap that can be bridged with a crossover channel, resulting in a three-dimensional fluidic pathway. Microchannel linewidths were 40 µm and the distances from the injection intersection to the sample reservoir (SR), buffer reservoir (BR) and sample waste reservoir (SW) were 0.5 cm. The separation channel was 2.5-cm-long from the injection point to the waste reservoir (WR); this distance includes a 0.5-cm-long crossover section located 1.75 cm downstream from the injection intersection (**Figure 6.2A**).

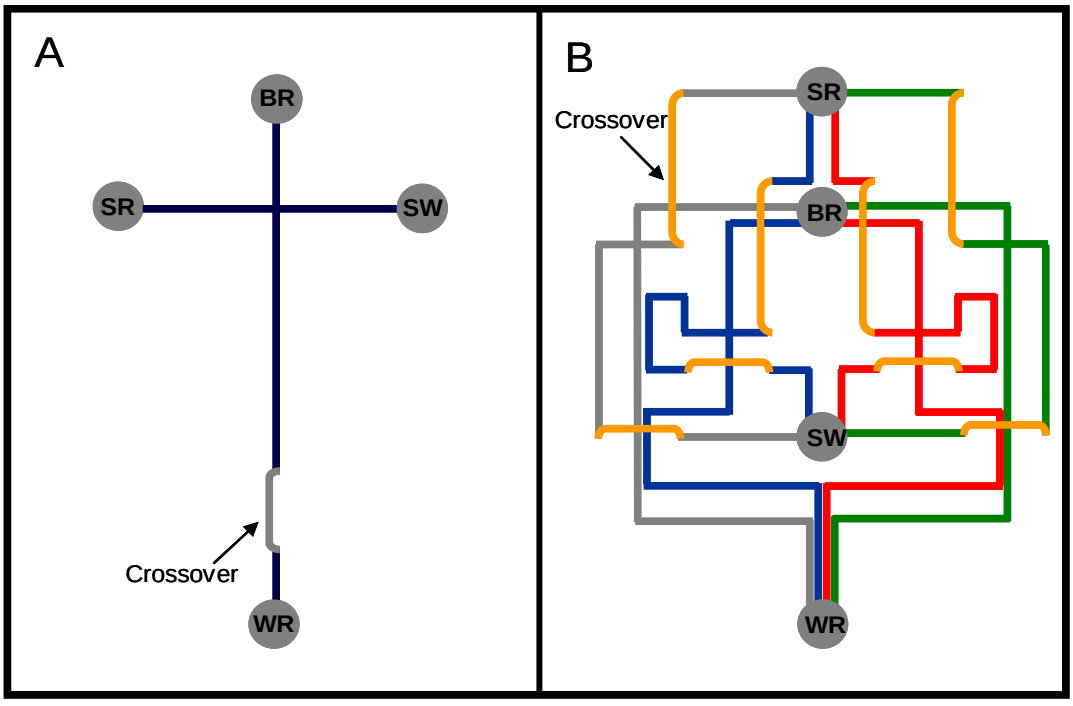

Figure 6.2 Microchip designs. (A) Microfluidic device for separations in crossover channels. (B) Design layout of a microdevice to run replicate analyses in parallel (*additional details are in the text*).

A multilayer microchip was designed to run an individual sample in parallel in four channels for simultaneous replicate analysis (**Figure 6.2B**). Each channel type (e.g., injection, separation, etc.) has identical length and number of crossover sections, which facilitates operation under a single set of injection and separation potentials. For each channel, the distance from the SR to the injection intersection was 2.75 cm, including a 1.0-cm-long crossover section. The distance from each injection intersection to the SW was 1.75 cm, including a 0.5-cm-long crossover. All separation channels were maintained in a single layer; the distance from the BR to each microchannel intersection was 1.25 cm, while the distance from the injection point to the WR was 3.5 cm.

6.2.4 Electrophoretic analysis

Amino acids and peptides were tagged fluorescently using FITC as described in Chapters 3 and 5.[15,18] For all electrophoretic analysis experiments, 10 mM carbonate (pH 9.2) having 0.5% (w/v) hydroxypropyl cellulose[19] (100 kDa average MW, Sigma-Aldrich) was used as the running buffer. Three FITC-labeled amino acids were injected and separated in a microchip with a crossover channel having the device layout illustrated in **Figure 6.2A**. Briefly, microchannels were filled with running buffer, and 15 μL of sample were loaded into the SR. For injection, +1.2 kV were applied at the SW for 20 s while keeping the other reservoirs grounded. To effect separation, the BR was grounded; the SR and SW were held at +1.2 kV, and 4.0 kV were applied at the WR. Laser induced fluorescence (LIF) of the separated amino acids was effected ~500 μm before and after the crossover region using the 488-nm line from an air-cooled Ar ion laser; the LIF detection system has been described previously.[17] I collected the fluorescence signal

using a 20x, 0.45 NA objective and a photomultiplier tube to detect photons passing through the aperture after spectral and spatial filtering. The sampling rate for data collection of the detector output on a personal computer was 10 Hz.

Multiplexed on-chip electrophoretic analysis of FITC-labeled FLEEI and ALAL was performed in a 2.5-mm-thick, 3.5 x 3.5 cm microchip having the device layout shown in **Figure 6.2B.** Sample placed in the SR was loaded using "pinched" injection[20] for 10-20 s with +1.2 kV applied at the SW. For separation, +4.5 kV were applied at the WR while keeping the SR and SW at +1.2 kV and grounding the BR. Replicates of injection and separation were performed simultaneously in all of the channels in the microdevice. For each separation, LIF detection was effected by aligning the laser beam manually with a channel ~800 μm from the WR, using the translation stage of an inverted optical microscope (TE300, Nikon, Tokyo, Japan).

6.3 RESULTS AND DISCUSSION

6.3.1 Separations in crossover microchannels

My initial work on PCSL-fabricated multilayer microdevices in Chapter 5 served to demonstrate the potential of using the PCSL approach to fabricate multilayer microdevices with both fluidically and electrically independent microchannels.[15] Even though some applications can be envisioned in these microdevices, the large diameters of the interconnects (~280 μm) relative to the microchannel widths (40 μm) prohibited high-performance separations in crossover channels. By using a thinner (250-μm-thick)

PMMA film as the intermediate layer, instead of the previous 1.6-mm thickness, smaller through-holes (<100 μm) can be formed, reducing the crossover volume up to fifty-fold. Importantly, thinner intermediate layers should allow the depth of focus of the machining laser beam to be more uniform across the substrate, resulting in a higher-fidelity and smaller-diameter cut.

Interestingly, I observed that laser-cut openings designed with a 100-μm diameter in 250-μm-thick PMMA films resulted in through-holes with 60-90-μm diameters. I hypothesize that the heat generated by the laser beam melts some PMMA around the opening, which then re-solidifies to produce narrower holes.

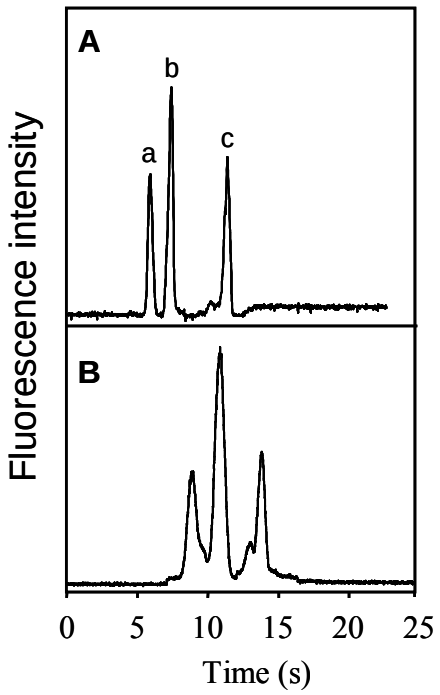

Figure 6.3 Separation in microchannels with a crossover section. (A) Detection before and (B) after the crossover. Peaks are: (a) glycine, (b) phenylalanine, and (c) arginine. ***Additional details are in the text.***

The benefits of having a reduced crossover volume are tremendous. **Figure 6.3** shows the separation and detection of three 0.5 μM FITC-labeled amino acids in a microchannel with a 5-mm-long crossover. Detection was performed both before (**Figure 6.3A)** and after (**Figure 6.3B)** the crossover. Importantly, all peaks were resolved at both detection points. The resolution for the Gly and Phe peaks was 1.6 in **Figure 6.3A** and 1.2 in **Figure 6.3B**. The efficiency of the phenylalanine peak was 3020 and 950 theoretical plates in **Figures 6.3A** and **6.3B,** respectively. The lower efficiency observed for

peaks detected after the crossover section is due to the change in cross-sectional area and the four turns experienced by the peaks as they traveled through the crossover. The effects of turns in microchannels have been studied before.[20-22] In general, bends or curves contribute to analyte dispersion due to variations in migration distance and electric field strength. Since the electric field is parallel to the microchannel walls in a turn, the same potential drop occurs over a shorter distance on the inner side of the curve than on the outer side. As a result, the inside edge of the curve experiences a stronger field than the outside edge. The faster migration of the solutes near the inner edge of the turn compared to the analytes in the outer edge creates band dispersion due to the so-called "race-track-effect."[22]

For the electric field to remain constant in a microchannel-crossover junction, the cross-sectional area of the through holes should be made to match the cross-sectional area of the microchannels at the interconnecting points. Differences in cross-sectional areas of the interconnecting vias and the microchannels cause variations in the electroosmotic flow rate (Q_{os}) according to:[23]

$$Q_{os} = \mu_{os} E S \qquad (6.1)$$

where S is the cross-sectional area of the microchannel, μ_{os} is the electroosmotic mobility and E is the applied potential. This difference in EOF in the crossover section compared to EOF in the microchannels also contributes to band broadening and can degrade separation efficiency in crossover channels.

Nevertheless, these results demonstrate that separations are feasible in crossover microchannels. The length of the crossover also affected separations. I performed experiments with microchannels having a shorter crossover, and for ten trials in two different devices; the Gly and Phe peaks were not resolved in microchips with a 1.0-mm-long crossover (results not shown).

6.3.2 Multichannel microdevices

As mentioned earlier, multilayer systems are attractive because they can potentially facilitate the development of complex microchips for multiplex analysis. **Figure 6.4** shows a photograph of a PCSL-fabricated PMMA microdevice having four separation channels in which four replicate analyses of a sample from a common reservoir can be run in parallel.

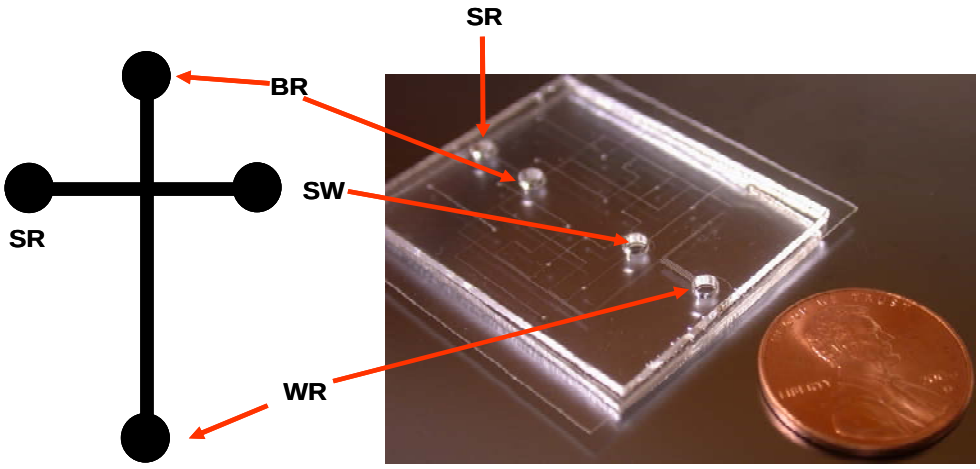

Figure 6.4 Photograph of a multilayer multichannel device to run replicate analyses in parallel. The device layout is shown in Figure 6.2B. The microchip is operated using the same number of control inputs as a microchip with a single channel.

Because of the ability to make crossover channels, only four reservoirs are needed to operate the device, which is the same number of inputs used to run a sample in a single channel microchip. Importantly, the symmetry of this design should allow more channels to be added without the need for extra reservoirs. Alignment of the micrometer-scale channels and openings in each layer is critical during fabrication. I used an x-y-z alignment and bonding station (Section 5.2.2.5 and Figure 5.1C),[15] which helped me obtain open fluidic vias in at least three out of four channels in most cases.

Etching crystalline silicon to pattern features with turns such as those in **Figure 6.2B** is problematic and usually results in "chopped" corners or even complete destruction of the micropattern. I resolved this issue by etching the Si templates to only 12 μm, which reduced the extent of corner cutting of features. Alternatively, SU-8 templates can be patterned using photolithography, resulting in microstructures with vertical side walls that can be transferred into PMMA substrates using solvent-assisted imprinting.[24] Thus, better-defined turns should be obtained easily using SU-8 templates.

6.3.3 Multiplexed separations

PCSL-fabricated multilayer multichannel microdevices were evaluated for the multiplexed analysis of two peptides. **Figure 6.5** shows three replicate separations of FLEEI and ALAL from three different channels. The relative standard deviation of the elution time for the ALAL peak was 2.8%. Small observed changes in the peak intensity and elution times can be attributed to variations in the injection efficiency and current through the different channels.

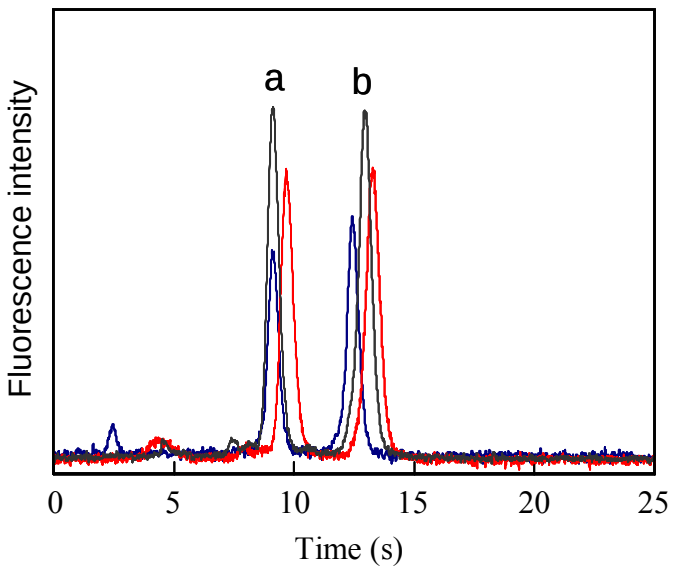

Figure 6.5 Multiplexed electrophoretic separation of 0.1 μM peptides. Peaks are: (a) FLEEI and (b) ALAL. The injection voltage was +1.2 kV and the separation voltage was +4.5 kV.

Although the chip design had four separation microchannels, only three channels were of use in the fabricated chip since there was no flow in the fourth channel due to misalignment at one of the crossover connections. The results obtained, however, demonstrate that crossover microchannels fabricated using the approach presented here are suitable for making microchannel arrays to facilitate the development of sophisticated microfluidic devices for multiplexed separations.

6.4 CONCLUSIONS

I have demonstrated that PCSLs can be used readily in the fabrication of multilayer microdevices having a 250-μm-thick intermediate layer. Reduction of the crossover volume allowed separations to be performed in a microchannel with a crossover and in multichannel multilayer microdevices for multiplexed analysis. Despite a decrease in efficiency and resolution when the peaks were detected after a crossover, the separation obtained was still acceptable. Both resolution and efficiency could be improved by using longer crossovers or making the through-hole diameters the same as the microchannel widths. Crossover microchannels facilitated the integration of multiple channels for

parallel analysis with a minimum number of control inputs. Fast (<15 s) separation of two peptides was achieved in three channels in parallel. The results obtained clearly demonstrate the potential of my fabrication strategy to develop a new generation of microfluidic chips. I anticipate that continued efforts and new ideas for multiplexing separations will further advance applications of microfluidics for the high-throughput analysis of proteomic samples.

6.5 REFERENCES

[1] Zubritsky, E., How analytical chemists saved the Human Genome Project, *Anal. Chem.* 74, 22A, 2002.

[2] Pang, H.-M., Kenseth, J., and Coldiron, S., High-throughput multiplexed capiollary electrophoresis in drug discovery, *Drug Discovery Today* 9, 1072, 2004.

[3] Dittrich, P. S., Tachikawa, K., and Manz, A., Micro total analysis systems. Latest advancements and trends, *Anal. Chem.* 78, 3887, 2006.

[4] Emrich, C. A., Tian, H. J., Medintz, I. L., and Mathies, R. A., Microfabricated 384-lane capillary array electrophoresis bioanalyzer for ultrahigh-throughput genetic analysis, *Anal. Chem.* 74, 5076, 2002.

[5] Woolley, A. T., Sensabaugh, G. F., and Mathies, R. A., High-speed DNA genotyping using microfabricated capillary array electrophoresis chips, *Anal. Chem.* 69, 2181, 1997.

[6] Liu, S. R., Ren, H. J., Gao, Q. F., Roach, D. J., Loder, R. T., Armstrong, T. M., Mao, Q. L., Blaga, I., Barker, D. L., and Jovanovich, S. B., Automated parallel DNA sequencing on multiple channel microchips, *Proc. Natl. Acad. Sci. USA* 97, 5369, 2000.

[7] Cheng, S. B., Skinner, C. D., Taylor, J., Attiya, S., Lee, W. E., Picelli, G., and Harrison, D. J., Development of a multichannel microfluidic analysis system employing affinity capillary electrophoresis for immunoassay, *Anal Chem* 73, 1472, 2001.

[8] Hongwei, X. and Ewing, A. G., *Anal. Chem.* 26, 4711, 2005.

[9] Landers, J. P. and Ferrance, J., Exploiting sensitive laser-induced fluorescence detection on electrophoretic microchips for executing rapid clinical diagnostics, *Luminiscence* 16, 79, 2001.

[10] Xue, Q. F., Foret, F., Dunayevskiy, Y. M., Zavracky, P. M., McGruer, N. E., and Karger, B. L., Multichannel microchip electrospray mass spectrometry, *Anal. Chem.* 69, 426, 1997.

[11] Dishinger, J. F. and Kennedy, R. T., Serial immunoassays in parallel on a microfluidic chip for monitoring hormone secretion from living cells, *Anal. Chem.* 79, 947, 2007.

[12] Liu, J., Hansen, C., and Quake, S. R., Solving the "world-to-chip" interface problem with a microfluidic matrix, *Anal. Chem.* 75, 4718, 2003.

[13] Anderson, J. R., Chiu, D. T., Jackman, R. J., Cherniavskaya, O., McDonald, J. C., Wu, H., Whitesides, S. H., and Whitesides, G. M., Fabrication of Topologically Complex Three-Dimensional Microfluidic Systems in PDMS by Rapid Prototyping, *Anal. Chem.* 72, 3158, 2000.
[14] Kelly, R. T., Pan, T., and Woolley, A. T., Phase-changing sacrificial materials for solvent bonding of high-performance polymeric capillary electrophoresis microchips, *Anal. Chem.* 77, 3536, 2005.
[15] Fuentes, H. V. and Woolley, A. T., Phase-changing sacrificial layer fabrication of multilayer polymer microfluidic devices, *Anal. Chem.* (in press), 2007.
[16] Fuentes, H. V. and Woolley, A. T., Using Sacrificial Materials to Fabricate Polymeric Microfluidic Devices, in *Handbook of Capillary Electrophoresis ans Miniaturized Techniques*, Landers, J. P. CRC, Boca Raton, 2007.
[17] Kelly, R. T. and Woolley, A. T., Thermal bonding of polymeric capillary electrophoresis microdevices in water, *Anal. Chem.* 75, 1941, 2003.
[18] Fuentes, H. V. and Woolley, A. T., Electrically actuated, pressure-driven liquid chromatography separations in microfabricated devices, *Lab Chip* 7, 1524, 2007.
[19] Sanders, J. C., Breadmore, M. C., Kwok, Y. C., Horsman, K. M., and Landers, J. P., Hydroxypropyl cellulose as an adsorptive coating sieving matrix for DNA separations: artificial neural network optimization for microchip analysis, *Anal. Chem.* 75, 986, 2003.
[20] Jacobson, S. C., Hergenroder, R., Koutny, L. B., Warmack, R. J., and Ramsey, J. M., Effects of Injection Schemes and Column Geometry on the Performance of Microchip Electrophoresis Devices, *Anal. Chem.* 66, 1107, 1994.
[21] Culbertson, C. T., Jacobson, S. C., and Ramsey, J. M., Dispersion sources for compact geometries on microchips, *Anal. Chem.* 70, 3781, 1998.
[22] Paegel, B. M., Hutt, L. D., Simpson, P. C., and Mathies, R. A., Turn geometry for minimizing band broadening in microfabricated capillary electrophoresis channels, *Anal. Chem.* 72, 3030, 2000.
[23] Grossman, P. D. and Colburn, J. C., Capillary Electrophoresis, Theory and Practice, Academic Press, San Diego, CA, 1992.
[24] Sun, X., Peeni, B. A., Yang, W., Becerril, H. A., and Woolley, A. T., Rapid prototyping of poly(methyl methacrylate) microfluidic systems using solvent imprinting and bonding, *J. Chromatogr. A* 1162, 162, 2007.

7. CONCLUSIONS AND FUTURE WORK

7.1. CONCLUSIONS

7.1.1 Electrically actuated, pressure-driven microfluidic pumps

The electrochemical pumps presented in Chapter 2 offer several advantages for microfluidic applications, including ease to fabricate, operate and integrate with a variety of substrates. Moreover, unlike electroosmotic pumps, electrochemical actuation requires relatively low voltages (<25 V), and they can be applied to fluid pumping of conductive and non-conductive solutions.

I performed pressure-driven pumping of water through poly(methyl methacrylate) (PMMA) microfluidic channels using electrochemically actuated micropumps. More than 150 experiments were carried out using different micropump-microchannel combinations. Using the ideal gas law and Faraday's equation, I developed an equation to predict the flow rate for a specific time and applied current. Measured flow rates ranged from 8.1 to 13 μL/min and were 1.5-3.3 times lower than predicted values. This difference was mostly due to the gas permeability of PDMS and leaks at the pump-microchannel interface. I observed that the flow rate in the microchannels could be adjusted by modifying the applied voltage. I also determined a maximum pump pressure of ~300 kPa. Electrochemical pumping holds great potential for pressure-driven applications in microfluidics. Indeed, in Chapter 3, I presented the application of electrically actuated pressure-driven pumping in a miniaturized LC system. Moreover,

evaluation of new designs and different materials should enable the use of these micropumps in other applications.

7.1.2 Electrically actuated, pressure-driven liquid chromatography separations in microfabricated devices

In Chapter 3, I described the capabilities of electrically actuated micropumps for pressure-driven microchip LC separations. I designed and fabricated microdevices having electrochemical micropumps integrated with microchannels in a glass substrate. Two independent micropumps controlled the flow of sample and mobile phase, which enabled the implementation of a pressure-balanced injection mode with no dead volume between injection and separation. Fast (<40 s) chromatographic separation of three fluorescently-tagged amino acids with an efficiency of >3000 theoretical plates was obtained in 2.5-cm-long glass microchannels coated with 10% (w/w) chlorodimethyloctadecylsilane as stationary phase.

Chapter 3 demonstrates the potential of electrochemical micropumps integrated with microchannels for performing rapid chromatographic separations in a microfabricated platform. Due to the stochastic formation of bubbles at electrode surfaces during electrolysis, pumping reproducibility decreased with longer electrolysis times. This issue can be resolved by decreasing bubble affinity for the electrodes or controlling the electrolysis using feedback loop current control.

7.1.3 Phase-changing sacrificial layer fabrication of polymeric microdevices for chemical analysis

PCSL work in Dr. Woolley's group was started by Kelly et al.[1] This approach has been demonstrated in the fabrication of microchips for high-efficiency electrophoretic separations,[1] electric field gradient focusing microdevices[2] and protein preconcentration systems.[3] In Chapter 4 of my dissertation, I reviewed the principles and experimental protocols used to fabricate polymer microfluidic devices using PCSLs.[4]

The flexibility of the PCSL approach makes it attractive in microfabrication for many reasons. First, by selecting the right combination of substrate, sacrificial material and solvent, this method can be extended easily to other polymers, which have not yet been explored for microfluidic applications. Second, the bonding step is carried out at room temperature, which prevents deformation of the patterned substrate observed in thermal bonding. Third, solvent-bonded polymeric microdevices can withstand internal pressures at least one order of magnitude higher than thermally bonded microchips. Finally, multiple substrates can be bonded together without affecting the properties of the previous layers, which should facilitate the fabrication of fluidically complex microstructures such as multidimensional microdevices.

Subsequently, I explored the use of PCSLs to make polymeric multilayer microfluidic devices. The work presented in Chapter 5 demonstrated for the first time the fabrication of multilayer structures with micrometer-sized channels in a thermoplastic material. I fabricated three-layered PMMA microchips having crossover microchannels. An

important achievement of this work was the ability to fill dead-end channels with the sacrificial material using capillary action instead of vacuum. I determined that crossover channels were fluidically and electrically independent, in that fluid flow and/or an applied electric field in a microchannel crossing over the main fluidic path had no effect on current or efficiency in the separation channel.[5]

My results in Chapter 5 motivated further studies to develop potential applications of multilayer devices with crossover channels. One important challenge to address was the reduction of the crossover volume. In initial designs, 40-µm-wide microchannels were interconnected via 280-µm-diamenter through-holes, which created a >100-nL dead volume at the crossover intersection. Therefore, the posibility of performing separations in a crossover channel was not realistic.

To overcome this issue, I used a 250-µm-thick PMMA film instead of a 1.6-mm-thick PMMA sheet to make the middle layer (Chapter 6). With this thin intermediate layer, I was able to laser cut through-holes with <100-µm diameters, which reduced the crossover volume by at least 50x compared to the devices presented in Chapter 5. The advantages of the new microchips with thinner intermediate layers were demonstrated in the separation of three fluorescently labeled amino acids in a microchannel with a crossover. Although the separation efficiency in the crossover channel was somewhat lower compared to that in a single-layer channel, resolution was still adequate to separate the three peaks. These results demonstrated potential for further integration and development of more sophisticated microchannel arrays in polymeric microchips.

The importance of having fluidically and electrically independent crossover channels was exploited in Chapter 6. I designed a microfluidic chip having only four input reservoirs for simultaneous replicate runs in four channels. The use of crossover microchannels simplified the design and reduced the space constraints, allowing more fluidic paths to be integrated in a specific device footprint. My experiments showed that multilayer multichannel microfluidic systems should be well suited for high-performance separations in parallel or series. As an example, I injected a sample from a single reservoir and separated two peptides simultaneously in three independent channels in <20 s. This experiment illustrated a significant gain in speed and throughput. Moreover, I have demonstrated that new microchip designs and fabrication strategies can help microfluidic devices better realize the promises and expectations of the μTAS concept.

7.2. FUTURE DIRECTIONS

7.2.1 Electrically actuated pumping

In my dissertation, I demonstrated the potential of electrically actuated micropumps for applications in microfluidics; however, the versatility of these micropumps can be improved and other applications should be explored. Electrochemical pumps have the potential to be actuated reversibly. By reversing the direction of the current, the electrolysis reaction can proceed in the opposite direction, converting gases into liquid again.[6,7] moreover, in my experiments water was electrolyzed, but other solutions and electrode combinations could also be explored.

The adhesion of the Cr/Au electrodes to glass in Chapter 3 was not optimal when exposed to KNO_3 solution and applied voltage. A device could be operated using these electrodes for only 15-20 runs before the metal delaminated. To overcome this issue Pt electrodes deposited on top of a Ti layer, which have better adhesion to glass[8] should be used instead. Ti/Pt electrodes can be placed on glass substrates by e-beam deposition.[9]

7.2.2 Pressure-driven separations in microfabricated devices

In 1990, Manz et al.[10] presented a paper in which theory indicated that miniaturization should improve the efficiency of LC separations. However, no microfabricated devices to date have achieved the separation power of conventional LC systems. My work in Chapter 3 demonstrated rapid LC microchip separations, but with lower efficiency and resolution compared to bench-top LC instruments.

To achieve the goal of higher separation efficiency, open-tubular microchannels can be made even narrower (<5 μm deep), which would improve the mass transfer from the mobile phase to the stationary phase. In addition, monoliths have been used as separation media for chip-based capillary electrochromatography (CEC).[11,12] Monoliths are well-suited for microfluidic devices because they eliminate column packing, since a monolith can be polymerized in-situ.[13,14] To generate monolithic stationary phases, different acrylate monomers in porogenic solvent systems can be polymerized according to published work.[11,14] By using UV-initiated polymerization, it is possible to cast monoliths only in desired regions in a channel.

To improve the resolution of chip-based LC separations, mobile phase gradient elution must be incorporated in the system. In the devices that I developed, this aim can be achieved easily by adding a second eluent pump and eluent reservoir. **Figure 7.1** illustrates a microchip layout similar to that in **Figure 3.1,** but in which a second electrochemical micropump has been connected to a second eluent reservoir, for mobile phase gradient elution delivery.

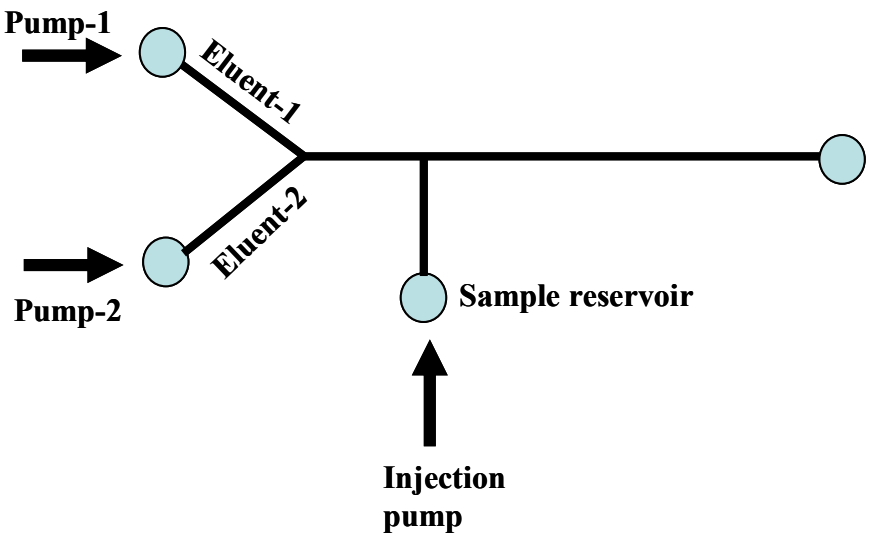

Figure 7.1 Layout of a microchip LC device with gradient elution capabilities.

In addition to the gain in speed and reduction in sample and reagent usage, micromachining facilitates the integration of multiple components or additional separation microchannels in a single substrate. **Figure 7.2** shows a schematic of a microdevice for multidimensional LC separations.

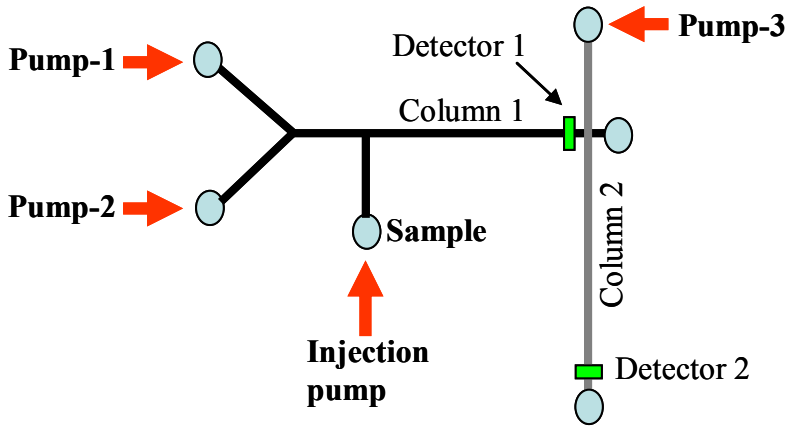

Figure 7.2 Layout of a microchip device for multidimensional LC separations.

In this design, sample can be separated in column 1 as demonstrated in Chapter 3. Then, the eluent from column 1 can be injected on a second separation column (column 2), driven by an additional micropump (**Figure 7.2**). If column 2 has a different stationary phase composition from column 1, the peak capacities of these microfabricated devices would be greatly improved over a one-dimensional separation.

7.2.3 Electrochemical detection

I have demonstrated separations in miniaturized devices, which can in principle be portable and used for on-site analyses. However, even with the reduced size of these microsystems, they still depend on bulky instrumentation for detection. For all experiments in my dissertation, I used LIF detection, which additionally requires non-fluorescent samples to be derivatized.

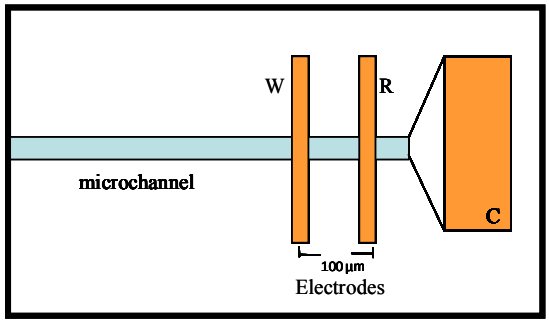

Figure 7.3.Diagram of a thin-film electrode configuration for EC detection in a microchip LC device. Legend: W, working electrode; R, reference electrode; C, counter electrode.

Miniaturization of the detection mechanism is thus highly desirable. Electrochemical (EC) detection could be implemented in the microchip LC devices fabricated in Chapter 3. **Figure 7.3** illustrates a potential arrangement and orientation of a microchannel and electrodes. Pt (2,000 Å) could be e-beam evaporated on top of a 200 Å Ti layer to form the electrodes. To optimize the EC detection system, one could study the effect of electrode spacing and width on detection sensitivity and performance, as well as chromatographic resolution. In addition, it would be useful to explore the deposition of different electrode materials to perform selective analyte detection.[15]

7.2.4 Microdevices for simultaneous CE analyses with different columns and potentials

In Chapter 6, I demonstrated replicate analyses in parallel using multichannel multilayer PCSL-fabricated microdevices. The same approach can be extended readily to make microdevices for simultaneous separations of a sample from a single reservoir using different columns and potentials. **Figure 7.4** illustrates such a device, which has a sample reservoir and four independent separation channels. This microchip layout should enable different CE separation modes to be performed simultaneously for a single sample.

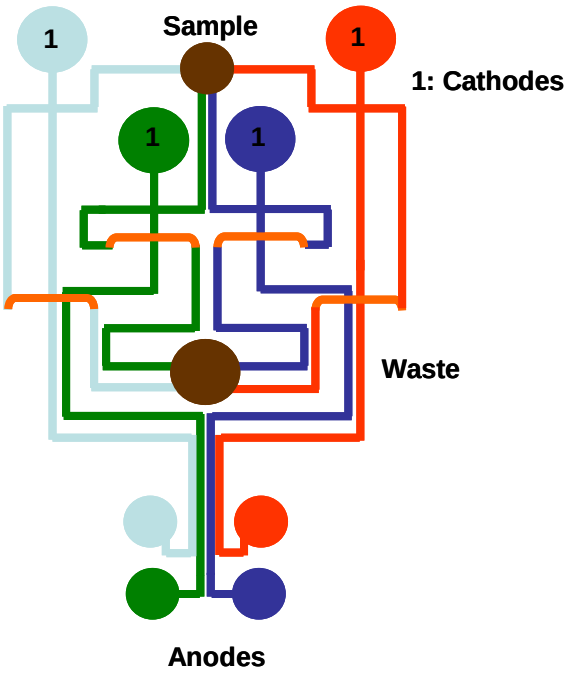

Figure 7.4 Microchip layout for simultaneous sample analyses with different columns or potentials.

For example, method development could be done faster since one could experiment with different buffers and potentials to optimize the conditions 4x faster compared to a microdevice with a single channel. Furthermore, with a single sample, one microchannel could run CZE separation, a second microchannel having an entangled polymer gel would enable CGE analysis;[16] and a third microchannel filled with a buffer containing micelles would allow MEKC separation of the neutral components in the sample. Finally, surface modification would enable the incorporation of a stationary phase in a fourth microchannel for CEC separation. Indeed, a microfluidic device with these capabilities would represent a tremendous advance in high-throughput separations and a step forward towards a new generation of chip-based analyses.

7.2.5 Multilayer microdevices for end-column labeling

Fluorescent labeling of proteins in the separation channel just before the detection point is advantageous to minimize band broadening due to differences in electrophoretic mobility of the same protein with different levels of derivatization.

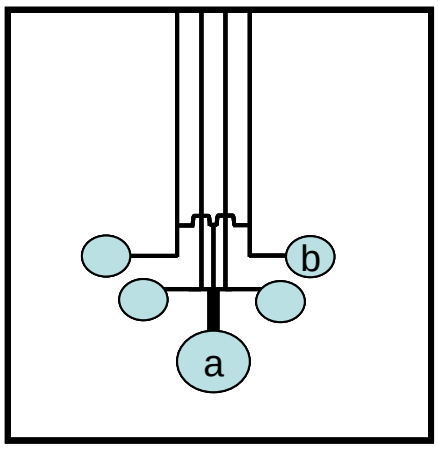

Figure 7.5 Microchip design for incorporating end-column labeling with multichannel separations in multilayer microdevices.

Although end-column labeling can be performed without multilayer devices, crossover channels should facilitate connecting a single reservoir containing the labeling reagent with several microchannels for simultaneous labeling. **Figure 7.5** depicts a microchip layout in which labeling reagent can be driven electrokinetically from reservoir a into four separation channels.

7.2.6 On-chip concentration and clean-up

Several groups have recognized the potential of microfabricated devices for incorporating sample processing steps such as preconcentration,[3,17] clean-up[18] and immunoassays.[19] One of the challenges associated with these applications is the incorporation of a membrane or a monolithic structure in a specific area of the microchannels (i.e., UV polymerization of monoliths) without affecting other sections or the device. The approach that I developed to fabricate multilayered microstructures

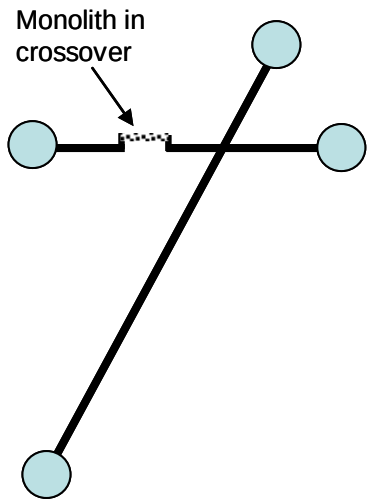

Figure 7.6 Device design of a microfluidic chip incorporating a crossover channel with a monolith structure for sample preconcentration.

with crossover channels allows connecting an independent channel section with a fluidic path in separated layers. The crossover microchannels section can thus be modified prior to being part of the completed fluidic path. **Figure 7.6** shows a schematic for a device containing a crossover channel with a monolith structure, which could be used for sample enrichment prior to separation.

In summary, in my dissertation I have developed tools to expand the applications of microfabricated devices. Further studies on electrochemical pumping, advances in microfabricated columns and electrochemical detection should move forward the field of chip-based LC separations. PCSL microfabrication was introduced over two years ago and continues to grow. My work pushes the frontiers of this fabrication technique and demonstrates strong potential for bioanalysis applications.

7.3 REFERENCES

[1] Kelly, R. T., Pan, T., and Woolley, A. T., Phase-Changing Sacrificial Materials for Solvent Bonding of High-Performance Polymeric Capillary Electrophoresis Microchips, *Anal. Chem.* 77, 3536, 2005.

[2] Kelly, R. T. and Woolley, A. T., Electric Field Gradient Focusing, *J. Sep. Sci.* 28, 1985, 2005.

[3] Kelly, R. T., Li, Y., and Woolley, A. T., Phase-changing sacrificial materials for interfacing microfluidics with ion-permeable membranes to create on-chip preconcentrators and electric field gradient focusing microchips, *Anal. Chem.* 78, 2565, 2006.

[4] Fuentes, H. V. and Woolley, A. T., Using Sacrificial Materials to Fabricate Polymeric Microfluidic Devices, in *Handbook of Capillary and Microchip Electrophoresis and Associated Microtechniques*, Landers, J. P., Ed., CRC, Boca Raton, FL, 2007.

[5] Fuentes, H. V. and Woolley, A. T., Phase-Changing Sacrificial Layer Fabrication of Multilayer Polymer Microfluidic Devices, *Anal. Chem.* (in press), 2007.

[6] Nyholm, L., Electrochemical techniques for lab-on-a-chip applications, *Analyst* 130, 599, 2005.

[7] Bohm, S., Timmer, B., Olthuis, W., and Bergveld, P., A closed-loop controlled electrochemical actuated micro-dosing system, *J. Micromech. Microeng.* 10, 498, 2000.

[8] Woolley, A. T., Lao, K. Q., Glazer, A. N., and Mathies, R. A., Capillary electrophoresis chips with integrated electrochemical detection, *Anal. Chem.* 70, 684, 1998.
[9] Madou, M. J., *Fundamentals of microfabrication*, CRC, Boca Raton, FL, 2nd edition, 193, 2002.
[10] Manz, A., Miyahara, Y., Miura, J., Watanabe, Y., Miyagi, H., and Sato, K., Design of an Open-Tubular Column Liquid Chromatograph Using Silicon Chip Technology, *Sens. Actuators B* 1, 249, 1990.
[11] Throckmorton, D. J., Shepodd, T. J., and Singh, A. K., Electrochromatography in microchips: Reversed-phase separation of peptides and amino acids using photopatterned rigid polymer monoliths, *Anal. Chem.* 74, 784, 2002.
[12] Yu, C., Svec, F., and Frechet, J. M. J., Towards stationary phases for chromatography on a microchip: Molded porous polymer monoliths prepared in capillaries by photoinitiated in situ polymerization as separation media for electrochromatography, *Electrophoresis* 21, 120, 2000.
[13] Tanaka, N., Kobayashi, H., Nakanishi, K., Minakuchi, H., and Ishizuka, N., Monolithic LC columns, *Anal. Chem.* 73, 420A, 2001.
[14] Rohr, T., Yu, C., Davey, M. H., Svec, F., and Frechet, J. M. J., Porous polymer monoliths: Simple and efficient mixers prepared by direct polymerization in the channels of microfluidic chips, *Electrophoresis* 22, 3959, 2001.
[15] Luo, P. F., Zhang, F. Z., and Baldwin, R. P., Constant potential amperometric detection of underivatized amino acids and peptides at a copper electrode, *Anal. Chem.* 63, 1702, 1991.
[16] Woolley, A. T. and Mathies, R. A., Ultra-High-Speed DNA Fragment Separations Using Microfabricated Capillary Array Electrophoresis Chips, *Proc. Natl. Acad. Sci. USA* 91, 11348, 1994.
[17] Foote, R. S., Khandurina, J., Jacobson, S. C., and Ramsey, J. M., *Anal. Chem.* 77, 57, 2005.
[18] Xu, N. X., Lin, Y. H., Hofstadler, S. A., Matson, D., Call, C. J., and Smith, R. D., A microfabricated dialysis device for sample cleanup in electrospray ionization mass spectrometry, *Anal. Chem.* 70, 3553, 1998.
[19] Cheng, S. B., Skinner, C. D., Taylor, J., Attiya, S., Lee, W. E., Picelli, G., and Harrison, D. J., Development of a multichannel microfluidic analysis system employing affinity capillary electrophoresis for immunoassay, *Anal. Chem.* 73, 1472, 2001.